

Analytical Studies on Diffusion and Intermittency in Chaotic Maps

Thesis submitted to

COCHIN UNIVERSITY OF SCIENCE AND TECHNOLOGY

in partial fulfilment of the requirements for the award of the degree of

DOCTOR OF PHILOSOPHY

By

Rajagopalan S.

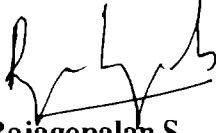
Department of Physics
Cochin University of Science and Technology
Kochi - 682 022, India
March 2002

Dedicated to the loving memory of my father

Declaration.

I hereby declare that the matter embodied in this thesis entitled **Analytical Studies on Diffusion and Intermittency in Chaotic Maps** is the result of investigations carried out by me under the supervision of Prof. M. Sabir in the Department of Physics, Cochin University of Science and Technology, Kochi-22 and that this work has not been included in any other thesis submitted previously for the award of any degree or diploma of any university.

Kochi-22,
4-3-2002.

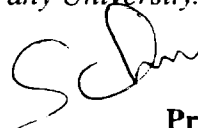


Rajagopalan S.

Certificate.

*Certified that the work contained in the thesis entitled **Analytical Studies on Diffusion and Intermittency in Chaotic Maps** is the bonafide work carried out by Rajagopalan S. under my supervision in the Department of Physics, Cochin University of Science and Technology, Kochi-22 in partial fulfilment of the requirements for the award of the degree of Doctor of Philosophy under the Faculty of Science and that the same has not been included in any other thesis submitted previously for the award of any degree or diploma of any University.*

Kochi-22,
4-3-2002.



Prof. M. Sabir

Preface.

Chaos is currently one of the most exciting topics in non-linear systems research. Simply put, a chaotic system is a deterministic system that exhibits complex behaviour. This is due to the existence of intrinsic trajectory instability of the dynamical system. It becomes difficult to understand the complex system in a predictable way, though the law of evolution is completely known. For this reason a statistical description is needed to understand the probabilistic behaviour in these systems. Concepts borrowed from thermodynamics and statistical mechanics are found to be useful in the qualitative and quantitative description of chaotic systems.

The study of simple chaotic maps for non-equilibrium processes in statistical physics has been one of the central themes in the theory of chaotic dynamical systems. Recently, many works have been carried out on deterministic diffusion in spatially extended one-dimensional maps. This can be related to real physical systems such as Josephson junctions in the presence of microwave radiation and parametrically driven oscillators. Transport due to chaos is an important problem in Hamiltonian dynamics also. A recent approach is to evaluate the exact diffusion coefficient in terms of the periodic orbits of the system in the form of cycle expansions. But the fact is that the chaotic motion in such spatially extended maps has two complementary aspects - diffusion and intermittency. These are related to the time evolution of the probability density function which is approximately Gaussian by central limit theorem. We noticed that the characteristic function

method introduced by Fujisaka and his co-workers is a very powerful tool for analysing both these aspects of chaotic motion. The theory based on characteristic function actually provides a thermodynamic formalism for chaotic systems. It can be applied to other types of chaos-induced diffusion also, such as the one arising in statistics of trajectory separation. We noted that there is a close connection between cycle expansion technique and characteristic function method. It was found that this connection can be exploited to enhance the applicability of the cycle expansion technique. In this way, we found that cycle expansion can be used to analyse the probability density function in chaotic maps. In our research studies we have successfully applied the characteristic function method and cycle expansion technique for analysing some chaotic maps. We introduced in this connection, two classes of chaotic maps with variable shape by generalizing two types of maps well known in literature.

This thesis is organized as follows: The first chapter provides an introduction to the basic concepts and theories needed for understanding the thesis. Fundamental ideas pertaining to periodic orbit, Frobenius-Perron operator, invariant density, topological conjugation, Markov partition etc are very briefly presented. Then we give the salient features of the characteristic function method somewhat in detail because a proper understanding of the same is quite essential for the thesis. The first chapter also contains an elementary introduction to cycle expansion technique.

In chapter 2 we discuss statistics of trajectory separation in one-dimensional maps. For any one dimensional map, fluctuations of local expansion rates produce fluctuations in the distance between nearby trajectories (trajectory separation). Fujisaka and his co-workers have shown that these fluctuations of local expansion rates produce a diffusion in the time evolution of trajectory separation. According to central limit theorem, the probability density function of the logarithmic distance between nearby trajectories will be approximately Gaussian. We examine the validity of Gaussian approximation by studying the case of pe-

riod three boundary map as an example. Analysis using characteristic function method reveals that in general the PDF shows appreciable deviation from Gaussian form. Approximation will be valid only if the standard deviation of LER is very small. The result is relevant to a class of one-dimensional maps conjugate to the PTB map. Exact expressions for quantities like diffusion coefficient and moments are evaluated.

In chapter 3, we generalize the spatially extended one-dimensional map introduced by R. Artuso. The generalized piecewise linear map (GPL map) proposed by us has a variable peak-shape and can have integer heights. We analyse the chaotic motion and its shape dependence in this map, using the characteristic function method. Exact expression for diffusion coefficient is obtained which reduces to the result of Artuso as a special case. Fluctuation spectrum obtainable from the characteristic function is used to analyse the probability density function. We note that the diffusion coefficient and the probability density function are highly influenced by the shape of the map. The important finding is that the non-Gaussian character of the probability density function and intermittency increase with increasing flatness and peak -height.

In chapter 4, we introduce a generalization of the map introduced by H.C. Tseng et al. The resulting map has a variable peak-shape and fractional peak-height, less than unity. We prove that for almost all arbitrary values of peak-height, these maps are Markov mappings. As such we call these generalized piecewise linear Markov maps. Closed form expressions for diffusion coefficient giving previously obtained results as special cases are derived in all cases. We show how the probability density function can be analysed using fluctuation spectrum obtainable from the characteristic function. Shape of the map is found to have a crucial role in determining the diffusion coefficient, intermittency and the probability density function. Our generalized piecewise linear maps are very good approximations to the sinusoidal maps which can be studied only numerically. We anticipate that these maps will be useful in the time series analysis of chaotic systems.

In Chapter 5, we show that cycle expansion technique which is usually applied for the evaluation of exact diffusion coefficient has more applications in the study of chaos-induced diffusion systems. This is done by linking it with the characteristic function method. We show how periodic orbits can be used to obtain the exact diffusion coefficient and fluctuation spectrum. The two complementary aspects of chaos-induced diffusion—diffusion and intermittency—can be analysed using the probability density function obtainable from fluctuation spectrum. We also present illustrative examples for the two types of systems referred to above - chaotic diffusion in spatially extended maps and the one associated with statistics of trajectory separation.

A part of the work reported in this thesis has been published in the form of two research papers. Two more papers have been prepared and communicated for publication

1. “Statistics of trajectory separation in one-dimensional maps”—S. Rajagopalan and M. Sabir, *Indian Journal of Physics* **74 A** (4), 439–445(2000).
2. “Analysis of chaotic motion and its shape dependence in a generalized piecewise linear map”—S. Rajagopalan and M. Sabir, *Physical Review E* **Vol 63**, 05 7201(2001).
3. “Analysis of diffusion and intermittency in generalized piecewise linear Markov maps with fractional peak-height”—S. Rajagopalan and M. Sabir, communicated to *Physical Review E*.
4. “Periodic orbits and the complementary dynamics of diffusion and intermittency in chaotic maps”—S. Rajagopalan and M. Sabir, communicated to *Physical Review E*.

Kochi-22,
4-3-2002.

RAJAGOPALAN S.

Acknowledgments

I wish to place on record my indebtedness to Dr. M. Sabir, Professor of Physics, for his keen interest, invaluable guidance and supervision throughout the course of my research studies. The stimulating and illuminating discussions we had on the subject were extremely beneficial for me to complete this work. Let me express my deep sense of gratitude to Dr. Elizabeth Mathai, Professor and Head of the Department of Physics, Cochin University of Science and Technology, for the interest she has shown in my studies. I am extremely thankful to other faculty members of the Department of Physics for their support and encouragement.

Let me gratefully acknowledge the assistance I have received from my fellow research scholars. I would like to thank all the members of the library and non-teaching staff of the Department for their kind hearted co-operation during the course of my research.

I wish to express my gratitude to the Principal, Sree Krishna College, Guruvayur for giving me permission to join for part time research. Completion of this work would not have been possible without the support of my colleagues. I would like to thank all of them.

I am extremely grateful to my wife Geetha Devi, son Arjun Sankar and daughter Lakshmi Devi for their understanding and unstinted support. My elder brother Dr. S. V. G. Menon, senior scientist at Bhabha Atomic Research Centre, Mumbai has helped me a lot in my work. Let me express my gratitude to him for the same.

I would like to thank Beeta Transcription Services, Tripunithura for their patience and efficiency in preparing the L^AT_EX version of this thesis. Thanks are also due to M. M. Book Binders, South Kalamassery for the neat binding.

RAJAGOPALAN S.

Contents

<i>Preface</i>	iv
<i>Acknowledgments</i>	viii
1 Introduction.	1
1.1 Essentials of chaotic maps.	1
1.1.1 Characterization of chaotic motion.	5
1.1.2 Topological conjugation.	7
1.1.3 Markov partition and symbolic dynamics.	7
1.1.4 Transition to chaos: Different routes.	9
1.2 Diffusion and intermittency in chaotic maps:	
Theory based on characteristic function.	10
1.2.1 Basic dynamics and characteristic function.	10
1.2.2 Probability density function (PDF).	13
1.2.3 Exponents μ and σ .	14
1.2.4 Fluctuation spectrum $\sigma(\alpha)$.	15
1.2.5 Evaluation of characteristic function λ_q .	18
1.2.6 Order q time correlation function $Q_t^{(q)}$	19
1.2.7 Thermodynamic formalism: connection with other theories.	20
1.3 Cycle expansion.	20

<i>CONTENTS</i>	x
2 Statistics of trajectory separation in one-dimensional maps.	25
2.1 Introduction.	25
2.2 Statistics of trajectory separation in one-dimensional maps: Characteristic function method.	27
2.3 Statistics of trajectory separation for the period-three boundary map.	29
2.3.1 Characteristic function and diffusion coefficient:	29
2.3.2 Moments and probability density function:	35
2.4 Results and conclusions.	36
2.5 Appendix-A.	41
2.6 Appendix B.	42
3 Analysis of chaotic motion and its shape dependence in a generalized piecewise linear map.	44
3.1 Introduction.	44
3.2 Model and characteristic function method.	46
3.3 Characteristic function, diffusion coefficient and fluctuation spectrum.	50
3.3.1 Special cases.	53
3.3.2 Limiting forms.	53
3.3.3 Shape dependence of diffusion coefficient and fluctuation spectrum.	54
3.4 Results and conclusions.	58
4 Analysis of diffusion and intermittency in generalized piecewise linear Markov maps with fractional peak height.	59
4.1 Introduction.	59
4.2 GPLM models and characteristic function method.	60
4.3 Exact results for diffusion coefficients.	65
4.4 Variation of diffusion coefficient and fluctuation spectrum.	75

<i>CONTENTS</i>	xi
4.5 Results and conclusions.	78
4.6 Appendix A.	81
4.7 Appendix B.	82
5 Periodic orbits and the complementary dynamics of diffusion and intermittency in chaotic maps.	84
5.1 Introduction.	84
5.2 Probability density function via periodic orbits.	86
5.3 Illustrative examples.	90
5.3.1 Spatially extended piecewise linear maps.	90
5.3.2 Dynamics of local expansion rates.	98
5.4 Results and conclusions.	107

Chapter 1.

Introduction.

1.1 Essentials of chaotic maps.

Today it is well known that even very low-dimensional, simple deterministic systems can exhibit an unpredictable, quasi-stochastic long-time behaviour. It has become common to call this phenomenon 'chaos'. The first system of this kind, namely the three body problem of classical mechanics, was investigated by Henri Poincaré at the end of nineteenth century [1]. Since then a large number of dynamical systems that exhibit chaotic behaviour have become known. Subsequent noteworthy early mathematical work on chaotic dynamics includes that of G. Birkhoff in the 1920s, M. L. Cartwright and J. E. Littlewood in the 1940s, S. Smale in the 1960s, and Soviet mathematicians, notably A. N. Kolmogorov and his co-workers. For non-linear systems, chaos appears to be a generic rather than an exotic phenomenon.

The time evolution of a dynamical system is determined by a deterministic evolution equation. For continuous-time dynamical systems it is a differential equation.

$$\frac{dx}{dt} = F(x) \tag{1.1}$$

and for discrete-time dynamical systems it is a recurrence relation known as a map or mapping. A map in a d -dimensional space with appropriate co-ordinates (Cartesian co-ordinates, for example) is given by

$$x_{t+1} = f(x_t) \quad (1.2)$$

where

$$x_t = (x_t^{(1)}, x_t^{(2)}, \dots, x_t^{(d)}) \quad (1.3)$$

is a vector in X , the phase space. Phase space is the set of all possible values of the co-ordinates.

$$f = (f^{(1)}, f^{(2)}, \dots, f^{(d)}) \quad (1.4)$$

is a vector-valued function. The dynamical system is called ‘nonlinear’ if the function $f(x)$ is nonlinear. Only nonlinear maps can exhibit chaotic behaviour. We start with an initial point x_0 and, iterate it step by step. Each point x_t is called an iterate. In a computer experiment, the number of iteration steps is very large — say of the order of 10^4 or larger. The sequence of iterates x_0, x_1, x_2, \dots is called a trajectory. It describes the motion of a point in the space X . Suppose each step from x_t to x_{t+1} takes the same time. Then the entire time is proportional to t , the total number of steps. We adopt the convention of calling the length of the trajectory the ‘time’

A trajectory may either become periodic, or stay aperiodic forever. In the first case after a certain number t of iterations, the iterates approach a sequence $x_t, x_{t+1}, x_{t+2}, \dots, x_{t+\xi}$, satisfying

$$x_{t+\xi} = x_t \quad (1.5)$$

The sequence $x_t, x_{t+1}, x_{t+2}, \dots, x_{t+\xi-1}$ is called a periodic orbit or cycle of f . The smallest possible ξ satisfying the above equation is called the length of the cycle.

A periodic orbit of length $\xi = 1$ is called a fixed point of the map f . A fixed point x^* is given by

$$x^* = f(x^*) \quad (1.6)$$

A periodic orbit of length ξ can be regarded as a fixed point of the ξ -times iterated function

$$f^\xi(x) = f(f(f(\dots f(x)))) \quad (\xi \text{ times}) \quad (1.7)$$

Hence one can restrict the discussion of periodic orbits to the discussion of fixed points.

It can be noted that the long-time behaviour of a non-linear map for a generic initial value is totally different for different kinds of maps. One can distinguish between so called Hamiltonian dynamical systems and dissipative dynamical systems. A Hamiltonian system is one which conserves the volume of an arbitrary volume element of the phase space during the time evolution. For a dissipative system, a small phase space volume either shrinks or expands and this usually depends on the position x in the phase space. In this case, a large number of trajectories approach a certain subset A of the phase space X in the limit $t \rightarrow \infty$. The subset A is called an attractor. There may be one or several attractors. In low-dimensional systems in many cases, there is just one attractor which attracts almost all trajectories. In further discussion we limit ourselves to dissipative systems.

One possible type of attractor is a stable fixed point. The fixed point x^* is called stable, if a large number of trajectories is attracted to it. For a one-dimensional map a Taylor series expansion of $f(x)$ around x^* shows that this will happen only if $|f'(x^*)| < 1$. This means that a stable fixed point for a 1- D map is characterized by the fact that its neighborhood is contracted under the action of f .

More generally, the attractor of a map may also be a stable periodic orbit of length ξ . The periodic orbit of length ξ is called stable, if the corresponding fixed

point f^k is stable. In this case the vicinity of the periodic orbit is contracting, and thus a large number of trajectories is attracted to it. An unstable periodic orbit is not an attractor, because it repels trajectories.

Chaotic attractors may have an extremely complicated structure (especially in dimensions $d \geq 2$). For such attractors there is at least one direction of the phase space where small distances expand on average. But in spite of that they are confined to a finite phase space. They often have a fractal structure [8–10]. This means that we observe a complicated structure on arbitrary length scales, which can be described by a ‘non-integer dimension’ Attractors with this property are called strange attractors [5–7, 40].

The logistic map [5, 16–18] has played an important role in the development of the theory of nonlinear dynamical systems. This is a one-dimensional map with range $[-1,1]$ of the real axis. The map is defined by

$$f(x) = 1 - \mu x^2 \tag{1.8}$$

μ is called the control parameter with possible values $\mu \in [0, 2]$. Familiar examples of two dimensional maps are (1) The Henon map [19] (2) Maps of Kaplan-Yorke type [20–23] (3) The standard map [7, 24].

One-dimensional non-invertible maps are the simplest systems capable of chaotic motion [5, 6]. They serve as a convenient starting point for the study of chaos. A surprisingly large proportion of phenomena encountered in higher dimensional systems is already present in some form in one-dimensional maps. As such, in this thesis, we have focused attention on the study of $1 - D$ chaotic maps.

There are many excellent textbooks giving detailed description of the different aspects of chaotic dynamics. We have listed a few of them in the bibliography [5–7, 24–28].

1.1.1 Characterization of chaotic motion.

A dynamical system is said to be chaotic if it possesses sensitive dependence on initial conditions. For a chaotic map, separation between two trajectories generated by very close initial values will increase exponentially and in the long run totally different trajectories will be produced.

We consider below certain quantitative measures for characterizing chaotic motion. Let us consider a one-dimensional discrete process $x_{t+1} = f(x_t)$ ($t = 0, 1, 2, \dots$). We are interested in the long-time average of a function $G(x_t)$,

$$\overline{G(x_t)} \equiv \lim_{N \rightarrow \infty} \frac{1}{N} \sum_{t=1}^N G(x_t). \quad (1.9)$$

Let us take an attractor Ω and assume that $f(x)$ is *ergodic* in Ω [24–29]. Namely, periodic orbits in Ω are all unstable and there exists a unique absolutely continuous invariant measure so that the long-time average (1.9) can be replaced by the space average

$$\langle G(x) \rangle \equiv \int_{\Omega} dx \rho(x) G(x) \quad (1.10)$$

for almost all initial values x_0 , where

$$\rho(x) \equiv \overline{\delta(x_t - x)} \quad (1.11)$$

is the invariant density independent of x_0 .

Let H be an operator defined as,

$$HG(x) \equiv \int_{\Omega} dy G(y) \delta(f(y) - x) = \sum_i G(y_i) / |f'(y_i)|, \quad (1.12)$$

where y_i is the i -th solution of $f(y_i) = x$ in the attractor Ω and $f'(x) = df(x)/dx$. It can be shown that [5–7] H determines the time evolution of the density of

iterates $\rho_t(x)$. The density at time $(t + 1)$ can be obtained from that at time t as

$$\rho_{t+1}(x) = H\rho_t(x) \tag{1.13}$$

H , defined in this fashion, is called the Frobenius-Perron operator. For ergodic systems, as $t \rightarrow \infty$, $\rho_t(x)$ becomes stationary (time independent). This gives the invariant density $\rho(x)$

$$\rho(x) = H\rho(x) \tag{1.14}$$

Therefore the ergodicity of f in Ω would be equivalent to the existence of a unique solution of (1.14) everywhere in Ω .

One important quantity which characterizes dynamical processes is the Lyapunov exponent which takes the form [5–7, 24–30].

$$\begin{aligned} \lambda &\equiv \lim_{N \rightarrow \infty} \frac{1}{N} \ln \left| \frac{d}{dx} f^{(N)}(x) \right|, \quad (x \in \Omega) \\ &= \lim_{N \rightarrow \infty} \frac{1}{N} \sum_{t=0}^{N-1} \ln | f'(f^{(t)}(x)) | \end{aligned} \tag{1.15}$$

This represents the mean expansion rate of the difference between two nearby orbits. If $\lambda(x) > 0$, then the orbit $f^{(t)}(x)$ is unstable. The ergodicity leads, for almost all x , to

$$\lambda = \int_{\Omega} dx \rho(x) \ln | f'(x) | \tag{1.16}$$

The time-correlation functions of ergodic processes are given by [31].

$$C_t(V, W) \equiv \langle V(f^{(t)}(x)) | W(x) \rangle \equiv \int_{\Omega} dx \rho(x) V(f^{(t)}(x)) W(x). \tag{1.17}$$

This can be transformed into

$$C_t(V, W) = \langle V(x) | \hat{H}^t W(x) \rangle \quad (1.18)$$

where \hat{H} is the linear operator introduced by Mori et al [31].

$$\hat{H}G(x) \equiv \frac{1}{\rho(x)} H[\rho(x)G(x)] \quad (1.19)$$

1.1.2 Topological conjugation.

Sometimes it is useful to change co-ordinates such that the transformed map is simpler or has other advantages. Such a transformation to new co-ordinates is called a topological conjugation. It connects a map with an equivalent one. Suppose the map $f(x)$ and $\tilde{f}(\tilde{x})$ are topologically conjugated. Then there is a conjugating function h yielding

$$\tilde{x} = h(x) \quad (1.20)$$

We have

$$x_{n+1} = f(x_n) \quad \tilde{x}_{t+1} = \tilde{f}(\tilde{x}_t) \quad (1.21)$$

Then the following is fulfilled

$$\tilde{f}(\tilde{x}_t) = \tilde{x}_{t+1} = h(x_{t+1}) = h(f(x_t)) = h(f(h^{-1}(\tilde{x}_t))) \quad (1.22)$$

We have assumed that h^{-1} exists. The composition of the three functions h^{-1} , f and h gives us \tilde{f}

1.1.3 Markov partition and symbolic dynamics.

To apply a statistical description to mappings we require a partition of the phase space to subsets. Suppose we make a partition of the phase space into cells I_ν of different sizes. Each cell is labeled by an index ν . The cells are disjoint and cover

the entire phase space X . That is

$$I_\nu \cap I_\mu = \Phi \text{ (null set); } \bigcup_{\nu=1}^R I_\nu = X \quad (1.23)$$

Partitions with these properties are called cells.

Suppose we iterate a certain initial value x_0 with the map f . The point x_0 will be in some cell. Suppose ν_0 is its index. Let the second iterate be in cell with index ν_1 , third in ν_2 and so on. So the sequence of cells will be $x_0 \rightarrow \nu_0, \nu_1, \nu_2, \dots, \nu_t$. Suppose each cell I_ν has a symbol. Then these symbols will be appearing in the above sequence. A mapping from phase space to the symbol space is called 'symbolic dynamics' [7]. It describes the trajectory in a coarse-grained way. As the size of the starting cell ν_0 is finite and as it contains many initial values x_0 , a given symbol sequence of finite length t can be associated with many different sequences x_0, x_1, \dots, x_t of iterates. On the other hand, not all symbol sequences may be allowed in general.

Among the allowed symbolic sequences some will occur more frequently than others. Hence we can attribute to each sequence ν_0, \dots, ν_t a certain probability $P(\nu_0, \dots, \nu_t)$ that it is observed. The hierarchy of all such probabilities with $t = 0, 1, 2, \dots$ defines a stochastic process. Below we define two kinds of processes [7].

Let $P(\nu_t | \nu_0, \dots, \nu_{t-1})$ represent the conditional probability which is the probability of the event ν_t provided we have observed the sequence ν_0, \dots, ν_{t-1} before. If the conditional probability does not depend on the entire history ν_0, \dots, ν_{t-1} , but on the last event ν_{t-1} only, the symbolic stochastic process is called a Markov chain. This means a Markov chain has the property

$$P(\nu_t | \nu_0, \dots, \nu_{t-1}) = P(\nu_t | \nu_{t-1}) \quad (1.24a)$$

Another important concept is that of a topological Markov chain defined by the

property

$$P(\nu_t | \nu_0, \dots, \nu_{t-1}) = 0$$

$$\text{if and only if } P(\nu_t | \nu_{t-1}) = 0 \text{ or } P(\nu_{t-1} | \nu_0, \dots, \nu_{t-2}) = 0 \quad (1.24b)$$

The meaning is the following: There are two ways in which the conditional probability $P(\nu_t | \nu_0, \dots, \nu_{t-1})$ to cell ν_t can be zero. Either it is not possible to reach the cell ν_t from the cell ν_{t-1} or the sequence ν_0, \dots, ν_{t-1} is already forbidden.

In general the stochastic process generated by a map f will be neither a Markov chain nor a topological Markov chain but a complicated non-Markovian process. Character of the process will depend on the partition chosen. But for some maps a partition indeed exists that makes the corresponding stochastic process a topological Markov chain. Such a partition is called a Markov partition. Technically one usually defines a Markov partition by a topological property of the partition, that is to say essentially by the fact that—atleast in the one-dimensional case—edges of the partition are mapped again onto edges [7]. For a generic chaotic map one does not know whether a Markov partition exists. Even if it does exist, there is no simple way to find it.

1.1.4 Transition to chaos: Different routes.

Different routes have been proposed for transition of a physical system from regular motion to chaotic motion. Feigenbaum analysed a logistic map of the form (1.8) and noticed that the iterates oscillate in time between stable values (fixed points) whose number doubles at distinct values of an external parameter. This continues until the number of fixed points become infinite at a finite parameter value, when the iterates become irregular. Feigenbaum noticed that the results are not restricted to logistic model but are in fact universal and are valid for every 1-D maps with a single maximum. There have been many theoretical and experimental studies [5, 6, 17, 32] on Feigenbaum route.

In the intermittency route [5, 6, 33–39], discovered by Manneville and Pomeau

the signal which behaves regularly (or laminary) in time becomes interrupted by statistically distributed periods of irregular motion (intermittent bursts). The average number of these bursts increases with the variation of an external control parameter until the motion becomes completely chaotic. This route also has universal features.

A third route has been found by Ruelle and Takens [40] and Newhouse [41]. Much earlier, Landau [42] had considered turbulence in time as the limit of an infinite sequence of instabilities each of which creates a new frequency. Ruelle, Takens and Newhouse showed that after only two instabilities, in the third step, the trajectory becomes attracted to a bounded region of phase space which are called strange attractors.

1.2 Diffusion and intermittency in chaotic maps: Theory based on characteristic function.

We give below the salient features of the characteristic function based theory for analysing diffusion and intermittency in chaotic systems. The theory has been developed by Fujisaka and his co-workers. The authors have set forth different aspects of the theory in a series of papers [43–54].

The theory can be applied to analyse diffusion and intermittency aspects of chaos-induced diffusion systems. Research studies on the possible applications of the theory form the subject matter of the subsequent chapters.

1.2.1 Basic dynamics and characteristic function.

Consider the dynamics of A_t governed by

$$A_{t+1} = B(x_t)A_t, \quad (t = 0, 1, 2, \dots) \quad (1.25)$$

with $A_0 = 1$, where $B(x_t)$ is a certain steady, positive definite function of x_t generated by

$$x_{t+1} = f(x_t) \quad (0 \leq x_t < 1) \quad (1.26)$$

The statistical dynamics of A_t can be discussed with the q -order moment $\langle A_t^q \rangle$, $(-\infty < q < \infty)$. Multiplicativity of the modulation B suggests one to introduce

$$\lambda_q = q^{-1} \lim_{t \rightarrow \infty} t^{-1} \ln \langle A_t^q \rangle = q^{-1} \lim_{t \rightarrow \infty} t^{-1} \ln \langle \exp \{ q \sum_{s=0}^{t-1} \ln B(x_s) \} \rangle, \quad (1.27)$$

where $\langle \cdot \cdot \rangle$ is the average over the steady ensemble $\rho(x)$ satisfying the Frobenius-Perron equation $\rho(x) = H\rho(x)$. Hence

$$\langle A_t^q \rangle = Q_t^{(q)} \exp(q\lambda_q t), \quad (1.28)$$

where $Q_t^{(q)}$ is non singular in the sense that $\lim_{t \rightarrow \infty} t^{-1} \ln Q_t^{(q)} = 0$. Therefore λ_q turns out to play a significant role in the long-time dynamics of A_t . We call it the characteristic function. By making use of the inequality $\langle A_t^{2q} \rangle \geq \langle A_t^q \rangle^2$, i.e., $q(\lambda_{2q} - \lambda_q) \geq 0$, λ_q turns out to be monotonical

$$d\lambda_q/dq \geq 0 \quad (1.29)$$

Consider the cumulant expansion

$$\langle A_t^q \rangle = \exp \{ q\lambda_0 t + \sum_{n=2}^{\infty} \langle (\ln A_t - \lambda_0 t)^n \rangle_c q^n / n! \}, \quad (1.30)$$

where $\langle \dots \rangle_c$ is the cumulant average. The above expansion indicates that λ_q can be expanded as a power series

$$\lambda_q = \lambda_0 + Dq + O(q^2), \quad (1.31)$$

where

$$\lambda_0 = \lim_{t \rightarrow \infty} t^{-1} \langle \ln A_t \rangle = \langle \ln B(x) \rangle, \quad (1.32)$$

$$D = \lim_{t \rightarrow \infty} \sigma_t / 2t. \quad \sigma_t \equiv \langle (\ln A_t - \langle \ln A_t \rangle)^2 \rangle. \quad (1.33)$$

λ_0 is the drift velocity of $\langle \ln A_t \rangle (= \lambda_0 t)$, and D the diffusion coefficient characterizing the diffusion law $\sigma_t \simeq 2Dt$ for $t \gg \tau$, τ being the correlation time of $\ln B(x_t)$. From eqs.(1.29) and (1.33) we note that $D \geq 0$.

We note that D can be transformed into [55–57]

$$D = \frac{C_0}{2} + \sum_{t=1}^{\infty} C_t \quad (1.34)$$

if C_t decays faster than $\propto t^{-1}$. C_t is the double-time correlation function [31, 32, 58, 59] defined as

$$C_{|s-l|} = \langle \delta \ln B(x_s), \delta \ln B(x_l) \rangle \quad (1.35)$$

Note that $C_{|s-l|}$ can be evaluated using eq (1.17). One has to put $V = W = \delta \ln B = \ln B - \lambda_0$ and $t = |s - l|$

For $q \rightarrow 0$, one obtains

$$\lambda_q = \lambda_0 + Dq \quad (1.36)$$

and for $t \gg \tau$

$$\langle A_t^q \rangle \propto \exp\{q(\lambda_0 + Dq)t\} \quad (1.37)$$

Assuming that $\lambda_{\pm\infty}$ exists, and furthermore that λ_q can be expanded as

$$\lambda_q = \lambda_{\theta\infty} - \lambda'_\theta q^{-1} + O(q^{-1}), \quad (1.38)$$

as $q \rightarrow \theta\infty$, ($\theta = \pm$), where λ'_θ is defined by $\lambda'_\theta = \lim_{q \rightarrow \theta\infty} \frac{d\lambda_q}{dq^{-1}}$ and is non-negative because of eq (1.29). Hence the q order moment is asymptotically given

by ($t \rightarrow \infty$ and $q \rightarrow 0$)

$$\langle A_t^q \rangle \propto \exp\{(\lambda_{\theta\infty} q - \lambda'_\theta)t\} \quad (1.39)$$

Note that the asymptotic form (1.38) is quite different from (1.31). These behaviors have a close connection with the violation of the Gaussian approximation for the probability distribution.

1.2.2 Probability density function (PDF).

From eq(1.25), we get

$$\ln A_{t+1} = \ln A_t + \ln B(x_t), \quad (1.40)$$

which can be integrated to yield $\ln A_t = \sum_{s=0}^{t-1} \ln B(x_s)$. If $\ln A_t$ is assumed to be Gaussian (the central limit theorem) as $t \rightarrow \infty$, the distribution for A_t takes the log-normal form [55, 60]

$$P(a, t) \simeq \frac{1}{\sqrt{2\pi}\sigma_t a} \exp\left\{-\frac{(\ln a - \lambda_0 t)^2}{2\sigma_t}\right\} \quad (1.41)$$

as $t \rightarrow \infty$. The q -order moment evaluated using the above PDF is

$$\langle A_t^q \rangle \simeq \exp(q\lambda_0 t + \sigma_t q^2/2) \propto \exp\{q(\lambda_0 + Dq)t\}. \quad (1.42)$$

Here we used $\sigma_t \simeq 2Dt$ for $t \gg \tau$. This indicates that λ_q takes the form (1.36) independently of q . Conversely, we can say that eqs.(1.36) and (1.37) will be valid if the probability density function (PDF) of $\ln A_t$ is Gaussian, which happens when the PDF of $\ln B(x_t)$ is Gaussian. But, usually the PDF of $\ln B(x_t)$ is not Gaussian. Even then, the PDF of $\ln A_t$ is approximately Gaussian due to central limit theorem, though it also has a non-Gaussian component. The first two terms in the expansion of λ_q can be attributed to the effect of Gaussian compo-

ment of the PDF. Which of the two component, Gaussian or non-Gaussian, will show its effect, depends on the value of q . Note that λ_q reduces to the form (1.36) when $|q| < b$, b being the convergence radius. In this range of q , one can ~~assume~~ assume Gaussian approximation for the PDF and moments $\langle A_t^q \rangle$ are given almost exactly by eq.(1.37). On the contrary, for $|q| > b$, λ_q is given by eq.(1.38) and $\langle A_t^q \rangle$ by eq.(1.39). Gaussian approximation for the PDF can no longer be assumed in this case. This finding can be explained further in the following way. The temporal evolution of $(B(x_t))^q$ strongly depends on q . When $|q| < b$, the fluctuations in $(B(x_t))^q$ get suppressed. As such the non-Gaussian character of $\ln A_t$ (resulting from fluctuations of $\ln B(x_t)$) does not become apparent. Central limit theorem gives moments almost exactly. For $|q| > b$, fluctuations in $(B(x_t))^q$ get amplified. Non-Gaussian character of $\ln A_t$ become conspicuous now and the moments deviate from (1.37) and behave like (1.39). That is, asymptotic laws for lower order moments are not valid for higher order moments. Amplitude fluctuations in $B(x_t)$ (equivalently in $\ln A_t$) is called intermittency.

Here after the regions of q called corresponding to (1.31) and (1.38) will be called diffusion and intermittency branch. Their boundaries can be estimated roughly as $q_\theta = \frac{\lambda_{\theta\infty} - \lambda_0}{D}$, ($\theta = \pm$)

It should be noted that the intermittency mentioned above is slightly different from that discussed by Manneville and Pomeau (See section 1.1.4). They use the word in relation to the dynamics $x_{t+1} = f(x_t)$, as a route by which x_t becomes chaotic. Here we mean the intermittency of $B(x_t)$ (or $\ln A_t$) which is a function of x_t which we assume, is already chaotic.

1.2.3 Exponents μ and σ .

To analyse deviation from Gaussian PDF, Fujisaka et al put forward exponents μ and σ . They are defined in relation to the dimensionless structure function [61].

$$\theta_q(t) \equiv \langle A_t^q \rangle / \langle A_t^2 \rangle^{q/2} \quad \theta_2(t) = 1. \quad (1.43)$$

From eq (1.28) $\theta_q(t) \propto \exp\{q(\lambda_q - \lambda_2)t\}$. $\theta_q(t) \rightarrow \infty$ both for $q < 0$ and $q > 2$, and $\theta_q(t) \rightarrow 0$ for $0 < q < 2$, as $t \rightarrow \infty$. Skewness S and flatness F are equal to θ_3 and θ_4 respectively. Exponents μ and σ are defined through

$$\langle A_t^2 \rangle \simeq \langle A_t^1 \rangle^2 e^{\mu t}, \quad S \sim F^\sigma \quad (1.44)$$

In terms of λ_q , they are given by

$$\mu = 2(\lambda_2 - \lambda_1), \quad \sigma = 3(\lambda_3 - \lambda_2)/4(\lambda_4 - \lambda_2). \quad (1.45)$$

which are non negative.

Diffusion branch approximation for $q = 1 \sim 4$ gives the limiting values

$$\mu = 2D, \quad \sigma = 3/8 \quad (1.46)$$

On the other hand, if we assume intermittency branch approximation for $q = 1 \sim 4$, the limiting values are

$$\mu = \lambda'_+, \quad \sigma = 1/2, \quad (1.47)$$

Comparison of μ and σ with the limiting values, enables us to find the range of parameter in $f(x)$, for which $q = 1 \sim 4$ will be in the diffusion branch. For this range of q , PDF of $\ln A_t$ can be assumed to be Gaussian.

1.2.4 Fluctuation spectrum $\sigma(\alpha)$.

In eq. (1.25), we defined the dynamics of A_t . Equivalently, one can consider the dynamics of the local time average α_t of a time series

$$\{u_j\} = u_0, u_1, u_2 \quad (1.48)$$

$$\alpha_t = \frac{1}{t} \sum_{j=0}^{t-1} u_j \quad (1.49)$$

where

$$u_j = u(x_j) = \ln B(x_j) \quad (1.50)$$

Characteristic function λ_q (eq (1.27)) is defined as [47, 49–54].

$$\lambda_q = \frac{1}{q} \lim_{t \rightarrow \infty} \frac{1}{t} \ln \langle \exp(qt\alpha_t) \rangle \quad (1.51)$$

The long time average $\alpha_\infty = \lim_{t \rightarrow \infty} \frac{1}{t} \sum_{j=0}^{t-1} u_j$ is no longer a fluctuating quantity. Note that it is equal to λ_0 , the drift velocity. Similarly, the diffusion coefficient D can be related to the variance of α_t through

$$\langle (\alpha_t - \alpha_\infty)^2 \rangle \simeq \frac{2D}{t} \quad (1.52)$$

Let $P_t(\alpha)$ represent the probability that α_t takes values between α and $\alpha + d\alpha$. This is related to the fluctuation spectrum $\sigma(\alpha)$ through [52, 54]

$$P_t(\alpha) \sim \sqrt{t} \exp[-\sigma(\alpha)t] \quad (1.53)$$

In some references the factor \sqrt{t} is not shown, it being part of normalization constant and also independent of α . Note that $P_t(\alpha) \rightarrow \delta(\alpha - \alpha_\infty)$ as $t \rightarrow \infty$. $P_t(\alpha)$ is related to λ_q as [47, 52–54]

$$\lambda_q = -\frac{1}{q} \min_\alpha [\sigma(\alpha) - q\alpha] \quad (1.54)$$

by employing the saddle point technique. This is equivalent to Legendre transform

$$\alpha = \frac{d(q\lambda_q)}{dq}, \quad \sigma(\alpha) = q^2 \frac{d\lambda_q}{dq} \quad (1.55)$$

It can be easily proved that [53]

$$\frac{d\alpha}{dq} \geq 0, \quad \frac{d^2\sigma(\alpha)}{d\alpha^2} > 0. \quad (1.56)$$

when $q = 0$, we get $\sigma = 0$ at $\alpha = \alpha_\infty = \lambda_0$. This is the single minimal value of $\sigma(\alpha)$.

For $|q| < b$ the asymptotic law (1.36) gives

$$\alpha = \lambda_0 + 2Dq \quad (1.57)$$

$$\sigma(\alpha) = \frac{(\alpha - \lambda_0)^2}{4D}. \quad (1.58)$$

The parabola (1.58) agrees with the central limit theorem result and is valid for $|\alpha - \lambda_0| \ll |\alpha(q = b) - \lambda_0|$. On the other hand, for $\theta q \gg b$, ($\theta = \pm$), we generally get

$$\lambda_q \simeq \lambda_{\theta\infty} - \frac{1}{q} \left[\frac{1}{\tau_\theta} - c_\theta \exp(-\eta_\theta |q|) \right] \quad (1.59)$$

where τ_θ , c_θ , and η_θ are positive constants. Its Legendre transformation gives

$$\alpha \simeq \lambda_{\theta\infty} - \theta c_\theta \eta_\theta \exp(-\eta_\theta |q|), \quad (1.60)$$

$$\sigma(\alpha) \simeq \frac{1}{\tau_\theta} - \frac{1}{\eta_\theta} |\alpha - \lambda_{\theta\infty}| \ln \left[\frac{a_\theta}{|\alpha - \lambda_{\theta\infty}|} \right] \quad (1.61)$$

where $\eta_\theta \sim O(1/b)$ and $a_\theta \equiv e c_\theta \eta_\theta$. The derivative $d\sigma(\alpha)/d\alpha$ logarithmically diverges as $\alpha \rightarrow \lambda_{\theta\infty}$.

The existence of the convergence radius b means that the statistical characteristics described with λ_q can be, roughly speaking, divided into three types $q \ll -b$; $|q| \ll b$; $q \gg b$, which can never be perturbatively connected to each other. In the sense that the parameter q selectively singles out the statistical characteristics relevant to it, it is called the filtering parameter.

1.2.5 Evaluation of characteristic function λ_q .

For evaluating λ_q one can use the linear operator defined by Mori et al (Section 1.1.1). Using eqns (1.19), (1.27), we get [43]

$$\lambda_q = q^{-1} \lim_{t \rightarrow \infty} t^{-1} \ln \langle (B(x))^q \underbrace{\hat{H}(B(x))^q}_{t^{-1}} \hat{H}(B(x))^q \rangle \quad (1.62)$$

If $\hat{H}(B(x))^q$ is a constant for the entire range of x ($0 \leq x < 1$), evaluation of λ_q using the above equation becomes trivial as in the case of Bernoulli map [43]. If this is not the case, one can get λ_q using the linear operator H_q defined as [49–53]

$$\begin{aligned} H_q G(x) &= \int_0^1 \delta(f(y) - x) e^{qu(y)} G(y) dy \\ &= H[\epsilon^{qu(x)} G(x)] \end{aligned} \quad (1.63)$$

with $H_0 = H$. From equations (1.25) and (1.63), it is easy to prove that

$$\langle .A_t^q \rangle = \int_0^1 [H_q]^t \rho(x) dx \quad (1.64)$$

Consider the eigen value equation of H_q

$$H_q \psi_q^{(n)}(x) = \phi_q^{(n)} \psi_q^{(n)}(x) \quad n = 0, 1, 2, \quad N \quad (1.65)$$

Let

$$\phi_q^{(0)} > |\phi_q^{(1)}| \geq |\phi_q^{(2)}| \quad (1.66)$$

Using equations (1.27), (1.64) we note that the characteristic function λ_q can be obtained as

$$\lambda_q = \frac{1}{q} \ln \phi_q^{(0)} \quad (1.67)$$

where $\phi_q^{(0)} = \max_n \{ \text{Re} \phi_q^{(n)} \}$. It is easy to prove that $\phi_q^{(0)}$ is not degenerate [51]. The meaning of other eigen values is pointed out in the next subsection.

1.2.6 Order q time correlation function $Q_t^{(q)}$.

So far nothing has been mentioned about $Q_t^{(q)}$, the function appearing in eq (1.28). For asymptotic behaviour, it is insignificant as $\lim_{t \rightarrow \infty} t^{-1} \ln Q_t^{(q)} = 0$. It depends on time only very slowly. One can find that λ_q describes the most dominant, ie. global behaviour of $\langle A_t^q \rangle$ while the non-global characteristics are contained in $Q_t^{(q)}$ [49–52]. Suppose $\{u_j\}$ is purely stochastic. Then $Q_t^{(q)} = 1$. If $\{u_j\}$ is periodic, then $Q_t^{(q)}$ is periodic with the same period. For a general chaotic dynamics $Q_t^{(q)}$ is neither unity nor a periodic function and contains information different from that in λ_q . It is known as order q time correlation function. It provides information regarding the temporal correlations in $\{u_j\}$. $Q_t^{(q)}$ can be expanded as [49–52]

$$Q_t^{(q)} = J_q^{(0)} + \sum'_n J_q^{(n)} e^{-(\gamma_q^{(n)} + iw_q^{(n)})t} \quad (1.68)$$

where

$$J_q^{(n)} = s_q^{(n)} \int_0^1 \psi_q^{(n)}(x) dx \quad (1.69)$$

$s_q^{(n)}$ being the expansion coefficients appearing in the expansion of $\rho(x)$

$$\rho(x) = \sum_{n=0}^N s_q^{(n)} \psi_q^{(n)}(x) \quad (1.70)$$

\sum'_n denotes the summation except $n = 0$. $\gamma_q^{(n)}$ and $w_q^{(n)}$ satisfy

$$\frac{\phi_q^{(n)}}{\phi_q^{(0)}} = e^{-(\gamma_q^{(n)} + iw_q^{(n)})} \quad (1.71)$$

$\{w_q^{(n)}\}$ and $\{\gamma_q^{(n)}\}$ are the sets of characteristic frequencies and decay rates of motions embedded in $\{u_j\}$.

1.2.7 Thermodynamic formalism: connection with other theories.

From the relations between q , λ_q , α and $\sigma(\alpha)$, one can note that these quantities are corresponding respectively to inverse temperature ($= \frac{1}{k_B T}$ with the Boltzmann constant k_B and the temperature T of the system), the Helmholtz free energy, the internal energy and entropy in thermodynamics. Hence the fluctuation spectrum theory is called a thermodynamic formalism [7, 14, 62–70]. It can be noticed further that the present approach has some similarity with some other theories on chaotic dynamics. Special reference is to be made of (1) multifractal theory [11–15] (2) velocity structure functions in developed turbulence [71]. These theories also aim at global characterization. They are also thermodynamic formalisms. In literature one can find a number of related works on strange attractors [2, 3], diffusion limited aggregations [72,73] and time correlations of intermittent maps [76]. Feigenbaum et al [4] have tried to study the correlations in strange objects in connection with global characterization. This is similar to the time correlation function discussed in the previous section. In ref [74, 75] one can find a similar approach to fluctuations utilizing the concept of generalized entropy.

1.3 Cycle expansion.

Cycle expansion [7, 62–64, 77–81] provides perturbation theory for chaotic systems of low dimensional phase space. The essence of this method is to express averages over chaotic orbits in terms of unstable short periodic orbits. The importance of periodic orbits has been already noted in the mathematical works on dynamical systems [1, 82]. Cycle expansion is actually the physics application of

the dynamical systems theory developed in [62–64, 80, 81].

Cycle expansion is an expansion on the dynamical ζ function of a dynamical system, which is obtained by the transfer operator technique. Transfer operator L is a linear evolution operator of the system which determines the evolution of the system under the deterministic map $x_{t+1} = f(x_t)$. The evolution operator used in the evaluation of the escape rate of a repeller is an example. The kernel of escape rate of a repeller is [77,79]

$$L(y, x) = \delta(y - f(x)). \quad (1.72)$$

Since the evolution of the system is completely determined by L , the evaluation of its eigen spectrum is the most important issue in the discussion of its dynamical properties. The eigen spectrum of L is related to the following determinant:

$$\begin{aligned} \det(1 - zL) &= \exp[\text{tr} \ln(1 - zL)] \\ &= \exp \left[- \sum_{n=1}^{\infty} \frac{z^n}{n} \text{tr}(L^n) \right] \end{aligned} \quad (1.73)$$

Due to the fact that $\text{tr}(L^n)$ picks up contributions from all repeats of prime cycles p (prime cycle explained below)

$$\text{tr}(L^n) = \sum_{n_p|n} n_p t_p^{n/n_p}, \quad (1.74)$$

where $n_p|n$ denotes that n_p is a divisor of n . The above determinant can be rewritten as

$$\det(1 - zL) = \prod_p (1 - z^{n_p} t_p). \quad (1.75)$$

In eq (1.75) all prime cycles p should appear in the product. The dynamical ζ function is defined as

$$\zeta^{-1}(z) = \det(1 - zL) = \prod_p(1 - T_p). \quad (1.76)$$

where $T_p = z^{n_p} t_p$. Eq (1.76) is exact and no approximation has been used up to this point. It is now clear that the eigen spectrum of L can be obtained from the zeros of ζ^{-1}

To show how cycle expansion can be done, we expand the Euler product (1.76)

$$\begin{aligned} \zeta^{-1} &= \prod_p(1 - T_p) = 1 - \sum_{p_1 p_2 \dots p_k} T_{p_1 + p_2 + \dots + p_k}, \\ T_{p_1 + p_2 + \dots + p_k} &= (-1)^{k+1} T_{p_1} T_{p_2} \dots T_{p_k} \end{aligned} \quad (1.77)$$

One may be tempted to think that the value of z should be very small so that the infinite sum makes sense. Actually this is not necessary, because the infinite sum will be truncated to a finite sum due to cancellation. To show how cancellation occurs, we take the example of the binary dynamics generated by a tent map. We have,

$$\begin{aligned} \zeta^{-1} &= (1 - T_0)(1 - T_1)(1 - T_{10})(1 - T_{100}) \dots \\ &= 1 - T_0 - T_1 - T_{10} - T_{100} - T_{110} \dots - T_{0+1} - T_{0+01} - \dots \end{aligned} \quad (1.78)$$

where the prime cycles are denoted by the symbolic sequences of two unrestricted symbols $\{0, 1\}$. A prime cycle is a single traversal of the orbit; its label is a non-repeating symbol string. There is only one prime cycle for each cyclic permutation class. For example $p = \overline{0011} = \overline{1001} = \overline{1100} = \overline{0110}$ is prime but $\overline{0101} = \overline{01}$ is not prime (bar denotes a symbol sequence with infinitely repeating basic block). The reorganization is done by grouping the terms of the same total symbol string

length

$$\zeta^{-1} = 1 - T_0 - T_1 - [T_{01} - T_0T_1] - [(T_{100} - T_{10}T_0) + (T_{101} - T_{10}T_1)] - \quad (1.79)$$

It is obvious in this expansion that T_0 and T_1 are the most important quantities since all longer orbits can be pieced together from them approximately. All the periodic orbits which cannot be approximated by shorter orbits are called fundamental cycles. In the above example, the fundamental cycles are T_0 and T_1 . The terms of the same total length which are grouped together in the brackets of (1.79) are called the curvature corrections c_n , where n denotes the total length. If all curvature corrections vanish, then ζ^{-1} is exactly given in terms of the fundamental cycles and this is the spirit of cycle expansion. For the case in which c_n are non vanishing, cycle expansion provides a systematic way to carry out corrections. For the case of binary dynamics generated by the tent map, it can be shown that all curvature corrections vanish identically. This is due to the uniform slope of line segments. In fact for all simple cases such as piecewise linear mapping the cancellation is exact.

In the case of binary dynamics generated by a tent map, all sequences of symbols in the alphabet $\{0, 1\}$ can be realised as a physical trajectory. The symbolic dynamics, in this case, is described by a complete unrestricted grammar. If some sequences are not allowed, we say that the symbolic dynamics is ‘pruned’. The word is suggested by ‘pruning’ of the branches corresponding to forbidden sequences for symbolic dynamics organised by a hierarchical tree. In such cases, the alphabet must be supplemented by a set of pruning rules which is called pruning grammar.

Cycle expansion provides a powerful tool for the analysis of deterministic chaos. For illustrating various aspects of the technique, Artuso et al have applied it [78] to a series of low-dimensional dynamically generated strange sets: the

skew Ulam map, the period-doubling repeller, the Henon-type strange sets and the irrational winding set for circle maps. Cycle expansion can be used for evaluating the decay rates of time correlations in chaotic dynamical systems [79]. Recently, many authors have applied this technique to evaluate exact diffusion coefficient in spatially extended maps exhibiting deterministic diffusion [95–97].

There is a connection between the cycle expansion technique and Fujisaka's characteristic function method. Exploiting this connection we found that the applicability of the cycle expansion for analysing chaos-induced diffusion systems can be enhanced. This work forms the subject matter of chapter 5.

Chapter 2.

Statistics of trajectory separation in one-dimensional maps.

2.1 Introduction.

One-dimensional transformations have proved to be useful for discovering and understanding properties of Hamiltonian systems and dissipate dynamical systems. Outstanding examples are Bernoulli shifts and β transformations in ergodic theory [29, 83], and the Henon dissipative mapping [19] and logistic model [16–18] for the onset of fluid turbulence. These have led to a deeper understanding of chaotic orbits and also to the discovery of new dynamic scaling laws in the vicinity of transition points [5, 17, 84, 85]. They are the simplest systems capable of chaotic motion. Piecewise linear maps, in particular, are very useful models for explaining the mechanisms leading to deterministic chaos [5, 6].

For one-dimensional map of the form:

$$x_{t+1} = f(x_t), \quad t = 0, 1, 2, \quad (0 < x_t < 1). \quad (2.1)$$

the distance between nearby trajectories evolves in time as

$$d_{t+1} = |f'(x_t)|d_t + O(d_t^2) \quad (2.2)$$

d_t exponentially grows in course of time, on the average, with the rate λ , the Lyapunov exponent (see subsection 1.1.1) when it is positive. The trajectory becomes unstable and is called chaotic. If λ is negative then d_t exponentially shrinks in the course of time and the trajectory is stable. Since the local expansion rate (LER) $\ln |f'(x_t)|$ [7, 53–55, 88] strongly depends on the phase point x_t , the trajectory separation fluctuates from

$$d_t = d_0 e^{\lambda t} + O(d_0^2), \quad (2.3)$$

d_0 being the initial separation. Fujisaka and coworkers [55] have shown that these fluctuations will produce a diffusion in the temporal evolution of trajectory separation. The probability density function (PDF) of trajectory separation for large t will be approximately log-normal according to central limit theorem. Equivalently, the PDF of the logarithmic separation will be Gaussian [43, 53, 55, 88]. It is this Gaussian component of PDF which leads to the diffusion of logarithmic distance between trajectories. Non-Gaussian component results from intermittency (in time) of the above stochastic process. This diffusion and intermittency are complementary aspects. This nature of trajectory separation is a matter of great theoretical interest as it arises in all one-dimensional maps [7, 53–55, 86–88].

In this chapter, we study the statistics of trajectory separation for a period-three boundary map (PTB Map). The motivations are the following:

- (i) It is a piecewise linear map and hence can be studied analytically. The study of trajectory separation of this map can bring out the relevant conditions for the validity of log-normal approximation for PDF. The result will be applicable to a class of $1 - D$ maps conjugate to the PTB map. This map

has a step like invariant density. So the result will not be influenced by the uniformity of the invariant density.

- (ii) The inference can be extended to stochastic motion in spatially extended maps [5, 24, 57, 58, 89–106]. Deterministic diffusion generated by such maps can account for the behavior of Josephson junctions [107–109] and of parametrically driven oscillators [110].
- (iii) It can provide a mathematical model to any chaotic series exhibiting deterministic diffusion. It can have applications in physical systems like Brownian motion.

We use Fujisaka's general theory based on characteristic function [43–54] to discuss the above dynamics. In Section 2.2, we describe how this can be done. In section 2.3, we consider the statistics of trajectory separation for the PTB map. Exact expressions for characteristic function and diffusion coefficient are obtained. Though we use the method suggested by Fujisaka, the procedure by which characteristic function is evaluated has not been reported so far. In section 2.3, the statistical quantities like moments and PDF are also got. To study variation from Gaussian character we evaluate the exponents μ and σ defined in subsection 1.2.3. In section 2.4 we analyse the results and discuss the significance and applications.

2.2 Statistics of trajectory separation in one-dimensional maps: Characteristic function method.

For every one dimensional map (eq. (2.1)) if we start with the nearby trajectory $d_0 (\ll 1)$ at the initial time, d_t becomes of the order of unity at the saturation time $t_s (\approx \lambda^{-1} \ln d_0^{-1})$. In the time range $0 < t < t_s$, $\ln d_t$ linearly depends on time, on the average, slope being equal to λ . For $t \geq t_s$, d_t is bounded by the scale of the

state space (≈ 1). In statistics of trajectory separation, we study the fluctuation effect of local expansion rates $\ln |f'(x)|$ on the dynamical behavior of d_t in the above time range [55]. In the limit, $d_0 \rightarrow 0$ the dynamics (2.2) can be written as

$$L_{t+1} = |f'(x_t)|L_t \quad (2.4)$$

Using L_t instead of d_t corresponds to taking the limit $t_s \rightarrow \infty$ as $d_0 \rightarrow 0$ i.e. there does not occur any cutoff time. Therefore if we neglect fluctuations of local expansion rates, we will get $L_t \propto e^{\lambda t}$ till $t = \infty$

Equation(2.4) can be integrated to yield

$$\ln L_t = \ln L_0 + \sum_{s=0}^{t-1} \ln |f'(x_s)|, \quad t > 0 \quad (2.5)$$

with the initial distance L_0 . Since x_t is uniquely determined by x_0 , L_t is also a unique function of x_0 . Therefore the average evolution of (2.5) is given by

$$\langle \ln L_t \rangle = \ln L_0 + \lambda t \quad (2.6)$$

where $\langle \cdot \rangle$ is the average over a steady ensemble $\rho(x)$ (invariant density). Note that λ , the Lyapunov exponent can be written as

$$\lambda = \frac{\langle \ln(L_t/L_0) \rangle}{t} = \langle \ln |f'(x)| \rangle \quad (2.7)$$

The fluctuation of $\ln L_t$ from the average motion(2.6) is measured with variance

$$\sigma_t = \langle (\ln L_t - \langle \ln L_t \rangle)^2 \rangle \quad (2.8)$$

This variance can be shown to be proportional to t for $t > \tau$, τ being the correlation time of $\ln |f'(x_t)|$ [55]. Hence we can define a diffusion coefficient D for $\ln L_t$ as

$$D = \lim_{t \rightarrow \infty} \frac{\sigma_t}{2t}, \quad t > \tau \quad (2.9)$$

This is similar to the deterministic diffusion studied in spatially extended maps by several authors [5, 24, 57, 58, 89–106].

Referring to section 1.2, it is quite easy to note that the dynamics (2.4) can be studied using Fujisaka's characteristic function method. In eq. 1.25 we have to make the substitutions

$$A_t = L_t; B(x) = |f'(x)| \quad (2.10)$$

The assumption $L_0 = 1$ will only change the scale of trajectory separation. Note that in this case λ_0 (characteristic function λ_q with $q = 0$) will become equal to the Lyapunov exponent λ (eq (2.7)). D is the diffusion coefficient of $\ln L_t$, the logarithmic separation between nearby trajectories. Variation from Gaussian character of the PDF can be analysed using exponents μ and σ introduced in subsection 1.2.3.

2.3 Statistics of trajectory separation for the period-three boundary map.

2.3.1 Characteristic function and diffusion coefficient:

In this section, we consider the statistics of trajectory separation for the period-three boundary map (figure 2.1) defined by

$$f(x) = \begin{cases} [\frac{(1-c)}{c}]x + c & (0 \leq x \leq c), \\ [\frac{1}{(1-c)}](1-x) & (c < x \leq 1). \end{cases} \quad (2.11)$$

The three points, $c, 1, 0$ are periodic points of period three, satisfying $x = f^{(3)}(x)$. In subsection 1.1.1 we defined the operator H as

$$HG(x) = \int_{\Omega} dy G(y) \delta(f(y) - x) = \sum G(y_i) / |f'(y_i)| \quad (2.12)$$

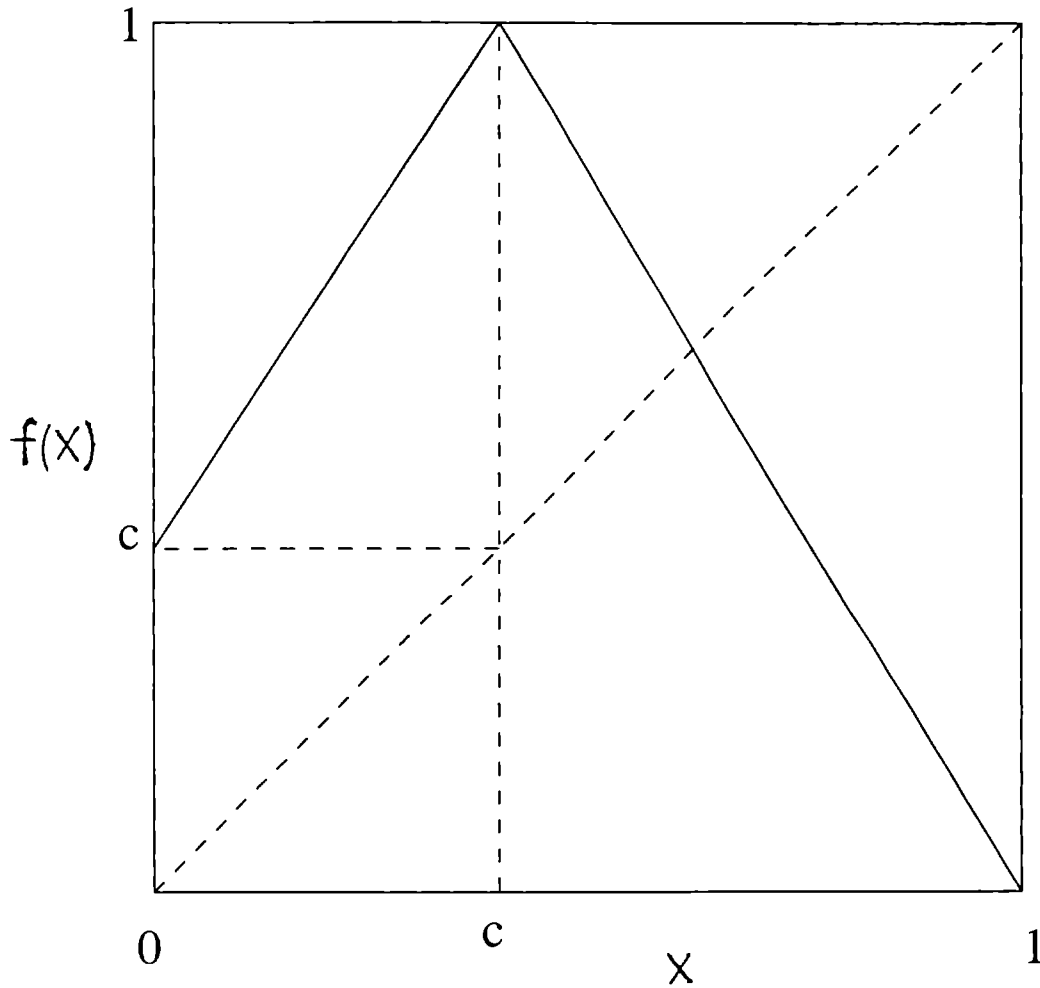


Figure 2.1: A transformation with the period-three boundary (PTB map) $-f(x)$ vs x . On both axes units are arbitrary.

y_i is the i th solution of $f(y_i) = x$ in the attractor Ω . For the PTB map.

$$HG(x) = \begin{cases} (1-c)G(y_2), & (0 \leq x \leq c) \\ [\frac{c}{(1-c)}]G(y_1) + (1-c)G(y_2), & (c < x \leq 1), \end{cases} \quad (2.13)$$

where

$$y_1 = [\frac{c}{(1-c)}](x-c); \quad y_2 = 1 - (1-c)x \quad (2.14)$$

Invariant density $\rho(x)$ is given by

$$H\rho(x) = \rho(x) \quad (2.15)$$

Eq. (2.13) leads to a step-like invariant density

$$\rho(x) = \begin{cases} \frac{1}{(1-c)}, & (0 \leq x \leq c), \\ \frac{1}{(1-c^2)}, & (c < x \leq 1) \end{cases} \quad (2.16)$$

Lyapunov exponent becomes

$$\lambda_0 = \langle \ln |f'(x)| \rangle = \left[\frac{1}{(1+c)} \right] \{-c \ln c - (1-c) \ln(1-c)\} \quad (2.17)$$

Since $\lambda_0 > 0$ the PTB map will produce trajectory instability.

For evaluating λ_q we use the linear operator introduced by Mori et al (subsection 1.1.1). The linear operator in eq. (1.19) takes the form

$$\widehat{H}G(x) = \begin{cases} G(y_2), & (0 \leq x \leq c) \\ cG(y_1) + (1-c)G(y_2), & (c < x \leq 1) \end{cases} \quad (2.18)$$

From the above equation, we note that $\widehat{H}|f'(x)|^q$ is not a constant for the entire range of x . When $\widehat{H}|f'(x)|^q$ is constant, the evaluation of λ_q using eq.(1.62) will become trivial, as in the case of Bernoulli map [43]. One can show that for

a tent map also this is the case. In fact, tent map gives the same result as the Bernoulli map. In contrast to these trivial cases, the PTB map produces temporal correlations. Referring to subsection 1.2.5, we note that usually in such cases one has to solve the eigen value equation for the linear operator H_q for evaluating λ_q . However, here we show a new procedure for getting λ_q using \widehat{H} (eq (2.18)) in eq (1.62).

Let us denote the function inside the expectation sign $\langle \cdot \rangle$ in eq. (1.62) by F_t . We note that it will be a step function for all t . Let $F_t(1)$ and $F_t(2)$ denote the values of this function for $0 \leq x \leq c$ and $c < x \leq 1$ respectively

$$F_1(1) = \left[\frac{1-c}{c} \right]^q, F_1(2) = \left[\frac{1}{1-c} \right]^q \quad (2.19)$$

First we show that $F_1(1) > F_1(2)$ guarantees $F_t(1) > F_t(2)$ by mathematical induction. Assume $F_t(1) > F_t(2) \Rightarrow F_{t+1}(1) > F_{t+1}(2)$. We can prove $F_{t+2}(1) > F_{t+2}(2)$.

$$\begin{aligned} F_{t+1}(1) &= |f'(x)|^q \widehat{H} F_t. \quad (0 \leq x \leq c) \\ &= \left(\frac{1-c}{c} \right)^q F_t(y_2) = \left(\frac{1-c}{c} \right)^q F_t(2) \end{aligned} \quad (2.20)$$

since $c < y_2 < 1$. Similarly,

$$\begin{aligned} F_{t+1}(2) &= \left(\frac{1}{1-c} \right)^q [cF_t(y_1) + (1-c)F_t(y_2)] \\ &= \left(\frac{1}{1-c} \right)^q [cF_t(1) + (1-c)F_t(2)], \quad (0 < y_1 < c) \end{aligned} \quad (2.21)$$

$$F_{t+2}(1) = \left(\frac{1-c}{c} \right)^q \left(\frac{1}{1-c} \right)^q [cF_t(1) + (1-c)F_t(2)] \quad (2.22)$$

$$F_{t+2}(2) = \left(\frac{1}{1-c}\right)^q \times \left\{ c \left(\frac{1-c}{c}\right)^q F_t(2) + (1-c) \left(\frac{1}{1-c}\right)^q [cF_t(1) + (1-c)F_t(2)] \right\} \quad (2.23)$$

Using assumed condition, we note

$$F_{t+2}(1) - F_{t+2}(2) > \left(\frac{1-c}{c}\right)^q \left(\frac{1}{1-c}\right)^q [cF_t(1) + (1-c)F_t(2)] - \left(\frac{1}{1-c}\right)^q \left[c \left(\frac{1-c}{c}\right)^q F_t(2) + (1-c) \left(\frac{1-c}{c}\right)^q F_t(2) \right] > 0 \quad (2.24)$$

The proof will be complete if $F_1(1) > F_1(2) \Rightarrow F_2(1) > F_2(2)$. This can be easily verified. Similarly, we can prove $F_1(1) < F_1(2) \Rightarrow F_t(1) < F_t(2)$ and $F_1(1) = F_1(2) \Rightarrow F_t(1) = F_t(2)$. Using $\rho(x)$, the expectation value $\langle F_t \rangle$ appearing in eq.(1.62) can be written as

$$\langle F_t \rangle = \frac{c}{(1+c)} F_t(1) + \frac{1}{(1+c)} F_t(2) \quad (2.25)$$

$t = t + 1$ gives

$$\langle F_{t+1} \rangle = \left(\frac{c}{1+c}\right) \left(\frac{1-c}{c}\right)^q F_t(2) + \frac{1}{1+c} \left(\frac{1}{1-c}\right)^q [cF_t(1) + (1-c)F_t(2)] \quad (2.26)$$

Some rearrangement will give us

$$\begin{aligned} \langle F_{t+1} \rangle &= \frac{1}{(1+c)} \left[c \left(\frac{1-c}{c}\right)^q + \left(\frac{1}{(1-c)}\right)^q \right] \\ &\quad \times \frac{1}{(1+c)} [cF_t(1) + F_t(2)] \\ &\quad \times \left\{ 1 - c^2 \left[\frac{\left(\frac{1}{1-c}\right)^q - \left(\frac{1-c}{c}\right)^q}{\left(\frac{1}{1-c}\right)^q + c \left(\frac{1-c}{c}\right)^q} \right] \left[\frac{F_t(2) - F_t(1)}{F_t(2) + cF_t(1)} \right] \right\} \quad (2.27) \end{aligned}$$

From results obtained above, we note the quantity inside the curly bracket will be less than 1, when $\left(\frac{1}{1-c}\right)^q \neq \left(\frac{1-c}{c}\right)^q$. It will be equal to 1 when $\left(\frac{1}{1-c}\right)^q = \left(\frac{1-c}{c}\right)^q$. Using results obtained above, we note

$$\langle F_{t+1} \rangle = \frac{1}{(1+c)} \left[c \left(\frac{1-c}{c} \right)^q + \left(\frac{1}{1-c} \right)^q \right] \langle F_t \rangle (1 - \chi_t), \quad (0 \leq \chi_t < 1) \quad (2.28)$$

This gives

$$\langle F_t \rangle = \left\{ \frac{1}{(1+c)} \left[c \left(\frac{1-c}{c} \right)^q + \left(\frac{1}{1-c} \right)^q \right] \right\}^t \Theta, \quad (0 < \Theta \leq 1), \quad (2.29)$$

where

$$\Theta = \prod_{i=1}^{t-1} (1 - \chi_i). \quad (2.30)$$

Eqs. (1.62) and (2.29) give

$$\lambda_q = \frac{1}{q} \lim_{t \rightarrow \infty} \frac{1}{t} \ln \langle F_t \rangle = \frac{1}{q} \ln \frac{1}{(1+c)} \left[c \left(\frac{1-c}{c} \right)^q + \left(\frac{1}{1-c} \right)^q \right] + \frac{1}{q} \lim_{t \rightarrow \infty} \frac{1}{t} \ln \Theta \quad (2.31)$$

Since $\langle F_t \rangle$ is the expectation value of absolute quantities, we note from eq. (2.29) that Θ will not tend to zero as $t \rightarrow \infty$, $0 < \Theta \leq 1$. Therefore,

$$\lim_{t \rightarrow \infty} \frac{1}{t} \ln \Theta = 0 \quad (2.32)$$

We provide a rigorous mathematical proof for this in the Appendix A. It may be noted that Θ in the above equation is the same as $Q_t^{(q)}$ in eq.(1.28) and is relevant to the correlations in $|f'(x_s)|$. The above equation actually proves that $\lim_{t \rightarrow \infty} \frac{1}{t} \ln Q_t^{(q)} = 0$, for the present case. One can put $Q_t^{(q)} \approx 1$ for large values of t . Thus

$$\lambda_q = \frac{1}{q} \ln \frac{1}{(1+c)} \left[c \left(\frac{1-c}{c} \right)^q + \left(\frac{1}{1-c} \right)^q \right] \quad (2.33)$$

Lyapunov exponent $\lambda_0 (= \lim_{q \rightarrow 0} \lambda_q)$ evaluated from λ_q agrees with eq.(2.17)

as it should. This shows the correctness of λ_q . A lengthy calculation gives the diffusion coefficient $D \left(= \lim_{q \rightarrow 0} \frac{d\lambda_q}{dq} \right)$,

$$D = \frac{c}{2} \left\{ \frac{1}{(1+c)} \ln \left[\frac{(1-c)^2}{c} \right] \right\}^2 \quad (2.34)$$

2.3.2 Moments and probability density function:

Asymptotic law for moments as $|q| \rightarrow 0$ can be obtained by substituting λ_0 and D in eq.(1.37)

$$\langle L_t^q \rangle \approx S^{qt} T^{q^2 t}, \quad (2.35)$$

where

$$S = c^{\frac{-c}{1+c}} (1-c)^{\frac{-(1-c)}{1+c}}; \quad T = \left[\frac{(1-c)^2}{c} \right]^{\frac{c}{2(1+c)^2} \ln \left[\frac{(1-c)^2}{c} \right]} \quad (2.36)$$

Probability density function corresponding to this, can be assumed to be log-normal.

$$P(L_t, t) = \frac{1}{2L_t \sqrt{\pi D t}} \exp \left\{ \frac{-[\ln(L_t S^{-t})]^2}{4Dt} \right\} \quad (2.37)$$

The following limits can be arrived at, after lengthy calculations. c^* is the solution of c in the range $0 < c < 1$ for which $\frac{(1-c)}{c} = \frac{1}{(1-c)}$. $c^* = \frac{3-\sqrt{5}}{2} = 0.381966$.

$$\lambda_{+\infty} = \max \left(\ln \frac{(1-c)}{c}, \ln \frac{1}{(1-c)} \right) \quad (2.38)$$

$$\lambda_{-\infty} = \max \left(\ln \frac{(1-c)}{c}, \ln \frac{1}{(1-c)} \right), \quad (2.39)$$

$$\lambda'_+ = \begin{cases} \ln \left(\frac{(1+c)}{c} \right), & (c < c^*), \\ \ln(1+c), & (c > c^*), \\ 0, & (c = c^*). \end{cases} \quad (2.40)$$

$$\lambda'_- = \begin{cases} \ln(1+c), & (c < c^*), \\ \ln\left(\frac{1+c}{\varepsilon}\right), & (c > c^*), \\ 0, & (c = c^*). \end{cases} \quad (2.41)$$

Using these limits, we get the asymptotic law for moments as $q \rightarrow \pm\infty$ from eq.(1.39)

$$\langle L_t^q \rangle = \begin{cases} \frac{1}{[(1+c)(1-c)^q]^t} & (c > c^*; q > 0) \quad (c < c^*; q < 0), \\ \left[\left(\frac{c}{1+c}\right) \left(\frac{1-c}{c}\right)^q \right]^t & (c < c^*; q > 0) \quad (c > c^*; q < 0), \\ \left(\frac{\sqrt{5}-1}{3-\sqrt{5}}\right)^{qt} & (c = c^*; q \text{ +ve or - ve}). \end{cases} \quad (2.42)$$

Intermittency exponent μ and exponent σ can be evaluated exactly as

$$\mu = \ln \left(\frac{(1+c)[c+(1-c)^4]}{c[1-(1-c)^2]^2} \right) \quad (2.43)$$

$$\sigma = \frac{\ln \left(\sqrt{\frac{(1+c)}{\varepsilon}} \frac{[c^2+(1-c)^6]}{[c+(1-c)^4]^{\frac{3}{2}}} \right)}{\ln \left(\frac{(1+c)[c^3+(1-c)^8]}{\varepsilon[c+(1-c)^4]^2} \right)} \quad (2.44)$$

2.4 Results and conclusions.

1. It follows from Fujisaka's general theory that Gaussian approximation for $\ln L_t$ is valid for moments with $|q| \rightarrow 0$ whereas non-Gaussian components of PDF will become dominant for moments with $q \rightarrow \pm\infty$. Whether a given value of q is in the diffusion branch or intermittency branch will be determined by the value of c . Their boundaries are roughly estimated as

$$q_{\theta} = \frac{\lambda_{\infty} - \lambda_0}{D}, \quad \theta = \pm. \quad (2.45)$$

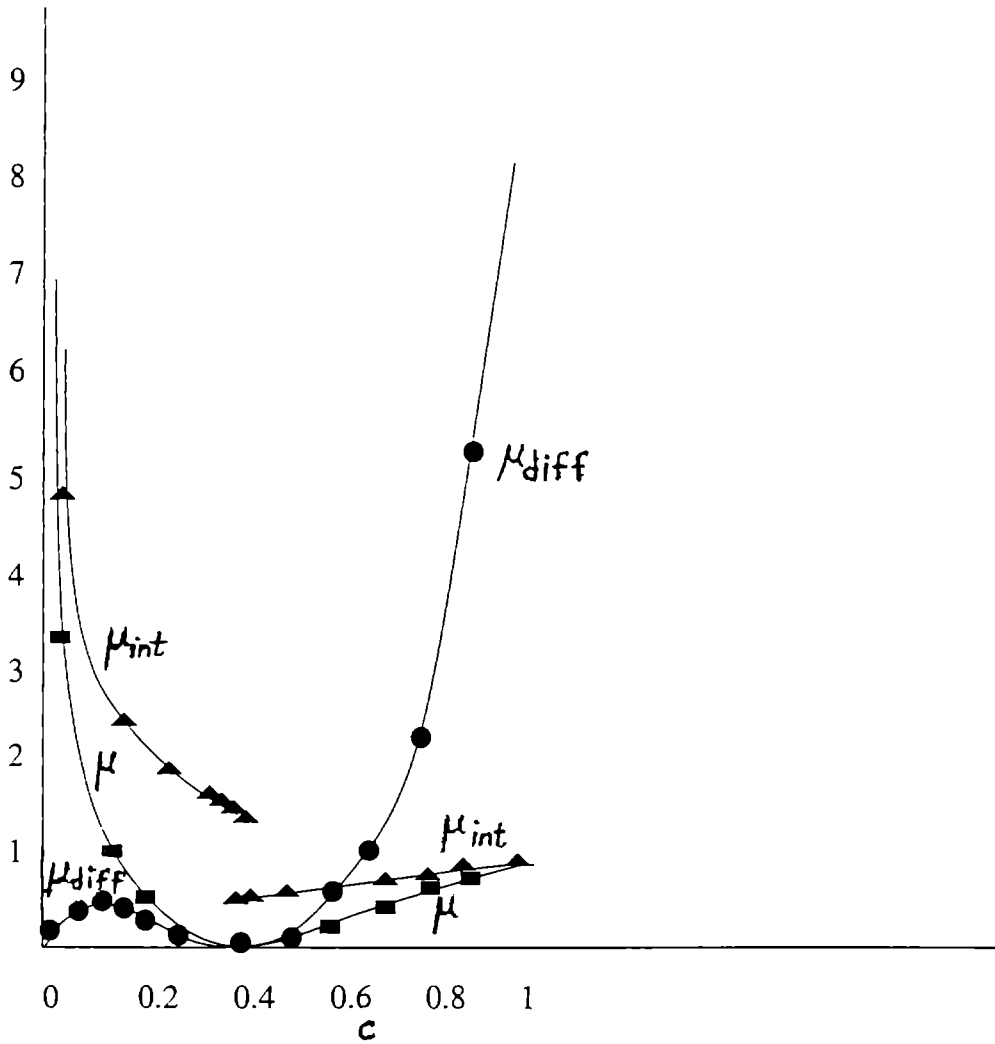


Figure 2.2: Intermittency exponent μ along with its limiting values μ_{diff} and μ_{int} vs c for the PTB map. On both axes units are arbitrary.

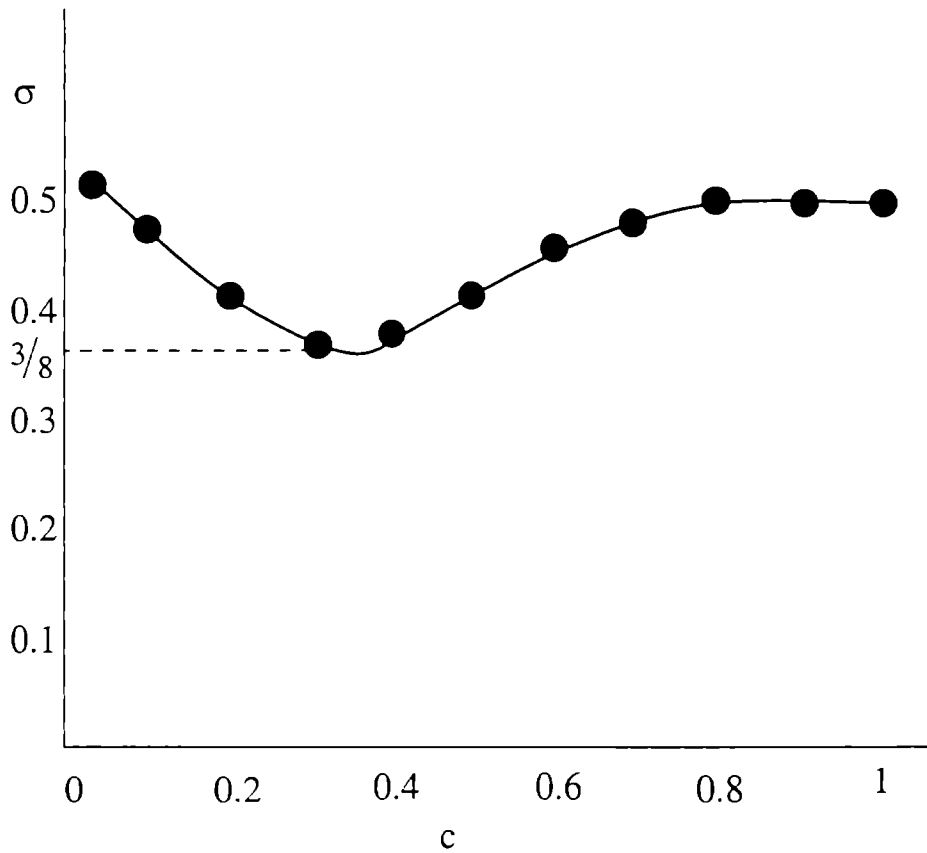


Figure 2.3: Exponent σ vs c for PTB map. On both axes units are arbitrary.

The condition for Gaussian approximation to hold good for a given value of q (say $q = 1 \sim 4$) is $q_- < q < q_+$

The curves μ and σ for the PTB map along with their limiting values can reveal the real implications of the above condition. These are shown in figures 2.2 and 2.3. Intermittency exponent μ is found to be globally similar to μ_{int} except around $c = c^*$. That is Gaussian approximation will hold good only when c is around c^* , say $0.375 < c < 0.4$. The average amplitude of $\ln |f'(x)|$ in the above range can be obtained as .037 which is only 7.7% of its value at c^* (0.4812). This is very small.

Characteristic exponent and diffusion coefficient are invariant under conjugation (see Appendix B). So the above result will be applicable for a family of one-dimensional maps conjugate to the PTB map. These conjugations can have non-linear portions and hence LER ($\ln |f'(x)|$) can have continuous parts also. From the above results, the following conclusions can be arrived at.

- (a) PDF of trajectory separation for large t is approximately log normal according to central limit theorem. Even for relatively lower order moments ($q = 1 \sim 4$) this will be valid only when the standard deviation of LER is very small (say, less than 7.7% of its mean value). For higher values of q , the standard deviation has to be still less. For most of the parameter values this condition will not be satisfied. Hence, in general, the PDF of trajectory separation will show appreciable departure from log-normal distribution. For $|q| \rightarrow 0$, these non-log normal components will get suppressed. When log normal approximation is valid, the moments will be given by eq. (2.35). Otherwise moments can be obtained using eq. (2.42)
- (b) Non-Gaussianity of $\ln L_t$, results from non-Gaussianity of local expansion rates ($\ln |f'(x)|$). Therefore in general, the PDF of LER will

have appreciable non-Gaussian components even when their standard deviation is very small. These non-Gaussian components influence even relatively lower order moments like $q = 1 \sim 4$. These results agree with the numerical results on logistic map as reported in reference [88]. The above conclusions are relevant to a class of 1-D maps conjugate to the PTB map.

2. Recently many works have been carried out on the stochastic motion in spatially extended, one-dimensional, periodic maps ascending along the bisector. They are used to describe deterministic diffusion of a dynamical variable. Example of such systems are: Josephson junctions in the presence of microwave radiation and parametrically driven oscillators. Fujisaka's method can be applied to study stochastic motion in such maps with $B(x) = \epsilon^{\Delta(x)}$, $\Delta(x)$ being the jump number [43]. From the above analysis, we note that stochastic motion in such maps will become more and more Gaussian when jump numbers become closer, *i.e.*, when the peaks of the extended maps come closer to the bisector.
3. Chaotic states occur widely in natural phenomena, but closed form mathematical models are rarely available. Linear maps are good approximations useful in analysing and predicting chaotic experimental data [25]. For example, they have been used in Chua circuits [111]. With c very near to c^* , the PTB map can describe deterministic diffusion of any dynamical variable ($X = \ln L_t$). Around c^* it gives the statistical properties of a Brownian motion with a drift velocity λ_0 . Like logistic map, it is a map with a single maximum. So it can be a good approximation for systems where the logistic models are applied.
4. We have followed a new procedure for deriving λ_q . The proposed method for systems with temporal correlations requires the solution of the eigen

value equation for the linear operator H_q defined in subsection 1.2.5. Instead, we compared values of the integral for successive values of t and took the limit $t \rightarrow \infty$ of the ratio. It will be applicable to systems where such comparison can be made.

2.5 Appendix-A.

To prove

$$\lim_{t \rightarrow \infty} \frac{1}{t} \ln \Theta = \lim_{t \rightarrow \infty} \frac{1}{t} \sum_{i=1}^{t-1} \ln(1 - \lambda_i) = 0, \quad (\text{A1})$$

we note,

$$\lambda_t = c^2 \frac{\left(\frac{1}{1-c}\right)^q - \left(\frac{1-c}{c}\right)^q}{\left(\frac{1}{1-c}\right)^q + c \left(\frac{1-c}{c}\right)^q} \times \frac{F_t(2) - F_t(1)}{F_t(2) + cF_t(1)} \quad (\text{A2})$$

Let $\left(\frac{1}{1-c}\right)^q > \left(\frac{1-c}{c}\right)^q$ The requirement $\lambda_{t+1} < \lambda_t$ implies

$$F_t(1)F_{t+1}(2) < F_{t+1}(1)F_t(2) \quad (\text{A3})$$

Substituting for $F_{t+1}(1)$, $F_{t+2}(2)$ eq (A3) leads to

$$F_{t+1}(1)F_{t+2}(2) > F_{t+2}(1)F_{t+1}(2) \quad (\text{A4})$$

i.e., $\lambda_{t+2} > \lambda_{t+1}$. Since eq.(A3) is true for $t = 1$, we get by mathematical induction

$$\lambda_1 > \lambda_2 < \lambda_3 > \lambda_4 < \lambda_5 \quad (\text{A5})$$

We examine the variation of alternate terms. The requirement $\lambda_{t+2} < \lambda_t$ reduces to equation (A3). Substitutions reveal that eq. (A3) will be valid with $t = t + 2$. Moreover $\lambda_3 < \lambda_1$. This gives

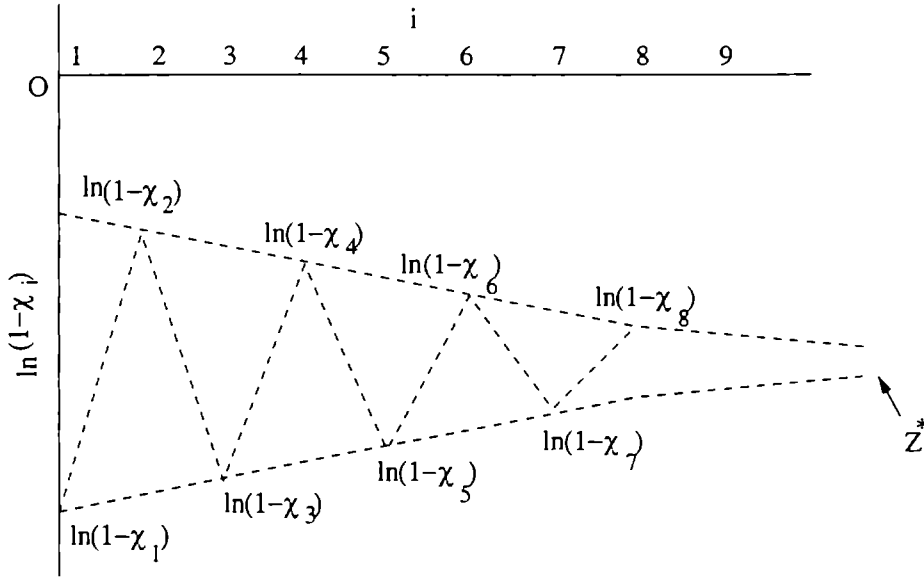


Figure 2.4: Variation pattern of terms $\ln(1 - \chi_i)$ for different values of i in the case of PTB map. $\ln(1 - \chi_i)$ tends to a finite limit z^* (negative) as $i \rightarrow \infty$

$$\chi_1 > \chi_3 > \chi_5 > \chi_7 \tag{A6}$$

Similarly,

$$\chi_2 < \chi_4 < \chi_6 \tag{A7}$$

Same result will be valid for $(\frac{1}{1-c})^q < (\frac{1-c}{c})^q$ When $(\frac{1}{1-c})^q = (\frac{1-c}{c})^q$ χ_i will be zeroes. Figure(4) shows the pattern of variation of $\ln(1 - \chi_i)$. We note $\lim_{t \rightarrow \infty} \frac{1}{t} \sum_{i=1}^{t-1} \ln(1 - \chi_i)$ will converge as two sums (one for odd values of i and other for even values of i) to a finite(negative) limit. This proves eq. (A1).

2.6 Appendix B.

It is easy to prove that the characteristic function λ_q associated with the statistics of trajectory separation is invariant under conjugation [43]. For a mapping $x_{t+1} =$

$f(x_t)$, λ_q is defined as

$$\lambda_q = q^{-1} \lim_{t \rightarrow \infty} t^{-1} \ln \left\langle \prod_{s=0}^{t-1} |f'(x_s)|^q \right\rangle \quad (\text{B1})$$

Let $\tilde{x} \in (\tilde{x}_i, \tilde{x}_f)$ be a one-to-one transformation of x $\tilde{x} = h(x)$, ($x = h^{-1}(\tilde{x})$). The dynamical law for \tilde{x}_t can be written as

$$\tilde{x}_{t+1} = h(f(h^{-1}(\tilde{x}_t))) \equiv \tilde{f}(\tilde{x}_t) \quad (\text{B2})$$

The characteristic function of the mapping (B2) is

$$\begin{aligned} \tilde{\lambda}_q &= q^{-1} \lim_{t \rightarrow \infty} t^{-1} \ln \left\langle \prod_{s=0}^{t-1} |\tilde{f}'(\tilde{x}_s)|^q \right\rangle_{\text{con}} \\ &= q^{-1} \lim_{t \rightarrow \infty} t^{-1} \ln \left\langle \exp \left\{ q \sum_{s=0}^{t-1} \ln |f'(x_s)| + q \ln |h'(x_t)/h'(x)| \right\} \right\rangle, \quad (\text{B3}) \end{aligned}$$

where $\langle \cdot \rangle_{\text{con}} \equiv \int_{\tilde{x}_i}^{\tilde{x}_f} d\tilde{x} \tilde{\rho}(\tilde{x}) \cdot \cdot$, and $\tilde{\rho}(\tilde{x}) = \rho(x)/|h'(x)|$ the invariant distribution for \tilde{x} .

One can show the invariance of characteristic function under conjugation in the following way. First, assume the inequality $0 < r < |h'(x_t)/h'(x)| < R < \infty$ with certain constants r and R for any choice of the initial values x and t . Inserting the inequality into (B3) yields $\tilde{\lambda}_q = \lambda_q$. Even if the above inequality does not hold, one can note that $\sum_{s=0}^{t-1} \delta \ln |f'(x_s)| \simeq O(\sqrt{t})$ and $\ln |h'(x_t)/h'(x)| = O(t^0)$, which implies the term $\ln |h'(x_t)/h'(x)|$ has no contribution to $\tilde{\lambda}_q$. This means $\tilde{\lambda}_q = \lambda_q$.

It is easy to note that Lyapunov exponent also is invariant under conjugation since its value is equal to λ_0 . Same is the case with diffusion coefficient D since $D = \lim_{q \rightarrow 0} \frac{d\lambda_q}{dq}$.

Chapter 3.

Analysis of chaotic motion and its shape dependence in a generalized piecewise linear map.

3.1 Introduction.

In physics and mathematics diffusion has been a subject of interest since the end of nineteenth century. One of the famous mechanisms is given by the thermal agitation of molecules and such motion has been named Brownian motion. It can be modeled theoretically by particle motion under the influence of a stochastic force term.

A diffusion like behaviour of a dynamical variable has been observed recently in a variety of physical systems. The amplitude of thermal noise, always present in experiments, is far too small to account for the observed diffusive behaviour. Examples of such systems are Josephson junctions in the presence of microwave radiation [107–109] and parametrically driven oscillators [110]. Recently, an explanation of this phenomenon has been given in terms of deterministic diffusion which can be noticed in simple spatially extended one dimensional maps which

are periodic along the bisector [5, 24, 57, 58, 89–106]. Transport due to chaos has become an outstanding problem in Hamiltonian dynamics also, both from a theoretical point of view (random processes exhibited by deterministic systems [112]), and in view of possible applications in different physical contexts, as celestial mechanics, confinement problems and so on.

Recently, some exactly solvable models of spatially extended 1- D maps have been analysed [95–97]. We note that the only aim in these studies is the evaluation of the exact diffusion coefficient using a cycle expansion technique [7, 62–64, 77–81]. It is a well known fact that the chaotic dynamics in spatially extended maps has two complementary aspects - diffusion and intermittency. These are related to the probability distribution which is approximately Gaussian by central limit theorem. Fujisaka's characteristic function method is a useful tool for analysing both these aspects of stochasticity in such maps. In this chapter, we apply the characteristic function method [43–54] to analyse the chaotic motion in a generalized piecewise linear (GPL) map with a variable shape. It is a generalization of the exactly solvable model introduced by Artuso [95] allowing analytical study. Exact expression for diffusion coefficient and a parametric representation for the fluctuation spectrum relating to the probability density function (PDF) are obtained. Generalization permits the study of the dependence of these quantities on the shape of the map. We also get analytically limiting forms of the above quantities when the peak shape becomes flat. We note that GPL map with flat peak is more suited to describe systems exhibiting intermittency in time. It can be noted that the generalization brings the map in [95] nearer to sinusoidal maps studied numerically in ref [58, 89–91]. A similar shape dependent piecewise linear model has been examined by S. Grossmann and S. Thomae [94] from the point of view of correlation times.

In section 3.2, we introduce the generalized piecewise linear (GPL) map and show how the characteristic function method introduced by Fujisaka et al can be applied to analyse the chaotic motion in it. Exact expressions for characteristic

function and diffusion coefficient and a parametric representation of fluctuation spectrum are obtained in section 3.3. We also discuss special cases of GPL models and limiting forms of the above mentioned quantities. The result of Artuso is regained as a special case of our general formula. Shape dependence of diffusion coefficient and fluctuation spectrum also is examined in section 3.3. Section 3.4 is devoted to results and conclusions.

3.2 Model and characteristic function method.

Chaos-induced diffusion systems have a general form [5, 43]

$$X_{t+1} = X_t + P_r(X_t) = Y_r(X_t), \quad P_r(X+1) = P_r(X) \quad (3.1)$$

where r is a control parameter. The sinusoidal map $P_r(X) = r \sin(2\pi X)$ is an example [58, 89–91]. After the decomposition $X_t = N_t + x_t$ where N_t is the cell number in which X_t is located, and x_t , ($0 \leq x_t < 1$) the distance measured from the relative origin $X = N_t$, eq. (3.1) can be uniquely rewritten as two dynamical laws:

$$N_{t+1} = N_t + \Delta(x_t), \quad x_{t+1} = f(x_t) \quad (3.2)$$

Here $\Delta(x)$ is the jumping number defined as the largest integer smaller than $x + P_r(x)$ and is free from N_t and $f(x) = x + P_r(x) - \Delta(x)$, satisfying $0 \leq f(x) < 1$. $f(x)$ is the reduced map of the extended map (3.1).

We analyse a piecewise linear map with variable shape of the type in fig.3.1. In the general case, the extended 1-D map consists of linear segments with slopes $\pm m_i, i = 0, 1, \dots, h, m_i < m_{i-1}$. For the cells on the bisector, the slope magnitude is m_0 . For the i^{th} cell above and below this cell on bisector, the slope magnitude changes to m_i . In the general case, the reduced map consists of $k = 4h + 3$ linear segments. For k increasing from 1 to $4h + 3$, these line segments have slopes $m_0, m_1, m_2, \dots, m_h, -m_h, -m_{h-1}, \dots, -m_0, -m_1, -m_2, \dots, -m_h, m_h,$

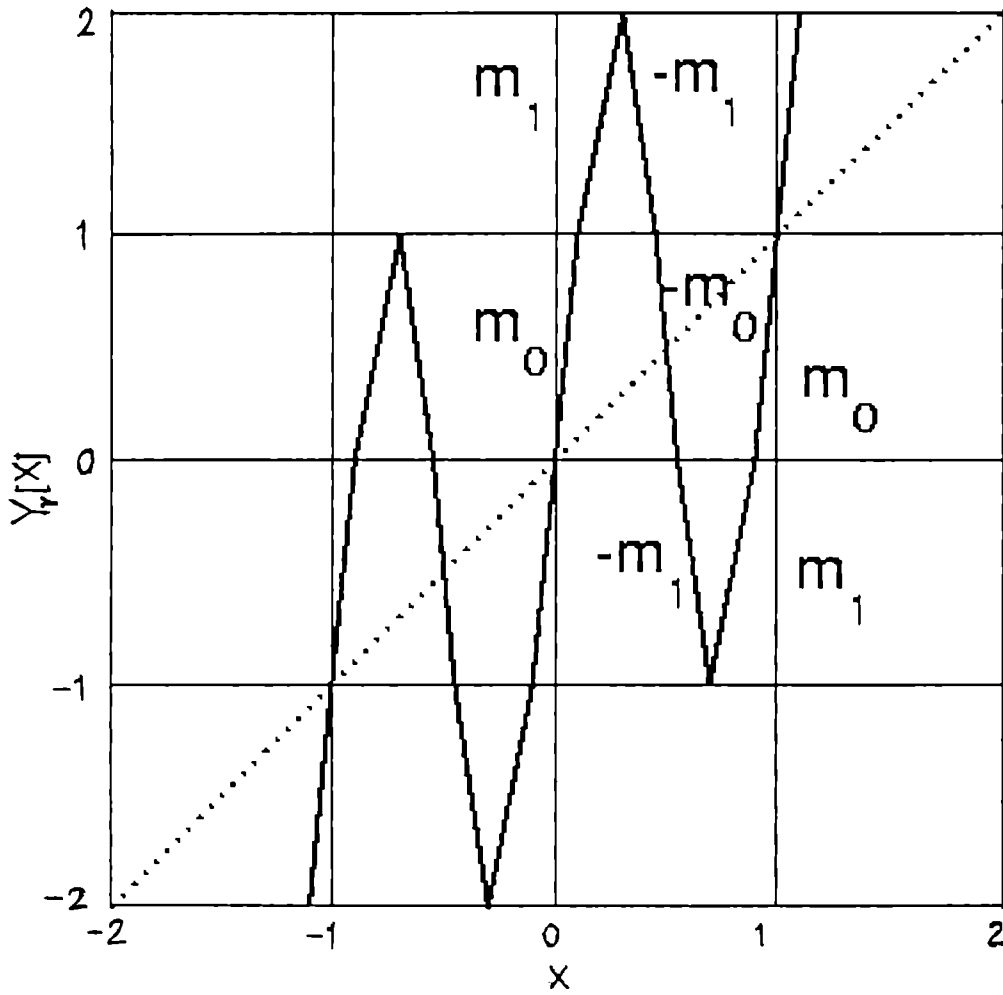


Figure 3.1: Generalised Piecewise Linear (GPL) map with a variable shape with $h = 1$. On both axes units are arbitrary.

$m_{h-1}, m_2, m_1, m_0,$ and m_i s satisfy the relation

$$\frac{3}{m_0} + \sum_{i=1}^h \frac{4}{m_i} = 1 \tag{3.3}$$

The extended map can be generated from the reduced map by giving suitable jump numbers $\Delta(x)$. For k increasing from 1 to $(4h + 3)$, the jump numbers $\Delta(x)$ (constant for a line segment) are $0, 1, 2, \dots, h, h, h - 1, \dots, 2, 1, 0, -1, -2, \dots, -h, -h, -(h - 1), \dots, -2, -1, 0$. Figs.3.1 and 3.2 show the map and the reduced map for $h = 1$.

Referring to section 1.2 we note that map (3.1) can be studied using the characteristic function method [43–54]. We have seen that in this method, the dynamics of A_t governed by $A_{t+1} = B(x_t)A_t$ ($t = 0, 1, 2, \dots$) with $A_0 = 1$ is studied. $B(x_t)$ is a steady function of x_t which evolves according to the chaotic map $x_{t+1} = f(x_t)$ ($0 \leq x_t < 1$) [43]. Equivalently, we have seen that one can consider the dynamics of the local time average of a time series $\alpha_t = \frac{1}{t} \sum_{j=0}^{t-1} \ln B(x_j)$ [47, 49–54]. Map (3.1) can be treated by putting $A_t = \exp(N_t - N_0)$; $B(x) = \exp(\Delta(x))$. We put $N_0 = 0$. Then $\alpha_t = \frac{N_t}{t}$. The long time dynamics of N_t can be discussed with the aid of Fujisaka’s characteristic function

$$\lambda_q = \frac{1}{q} \lim_{t \rightarrow \infty} \frac{1}{t} \ln[\langle \exp(qN_t) \rangle] \tag{3.4}$$

$\langle \exp(qN_t) \rangle$ is average over a steady ensemble and is the q -order moment of $\exp(N_t)$. λ_q can be expanded in the series of cumulants. The expansion converges for $|q| < b$, b being the convergence radius. b separates three typical regions of q : ($q \ll -b, |q| \ll b: q \gg b$). For $|q| \ll b$, we found that λ_q can be approximated as

$$\lambda_q = \lambda_0 + D q \tag{3.5}$$

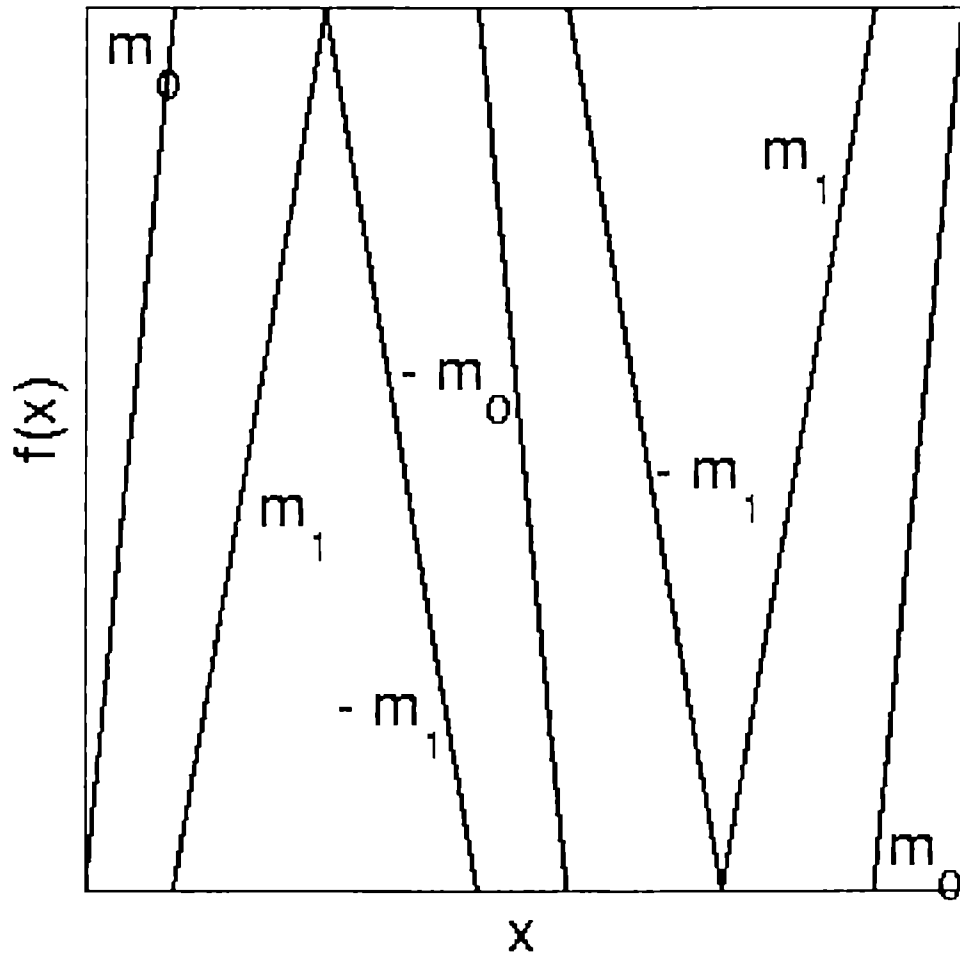


Figure 3.2: Reduced map of GPL map in fig.3.1. On both axes units are arbitrary.

where λ_0 is the drift velocity defined as,

$$\lambda_0 = \alpha_\infty = \lim_{t \rightarrow \infty} \frac{N_t}{t} \quad (3.6)$$

D is the diffusion coefficient given by

$$\sigma_t = \langle (N_t - \lambda_0 t)^2 \rangle \approx 2 D t \quad (3.7)$$

for large values of t . σ_t is the variance of N_t . In section 1.2.2 it was shown that the asymptotic PDF of α_t has a Gaussian component (central limit theorem) and a non-Gaussian component. For $|q| \ll b$, the moment $\langle \exp(q N_t) \rangle$ is determined by the Gaussian component. This is called the diffusion branch of q . For $|q| \gg b$, it is determined by the non-Gaussian component and this range is the intermittency branch of q .

The probability density $P_t(\alpha)$ that α_t takes values between α and $\alpha + d\alpha$ can be obtained as $P_t(\alpha) \sim \sqrt{t} \exp[-\sigma(\alpha)t]$. $\sigma(\alpha)$ is the fluctuation spectrum and $P_t(\alpha) \rightarrow \delta(\alpha - \alpha_\infty)$ as $t \rightarrow \infty$. We have seen that $P_t(\alpha)$ can be obtained from λ_q in parametric form using the Legendre transform $\alpha = \frac{d}{dq}(q\lambda_q)$, $\sigma(\alpha) = q^2 \frac{d}{dq} \lambda_q$.

3.3 Characteristic function, diffusion coefficient and fluctuation spectrum.

For simplicity, we first consider the case with $h = 1$. The reduced map consists of $\bar{\tau}$ line segments with slopes (from left) $m_0, m_1, -m_1, -m_0, -m_1, m_1, m_0$. These satisfy (3.3). The operator H (subsection 1.1.1) in the present case becomes

$$HG(x) = \sum_{k=1}^{\bar{\tau}} \frac{G(y_k)}{|f'(y_k)|} = \sum_{k=1}^{\bar{\tau}} \frac{G(y_k)}{|m_k|} \quad (3.8)$$

where y_k is the k^{th} solution of $f(y_k) = x$ and $f'(x) = \frac{d}{dx}f(x)$. m_k is the slope of the k^{th} line segment of the reduced map. The invariant density $\rho(x)$ can be obtained as the solution of

$$H\rho(x) = \rho(x) \quad (3.9)$$

We note that $\rho(x)$ is uniform in the interval $0 \leq x \leq 1$ ($\rho(x) = 1$). The Lyapunov exponent λ can be obtained as

$$\lambda = \frac{3}{m_0} \ln(m_0) + \frac{4}{m_1} \ln(m_1) \quad (3.10)$$

Since $m_i > 1$, it is easy to note that $\lambda > 0$ and therefore the reduced map is always chaotic.

To evaluate λ_q we can use the linear operator defined by Mori et al (eq.(1.19))

$$\widehat{H}G(x) = \frac{1}{\rho(x)} H[G(x)\rho(x)] \quad (3.11)$$

For our model $H = \widehat{H}$. Characteristic function λ_q can be evaluated as (eq.(1.62))

$$\lambda_q = \frac{1}{q} \lim_{t \rightarrow \infty} \frac{1}{t} \ln \left\langle e^{q\Delta x} \underbrace{\widehat{H} e^{q\Delta x} \widehat{H} e^{q\Delta x} \dots \widehat{H} e^{q\Delta x}}_{t-1} \right\rangle \quad (3.12)$$

$\Delta(x)$, the jump numbers which are constant over a line segment are (from left) 0, +1, +1, 0, -1, -1, 0. Hence we get from eqs.(3.8) and (3.11)

$$\begin{aligned} \widehat{H} e^{q\Delta x} &= \frac{3}{m_0} + \frac{2}{m_1} e^q + \frac{2}{m_1} e^{-q} \\ &= \frac{3}{m_0} + \frac{4}{m_1} \cosh(q) \end{aligned} \quad (3.13)$$

Using this in eq.(3.12) we have

$$\lambda_q = \frac{1}{q} \ln \left[\frac{3}{m_0} + \frac{4}{m_1} \cosh(q) \right] \quad (3.14)$$

The result can be generalized for integer values of h . Slope of the line segments m_k and jump numbers $\Delta(x)$ are given in sec.3.2. Again, slopes satisfy relation (3.3). Eq.(3.9) again leads to uniform invariant density $\rho(x) = 1$. Lyapunov exponent λ is given by

$$\lambda = \frac{3}{m_0} \ln(m_0) + \sum_{i=1}^h \frac{4}{m_i} \ln(m_i) \quad (3.15)$$

Since $m_i > 1$, it can be easily proved that $\lambda > 0$, again making the map fully chaotic. Evaluation of λ_q using eq.(3.12) gives

$$\lambda_q = \frac{1}{q} \ln\left[\frac{3}{m_0} + \sum_{i=1}^h \frac{4}{m_i} \cosh(iq)\right] \quad (3.16)$$

It is easy to verify that the drift velocity $\lambda_0 = 0$, always. The diffusion coefficient D is obtained as

$$D = \lim_{q \rightarrow 0} \frac{d}{dq} \lambda_q = \sum_{i=1}^h \frac{2i^2}{m_i} \quad (3.17)$$

To obtain α and $\sigma(\alpha)$ one can effect the Legendre transforms given in section 3.2. Relation between α and fluctuation spectrum $\sigma(\alpha)$ can be got in the parametric form.

$$\alpha = \frac{\sum_{i=1}^h \frac{4i}{m_i} \sinh(iq)}{\frac{3}{m_0} + \sum_{i=1}^h \frac{4}{m_i} \cosh(iq)} \quad (3.18a)$$

$$\sigma(\alpha) = q \frac{\sum_{i=1}^h \frac{4i}{m_i} \sinh(iq)}{\frac{3}{m_0} + \sum_{i=1}^h \frac{4}{m_i} \cosh(iq)} - \ln\left[\frac{3}{m_0} + \sum_{i=1}^h \frac{4}{m_i} \cosh(iq)\right] \quad (3.18b)$$

$q = 0$ gives $\alpha = 0$; $\sigma(\alpha) = 0$. If $+q$ gives $+\alpha$, $-q$ will give $-\alpha$ without changing $\sigma(\alpha)$. ie. $\sigma(\alpha)$ is a symmetric function of α . It can also be noted that maximum value of α is obtained by putting $q \rightarrow \infty$. We have

$$\alpha_{max} = h \quad \sigma(\alpha_{max}) = \ln\left(\frac{m_h}{2}\right) \quad (3.19)$$

3.3.1 Special cases.

In the special case when all m_i 's are equal ($=m_0$), eq.(3.17) can be summed to obtain a closed form expression for D . in this case, eq.(3.3) gives $m_0 = 3 + 4h$ and we get

$$D = \frac{h(h+1)(2h+1)}{3(4h+3)} \quad (3.20)$$

With $h+1 = \beta$,

$$D = \frac{(\beta-1)\beta(2\beta-1)}{3(4\beta-1)} \quad (3.21)$$

which reduces to $D = 2/7$ for $\beta = 2$. These results have been obtained previously in ref. [95].

Closed form expression can be got also for the special case $m_i/m_{i-1} = r = a$ constant, $0 < r < 1$. Then $m_i = m_0 r^i$. From eq.3.3, we have

$$m_0 = 3 + \frac{4(1-r^h)}{r^h(1-r)} \quad (3.22)$$

Summation appearing in eq.(3.17) can be performed for this special case using the above values of m_0 and m_i and an exact analytical expression for diffusion coefficient can be obtained. We get

$$D = \frac{2[h^2 + (1 - 2h - 2h^2)r + (h+1)^2 r^2 - r^{h+1} - r^{h+2}]}{[3r^h(1-r) + 4(1-r^h)](1-r)^2} \quad (3.23)$$

For every r between 0 and 1, the above model becomes an exactly solvable case with D given by eq.(3.23).

3.3.2 Limiting forms.

Limiting forms of the above quantities can be obtained for a constant h as the peak shape becomes maximum flat. These can be arrived at by taking limit $r \rightarrow 0$.

From eq.(3.23), we find that D behaves like

$$D = \frac{h^2}{2} \quad (3.24)$$

Note from eq.(3.22) that the above limit can also be obtained by putting $m_i \rightarrow \infty (i = 0, \dots, h - 1)$ and $m_h \rightarrow 4$. Applying this we get

$$\lim_{r \rightarrow 0} \lambda_q = \frac{1}{q} \ln[\cosh(qh)] \quad (3.25)$$

$$\lim_{r \rightarrow 0} \alpha = h \tanh(qh) \quad (3.26)$$

One can also obtain the following limiting form for $\sigma(\alpha)$. For $r \rightarrow 0$ we get

$$\lim_{r \rightarrow 0} \sigma(\alpha) = \ln\left[\frac{h^2 - \alpha^2}{h^2}\right]^{1/2} \left[\frac{h + \alpha}{h - \alpha}\right]^{\alpha/2h} \quad (3.27)$$

3.3.3 Shape dependence of diffusion coefficient and fluctuation spectrum.

In fig.3.3 we plot diffusion coefficient versus r for $h = 2$. It can be observed that D increases with increasing flatness of the peak shape. D varies from 0.9 to 2 when r is varied from 1 to 0. Increasing h , keeping $m_i = m_0 (i = 1, 2, \dots, h)$ appears to have more influence on increasing D . This is because $D = 2/\pi = 0.29$ for $h = 1$, whereas it goes to 0.909 for $h = 3$ (eq. (3.20)).

For $|q| \ll b$, λ_q is approximately given by eq. (3.5). This range of q will give small (absolute) values of α . α and $\sigma(\alpha)$ take the form (eqs. (1.57) and (1.58))

$$\alpha = \lambda_0 + 2Dq \quad (3.28)$$

$$\sigma(\alpha) = \frac{(\alpha - \lambda_0)^2}{4D} \quad (3.29)$$

For the present model $\lambda_0 = 0$ and generally D is given by eq.(3.17). For $|q| \gg b$,

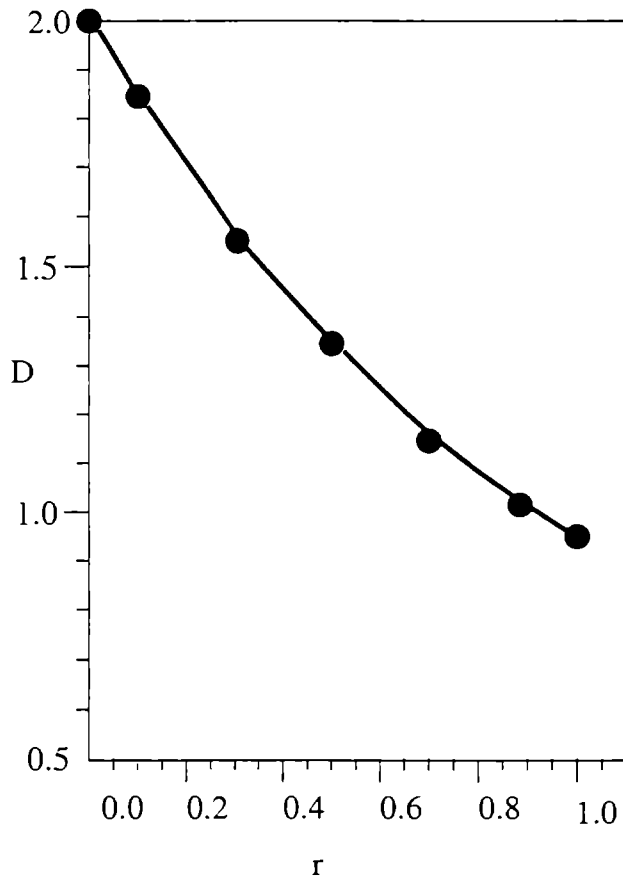


Figure 3.3: Variation of diffusion coefficient D with r for $h = 2$. On both axes units are arbitrary.

λ_q behaves like eq. (1.38). This range of q gives the extreme values of α . α and $\sigma(\alpha)$ are given by (1.60) and (1.61) respectively.

$$\alpha \approx \lambda_{\theta\infty} - \theta c_\theta \eta_\theta \exp(-\eta_\theta |q|) \quad (3.30)$$

$$\sigma(\alpha) \approx \frac{1}{\tau_\theta} - \frac{1}{\eta_\theta} |\alpha - \lambda_{\theta\infty}| \ln\left[\frac{a_\theta}{|\alpha - \lambda_{\theta\infty}|}\right] \quad (3.31)$$

where $\lambda_{\theta\infty}$ and the positive constants τ_θ , c_θ and η_θ ($\theta = \pm$) can be shown to be

$$\begin{aligned} \lambda_{+\infty} = h; \quad \lambda_{-\infty} = -h; \quad \tau_+ = \tau_- = \frac{1}{\ln(\frac{m_h}{2})} \\ c_+ = c_- = \frac{m_h}{m_{h-1}}; \quad \eta_+ = \eta_- = +1 \end{aligned} \quad (3.32)$$

The probability distribution function for N_t , the distance from the origin, can be obtained using the fluctuation spectrum $\sigma(\alpha)$. From eq. (1.53), we have

$$P_t(N) \sim \frac{1}{\sqrt{t}} \exp\left[-\sigma\left(\frac{N}{t}\right) t\right] \quad (3.33)$$

$P_t(N)$ being the PDF that N_t takes values between N and $N + dN$. This PDF is approximately Gaussian by central limit theorem. In fig. 3.4 we plot $\sigma(\alpha)$ for different maps and compare with the Gaussian form given in eq.(3.29). Actually eq.(3.29) which is applicable for small (absolute) values of α represents the Gaussian part of $\sigma(\alpha)$. Eq.(3.31), is applicable for extreme values of α and it represents the non-Gaussian part of $\sigma(\alpha)$. From this equation and also from fig. 3.4, we note that the derivative $\frac{d\sigma(\alpha)}{d\alpha}$ logarithmically diverges at extreme values of α . For Gaussian approximation to hold good in this range of α , it follows that the slope of $\sigma(\alpha)$ represented by eq. (3.29) should tend to a maximum. This will happen when D tends to a minimum. It becomes clear that the non-Gaussian character of the PDF will increase with increasing peak-height and flatness of the map. Among these two factors increase in h appears to have more influence in produc-

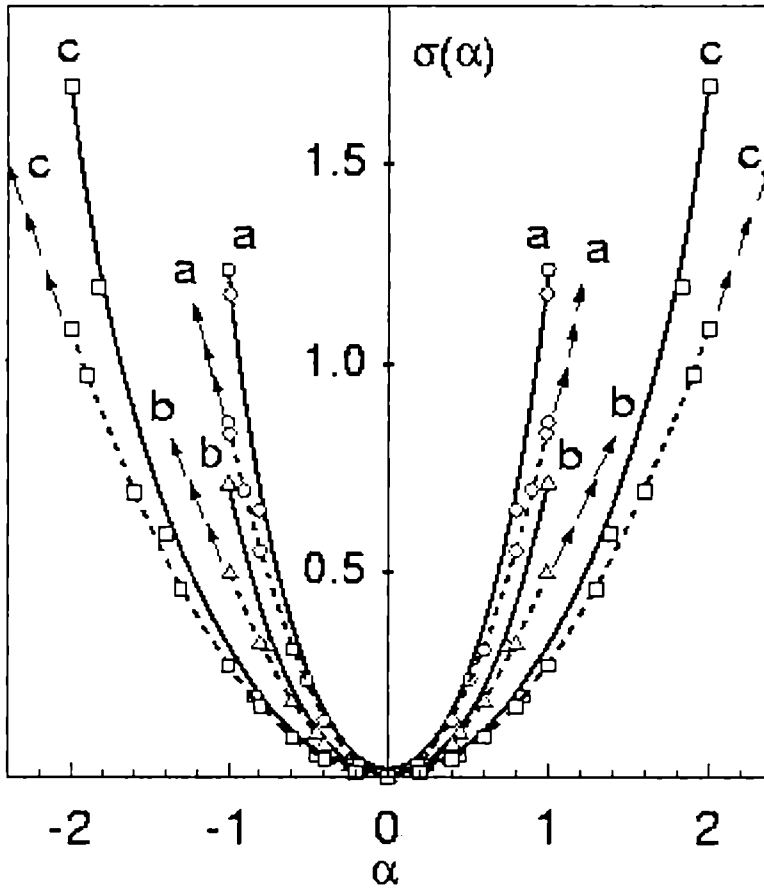


Figure 3.4: Fluctuation Spectrum $\sigma(\alpha)$ versus α for different cases. Solid lines represent actual $\sigma(\alpha)$ while dotted lines give corresponding Gaussian forms. (a) $h = 1$, $m_0 = m_1 = 7$ (b) $h = 1$, $m_0 = 100$, $m_1 = 4.1237$ (c) $h = 2$, $m_0 = m_1 = m_2 = 11$. On both axes units are arbitrary.

ing non-Gaussian character of the PDF. Thus, we find that intermittency in the generalized piecewise linear map increases with increasing flatness and the height of the peak, though the influence become more pronounced when the height is increased.

3.4 Results and conclusions.

In this chapter we applied the characteristic function formalism to analyse a generalized piecewise linear map and derived exact expressions for diffusion coefficient and characteristic function. Previous result on closed form expression for diffusion coefficient is obtained as a special case. The fluctuation spectrum relating to the probability distribution is got in a parametric form. Analysis of the PDF with fluctuation spectrum brings out that non-Gaussian character of the PDF increases with increasing peak-height and flatness of the map, height exercising more effect. This is important when one selects models for describing experiments relating to diffusion. For example, systems exhibiting chaotic motion similar to Brownian motion should have a Gaussian distribution. GPL Maps with linear segments having constant slope and minimum peak-height are useful in cases like this. Maps with greater height with peaks becoming more flat will be best suited in describing diffusion systems showing intermittency in time. With flatness becoming maximum, diffusion coefficient behaves like $\frac{h^2}{2}$, h being the peak-height. Corresponding limiting forms for characteristic function and fluctuation spectrum are also obtained. The limiting form of fluctuation spectrum is quite different from the Gaussian form following from central limit theorem.

Chapter 4.

Analysis of diffusion and intermittency in generalized piecewise linear Markov maps with fractional peak height.

4.1 Introduction.

In the last chapter we analysed the chaotic motion and its shape dependence in a generalized piecewise linear (GPL) map. We found that the complementary dynamics of diffusion and intermittency in spatially extended maps of this kind can be analysed very effectively using the characteristic function method proposed by Fujisaka et al. GPL maps have variable peak-shape and integer peak-heights. In this chapter we introduce another class of spatially extended piecewise linear maps with variable peak-shape. Peak-height in this case can take fractional values less than unity. These are generalizations of the maps discussed by Tseng et al [96]. We prove that for almost all arbitrary values of fractional peak-height, these are exactly solvable Markov mappings. Hence we call these maps generalized

piecewise linear Markov (GPLM) maps. Applying characteristic function method, we derive closed form expressions for diffusion coefficient from which the results obtained previously by Tseng et al can be regained as special cases. We show how fluctuation spectrum obtainable from characteristic function can be used to investigate probability density function (PDF). The dependence of these quantities on the shape the map is analysed. We note that intermittency and non-Gaussian character of the PDF can be related to the shape of the map. GPLM maps with flat peaks is found to be more suited in time series analysis of systems showing intermittency whereas those with sharp peaks are to be preferred for describing diffusive behaviour similar to Brownian motion. Another significance of the result is that conjecture regarding the fractal nature of diffusion coefficient for piecewise linear maps [98] is found to be non justifiable, it being analytical and exact in all cases. GPLM maps are very good approximations for sinusoidal maps which can be analysed only numerically [58, 89–91]. We note that shape dependence of chaotic motion has been investigated for a similar model in [94].

In section 4.2, we introduce the generalized piecewise linear Markov (GPLM) maps and show how the characteristic function method can be applied to study the chaotic motion in them. In section 4.3, we give the derivation of exact diffusion coefficient in each case. In section 4.4, we discuss the variation of diffusion coefficient with the shape of the map and how PDF can be analysed using fluctuation spectrum. Section 4.5 is devoted to results and conclusions.

4.2 GPLM models and characteristic function method.

We consider in this paper generalized piecewise linear Markov maps with fractional peak-heights and variable shape ascending along the bisector as shown in fig(4.1). The map consists of linear segments with slopes m_0 and m_1 , $m_1 \leq m_0$.

For the cells on the bisector, the slope magnitude is m_0 . For cells above and below this cell on the bisector, the slope magnitude changes to m_1 . The peak-height in these cells above and below the bisector is denoted as h . Note that in [96], we get a special case of this with $m_0 = m_1$. In chapter 3 we found that such chaos induced diffusion systems can be represented as [5, 43].

$$X_{t+1} = X_t + P_r(X_t) = Y_r(X_t), \quad P_r(X + 1) = P_r(X) \quad (4.1)$$

r being the control parameter. After the decomposition $X_t = N_t + x_t$ where N_t is the cell number in which X_t is located and x_t , ($0 \leq x_t < 1$) the distance measured from the relative origin $X = N_t$, the equation (4.1) becomes two dynamical laws.

$$N_{t+1} = N_t + \Delta(x_t), \quad x_{t+1} = f(x_t) \quad (4.2)$$

$\Delta(x)$ is the jumping number defined as the largest integer smaller than $x + P_r(x)$ and is free from N_t and $f(x) = x + P_r(x) - \Delta(x)$, ($0 \leq f(x) < 1$) is the reduced map of the extended map represented by eq.(4.1). One can note that our generalized map is a very good approximation for the sinusoidal map $P_r(X) = r \sin(2\pi X)$ which has been studied numerically in ref [58, 89–91].

The figure 4.2 show the reduced maps of the 6 cases of GPLM maps which we consider in this paper. Each of them consists of 7 linear segments marked as solid lines. From left these segments have slopes $m_0, m_1, -m_1, -m_0, -m_1, m_1, m_0$. The extended map can be generated from the reduced map by giving, suitable jump numbers $\Delta(x)$ (constant for a line segment). These jump numbers (from left) are 0, 1, 1, 0, -1, -1, 0. The dotted lines show the Markov partition of the interval $[0, 1]$. The partition points get mapped on to other partition points by the map $f(x)$. In between two partition points map is linear. Hence the reduced maps $f(x)$ are piecewise linear Markov maps.

We note that the map (4.1) can be studied using Fujisaka's characteristic function method: We have to put $A_t = \exp(N_t - N_0)$ and $B(x) = \exp(\Delta(x))$. Then

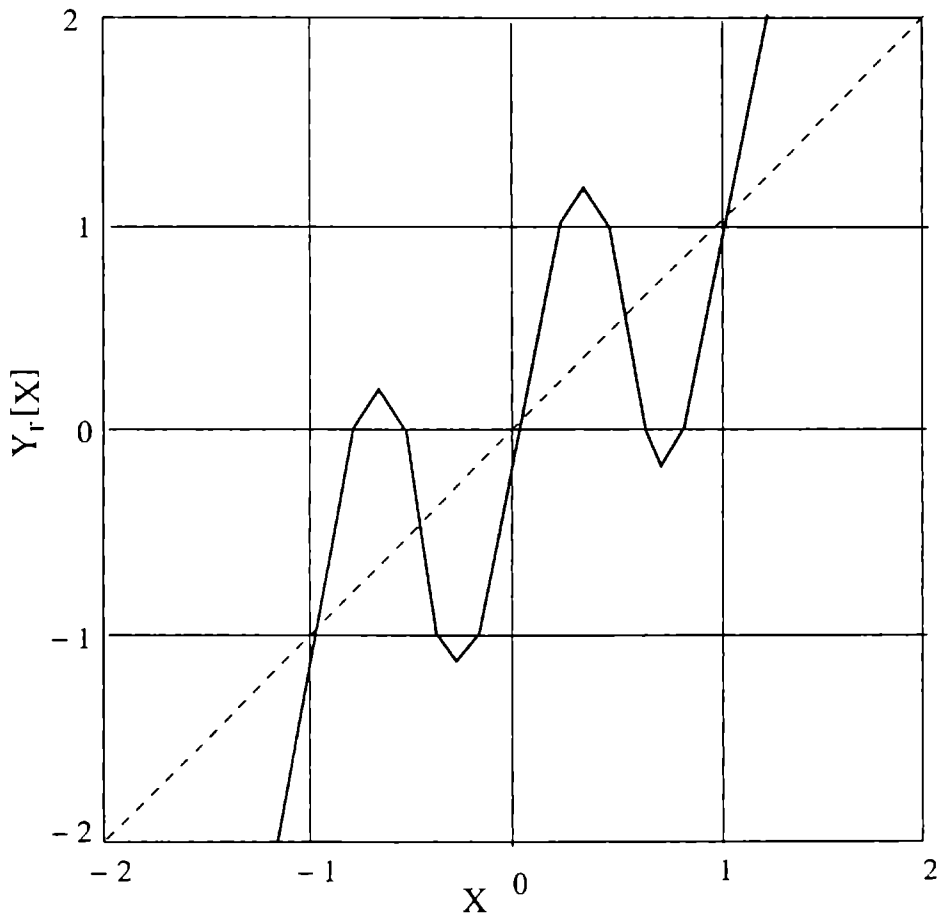


Figure 4.1: Generalized piece wise linear Markov map (GPLM map) with fractional peak height and variable shape ascending along the bisector. The slope magnitude of line segments in the cells on the bisector is m_0 . In cells above and below the bisector the slope magnitude changes to m_1 . On both axes units are arbitrary.

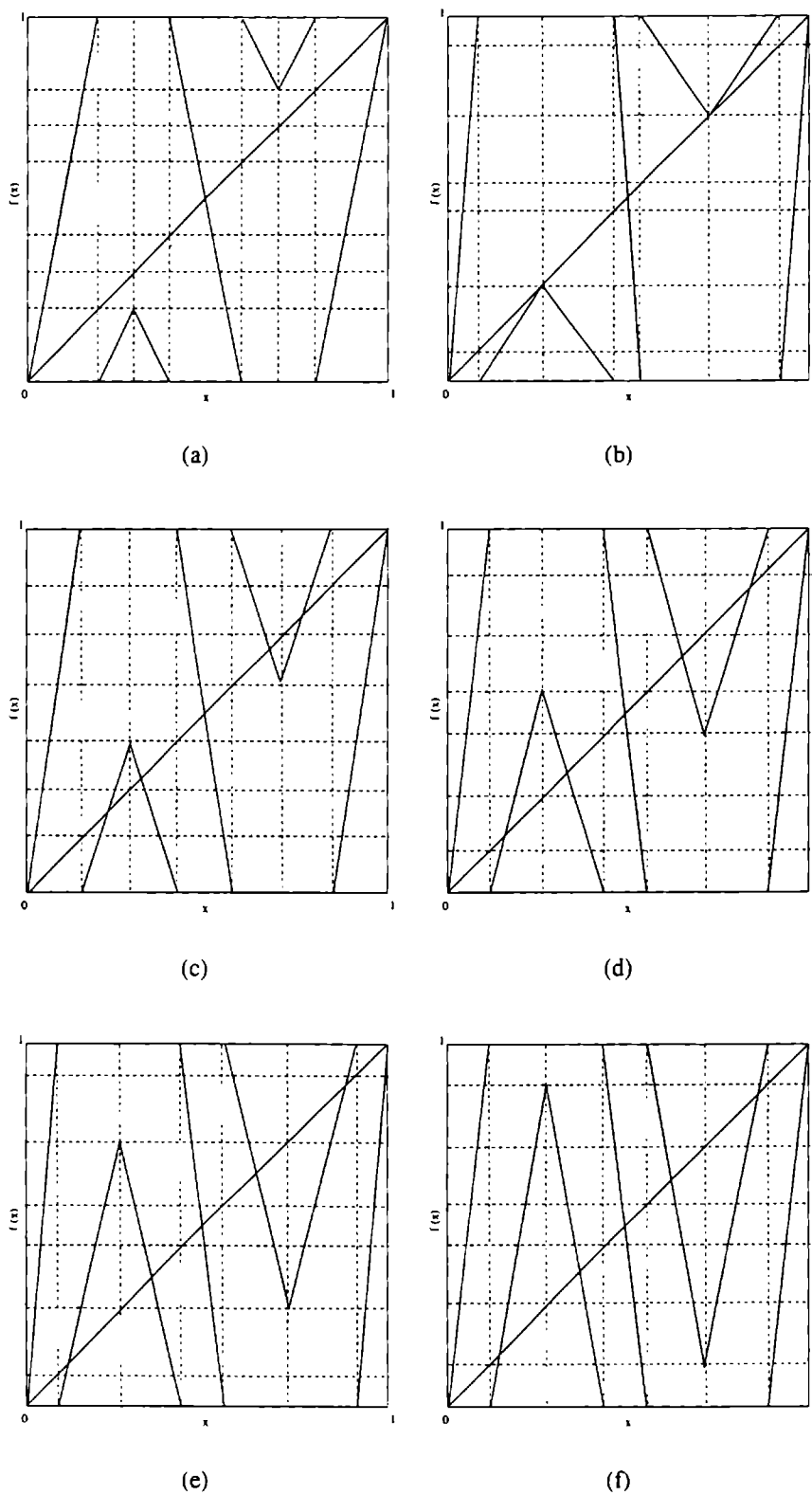


Figure 4.2: Reduced maps of the 6 cases (a to f) of GPLM maps. The 3 longer line segments have slope magnitude m_0 and the 4 shorter line segments have slope magnitude m_1 . On both axes units are arbitrary.

$u_j = \Delta(x_j)$. We put $N_0 = 0$ for convenience. Then $\alpha_t = \frac{N_t}{t}$. For studying the long time dynamics of A_t or α_t , one has to evaluate the characteristic function λ_q . Referring to subsection 1.2.5 we note that for evaluating λ_q , one requires the eigenvalues of the linear operator H_q (eq. (1.63)). The advantage of Markov partitioning of the reduced map $f(x)$ is that the eigenvalue problem of the operator H_q can be reduced to that of the generalized transition matrix of a 7 state Markov model. Let the ν^{th} partition from the left be denoted as I_ν . Let δ_ν be the length of the ν^{th} partition, f'_ν , the constant slope of the corresponding line segment and Δ_ν the corresponding jump number. The operator H (section 1.1.1) can be represented by a 7×7 matrix as [87].

$$H_{\mu\nu} = \Gamma_{\mu\nu} |f'_\nu|^{-1} \quad \mu, \nu = 1, 2, \dots, 7 \quad (4.3)$$

with

$$\begin{aligned} \Gamma_{\mu\nu} &= 1 && \text{if } f(I_\nu) \supseteq I_\mu \\ &= 0 && \text{otherwise} \end{aligned} \quad (4.4)$$

For a proof see Appendix A. The transition matrix is given by [7, 50, 87]

$$\bar{H}_{\mu\nu} = H_{\mu\nu} \frac{\delta_\mu}{\delta_\nu} \quad (4.5)$$

$\bar{H}_{\mu\nu}$ satisfy the normalisation condition

$$\sum_{\mu} \bar{H}_{\mu\nu} = 1 \quad (4.6)$$

Invariant probabilities p_ν can be obtained as the solution of [7, 50].

$$p = \bar{H}p \quad (4.7)$$

where $p = \text{col}(p_1, p_2, p_3, p_4, p_5, p_6, p_7)$. From p_ν one can evaluate the invariant densities ρ_ν .

$$\rho_\nu = p_\nu / \delta_\nu \tag{4.8}$$

Then, the generalised transition matrix is given by [49, 50, 52]

$$(\overline{H}_q)_{\mu\nu} = \overline{H}_{\mu\nu} e^{q\Delta_\nu} \tag{4.9}$$

It is an easy matter to verify that the eigenvalues of the generalised transition matrix \overline{H}_q and those of the linear operator H_q will be the same. Transition matrix \overline{H} can be obtained from \overline{H}_q (putting $q = 0$). Invariant probabilities and invariant densities can be evaluated using eq. (4.7) and (4.8) respectively.

4.3 Exact results for diffusion coefficients.

We take the six cases of GPLM maps one by one. To avoid negative Lyapunov exponents and stable periodic orbits, we consider only maps expanding everywhere ie, $m_0, m_1 > 1$. In each case $m_0 = m_1$ corresponds to the reduced map discussed in [96]. For all reduced maps shown in fig. 4.2 it is easy to note that

$$\delta_1 = \delta_4 = \delta_7 = \frac{1}{m_0} \quad \delta_2 = \delta_3 = \delta_5 = \delta_6 = \frac{h}{m_1} \tag{4.10}$$

This means m_0 and m_1 should always satisfy

$$\frac{3}{m_0} + \frac{4h}{m_1} = 1 \tag{4.11}$$

Case 1.

Consider fig (4.2a). We note that $\frac{1}{m_0} = h$. Solving this relation with equation eq.(4.11), we get

$$m_0 = \frac{1}{h} \quad m_1 = \frac{4h}{1-3h} \quad (4.12)$$

Generalization permits the peak height h to vary continuously such that $\frac{1}{7} < h \leq \frac{1}{4}$. When h increases from $1/7$ to $1/4$, it can be noted that m_0 decreases from 7 to 4 whereas m_1 increases from 1 to 4 . Therefore, in the range of h given above, both m_0 and m_1 are greater than 1 and always $m_0 \geq m_1$ ensuring that map is 'everywhere expanding' Transition matrix $\overline{H}_{\mu\nu}$ and the generalised transition matrix $(\overline{H}_q)_{\mu\nu}$ are given by eq. (4.5) and eq.(4.9) respectively. We get

$$(\overline{H}_q)_{\mu\nu} = \begin{bmatrix} h & e^q & e^q & h & 0 & 0 & h \\ (\frac{1-3h}{4}) & 0 & 0 & (\frac{1-3h}{4}) & 0 & 0 & (\frac{1-3h}{4}) \\ (\frac{1-3h}{4}) & 0 & 0 & (\frac{1-3h}{4}) & 0 & 0 & (\frac{1-3h}{4}) \\ h & 0 & 0 & h & 0 & 0 & h \\ (\frac{1-3h}{4}) & 0 & 0 & (\frac{1-3h}{4}) & 0 & 0 & (\frac{1-3h}{4}) \\ (\frac{1-3h}{4}) & 0 & 0 & (\frac{1-3h}{4}) & 0 & 0 & (\frac{1-3h}{4}) \\ h & 0 & 0 & h & e^{-q} & e^{-q} & h \end{bmatrix} \quad (4.13)$$

$q = 0$ in the above matrix gives $\overline{H}_{\mu\nu}$ which can be used for obtaining invariant probabilities p_ν (eq. (4.7)). We get

$$p_1 = p_7 = \frac{(1-h)}{2(2-3h)} \quad p_2 = p_3 = p_5 = p_6 = \frac{(1-3h)}{4(2-3h)} \quad \text{and} \quad p_4 = \frac{h}{(2-3h)} \quad (4.14a)$$

Using eq (4.8), the invariant densities can be evaluated as

$$\rho_1 = \rho_7 = \frac{(1-3h)}{2h(2-3h)} \quad \rho_2 = \rho_3 = \rho_4 = \rho_5 = \rho_6 = \frac{1}{(2-3h)} \quad (4.14b)$$

Note that p_ν and $\rho_\nu, \nu = 1, 2, \dots, \bar{\tau}$ are all positive. Hence Lyapunov exponent evaluated from $\lambda = \sum_\nu \ln |m_\nu| p_\nu$ is positive ensuring that the map is fully chaotic. Solution of the eigenvalue equation for \bar{H}_q shows that five out of the seven eigenvalues are zeros. The remaining 2 eigen values are the solutions of the quadratic equation.

$$o_q^2 - 3ho_q - (1 - 3h) \cosh q = 0 \quad (4.15)$$

We have

$$o_q = \frac{3h \pm \sqrt{9h^2 + 4(1 - 3h) \cosh q}}{2} \quad (4.16)$$

Hence, from eq. (1.67),

$$\lambda_q = \frac{1}{q} \ln \frac{3h + \sqrt{9h^2 + 4(1 - 3h) \cosh q}}{2} \quad (4.17)$$

Drift velocity λ_0 and diffusion coefficient D can be evaluated from λ_q using eq. (1.31).

$$\lambda_0 = \lim_{q \rightarrow 0} \lambda_q = 0 \quad (4.18)$$

$$D = \lim_{q \rightarrow 0} \frac{d\lambda_q}{dq} = \frac{(1 - 3h)}{2(2 - 3h)} \quad (4.19)$$

It can be noted that for $h = \frac{1}{4}$ (ie. $m_0 = m_1$) the above expression for D reduces to $D = 0.1$, the result obtained previously in [96].

Case 2.

On examining fig (4.2b) it can be noted that $\frac{1}{m_0} + \frac{h}{m_1} = h$. This relation can be solved with eq.(4.11) and we get

$$m_0 = \frac{1}{4h - 1} \quad m_1 = \frac{h}{1 - 3h} \quad (4.20)$$

In this case h varies such that $\frac{1}{4} < h \leq \frac{\sqrt{5}-1}{4}$. When h increases from $\frac{1}{4}$ to $\frac{\sqrt{5}-1}{4}$, m_0 decreases from infinity to $(\sqrt{5} + 2)$, whereas m_1 increases from 1 to $(\sqrt{5} + 2)$. Hence in the above range of h , m_0 and m_1 are greater than 1 and always $m_0 \geq m_1$. Thus the reduced map is expanding everywhere. Transition matrix $\overline{H}_{\mu\nu}$ and the generalised transition matrix $(\overline{H}_q)_{\mu\nu}$ can be considered as in case 1. Invariant probabilities evaluated from $\overline{H}_{\mu\nu}$ (eq. (4.7)) are

$$p_1 = p_7 = \frac{(4h - 1)}{(6h - 1)} \quad p_2 = p_6 = \frac{(1 - 3h)}{(6h - 1)}$$

$$p_3 = p_5 = \frac{(1 - 3h)(4h - 1)}{(1 - 2h)(6h - 1)} \quad p_4 = \frac{(4h - 1)^2}{(1 - 2h)(6h - 1)} \quad (4.21a)$$

Invariant densities, ρ_ν become (eq.(4.8))

$$\rho_1 = \rho_2 = \rho_6 = \rho_7 = \frac{1}{6h - 1} \quad \rho_3 = \rho_4 = \rho_5 = \frac{(4h - 1)}{(1 - 2h)(6h - 1)} \quad (4.21b)$$

p_ν and ρ_ν , $\nu = 1, 2, \dots, 7$ are all positive which means Lyapunov exponent λ is positive. Thus the map is fully chaotic. On solving the eigen value equation for \overline{H}_q , we find that four eigenvalues are zeros. The remaining 3 are to be obtained as the solutions of the general cubic equation.

$$\phi_q^3 + A\phi_q^2 + B\phi_q + C = 0 \quad (4.22)$$

With

$$A = -[3(4h - 1) + \frac{2(1 - 3h)}{h} \cosh q]$$

$$B = \frac{(1 - 3h)^2}{h^2} + 2(4h - 1)\left(\frac{1 - 3h}{h}\right) \cosh q \quad C = (4h - 1)\frac{(1 - 3h)^2}{h^2} \quad (4.23)$$

Though the general cubic equation can be solved by Cardon's method, we note that for arbitrary values of h and q , the solution will be very cumbersome. But, for

evaluating analytical expression for D , the solution with $q = 0$ is sufficient. The solution set is $\{1, \frac{(1-3h)}{h}, -(4h-1)\frac{(1-3h)}{h}\}$. The maximum among these solutions is 1. That is, $\phi_q^{(0)}$, the maximum eigenvalue required for the evaluation of λ_q (eq. (1.67)) satisfy eq. (4.22) and reduces to $\phi_0^{(0)} = 1$ as $q \rightarrow 0$. In this case it is easy to show that the limits yielding drift velocity λ_0 and diffusion coefficient D can be expressed in terms of $(\frac{d\phi_q^{(0)}}{dq})_{q=0}$ and $(\frac{d^2\phi_q^{(0)}}{dq^2})_{q=0}$. These can be got by differentiating the equation satisfied by $\phi_q^{(0)}$ and also applying $\phi_0^{(0)} = 1$. We get

$$\lambda_0 = (\frac{d\phi_q^{(0)}}{dq})_{q=0} = - \left[\frac{\frac{d}{dq}(A+B)}{(3+2A+B)} \right]_{q=0} \tag{4.24}$$

$$D = \frac{1}{2} (\frac{d^2\phi_q^{(0)}}{dq^2})_{q=0} = -\frac{1}{2} \left[\frac{\frac{d^2}{dq^2}(A+B)}{(3+2A+B)} \right]_{q=0} \tag{4.25}$$

For the present case, we obtain the following values

$$\lambda_0 = 0 \tag{4.26}$$

$$D = \frac{2h(3h-1)(1-2h)}{48h^3 - 44h^2 + 12h - 1} \tag{4.27}$$

It can be easily verified that the above expression for D reduces to $D = \frac{1}{10}\sqrt{5}$ for $h = \frac{\sqrt{5}-1}{4}$ ($m_0 = m_1$), the result obtained previously in [96].

Case 3.

We consider fig (4.2c), In addition to the relation given by eq. (4.11), we note $\frac{1}{m_0} = 1 - 2h$. On solving,

$$m_0 = \frac{1}{1-2h} \quad m_1 = \frac{2h}{3h-1} \tag{4.28}$$

In this case $(\frac{\sqrt{17}-1}{8}) \leq h < 0.5$. When h increases from the lower limit to the upper limit, m_0 increases from $(\frac{4}{5-\sqrt{17}})$ to infinity whereas m_1 decreases from $\frac{4}{5-\sqrt{17}}$ to 2. Hence in the above range of h , m_0 and m_1 are greater than 1 and always $m_0 \geq m_1$. The invariant probabilities got from $\overline{H}_{\mu\nu}$ are

$$p_1 = p_7 = \frac{(1-2h)h}{6h^2-4h+1} \quad p_2 = p_3 = p_5 = p_6 = \frac{(3h-1)h}{2(6h^2-4h+1)} \\ p_4 = \frac{(1-2h)^2}{6h^2-4h+1} \quad (4.29a)$$

From p_ν , one can obtain the invariant densities,

$$\rho_1 = \rho_2 = \rho_3 = \rho_5 = \rho_6 = \rho_7 = \frac{h}{(6h^2-4h+1)} \quad \rho_4 = \frac{(1-2h)}{(6h^2-4h+1)} \quad (4.29b)$$

Since these are all positive, λ is positive. Thus, the reduced map is an expanding map and is fully chaotic. Solution of the eigenvalue equation of (\overline{H}_q) reveals that four eigenvalues are zeros. The remaining 3 eigenvalues are obtainable as the solutions of the general cubic given by eq. (4.22) with

$$A = -[3(1-2h) + \frac{2(3h-1)}{h} \cosh q] \\ B = \frac{(3h-1)^2}{h^2} + 4\frac{(1-2h)(3h-1)}{h} \cosh q \\ C = -(1-2h)\frac{(3h-1)^2}{h^2} \quad (4.30)$$

The solution set of eq. (4.22) with $q = 0$ is $\{1, \frac{(3h-1)}{h}, (1-2h)\frac{(3h-1)}{h}\}$. As in case 2, we note that in this case also $\varphi_0^{(0)} = 1$. Hence λ_0 and D can be evaluated using equations (4.24) and (4.25). We get

$$\lambda_0 = 0 \quad (4.31)$$

$$D = \frac{h(12h^2 - 7h + 1)}{(-12h^3 + 14h^2 - 6h + 1)} \quad (4.32)$$

The result presented in [96], $D = \frac{2}{17}\sqrt{17}$, can be obtained as a special case from eq. (4.32) by putting $h = \frac{\sqrt{17}-1}{8}$, the case with $m_0 = m_1$.

Case 4.

From fig (4.2d) we note that $h + \frac{2h}{m_1} + \frac{1}{m_0} = 1$. Solving this relation with eq. (4.11), we get

$$m_0 = \frac{1}{2h-1} \quad m_1 = \frac{2h}{2-3h} \quad (4.33)$$

It is easy to note that $0.5 < h \leq \frac{\sqrt{33}-1}{8}$. When h increases from 0.5 to $\frac{\sqrt{33}-1}{8}$, m_0 decreases from infinity to $\frac{4}{\sqrt{33}-5}$ whereas m_1 increases from 2 to $\frac{4}{\sqrt{33}-5}$. Thus $m_0, m_1 > 1$ and always $m_0 \geq m_1$ in the range of h shown. As in previous cases, $\overline{H}_{\mu\nu}$ gives the invariant probabilities.

$$p_1 = p_7 = \frac{(2h-1)h}{2(3h-1)(1-h)} p_2 = p_3 = p_5 = p_6 = \frac{(2-3h)h}{4(3h-1)(1-h)} \quad (4.34a)$$

$$p_4 = \frac{(2h-1)}{(3h-1)}$$

Invariant densities, in this case, are

$$\rho_1 = \rho_2 = \rho_3 = \rho_5 = \rho_6 = \rho_7 = \frac{h}{2(3h-1)(1-h)} \quad \rho_4 = \frac{1}{(3h-1)} \quad (4.34b)$$

λ is positive, since p_ν and ρ_ν all are positive. Hence the reduced map is fully chaotic. Eigen value equation of (\overline{H}_q) shows that four eigenvalues are zeros. The

remaining 3 eigenvalues are the solutions of the general cubic eq. (4.22) with

$$A = -[3(2h-1) + \frac{2(2-3h)}{h} \cosh q] \quad B = \frac{(2-3h)^2}{h^2} + 2(2h-1) \frac{(2-3h)}{h} \cosh q$$

$$C = (2h-1) \frac{(2-3h)^2}{h^2} \quad (4.35)$$

For $q = 0$, the solution set is $\{1, \frac{(2-3h)}{h}, -(2h-1)\frac{(2-3h)}{h}\}$. $\phi_0^{(0)} = 1$ and therefore λ_0 and D can be evaluated using equations eq. (4.24) and eq. (4.25). We get

$$\lambda_0 = 0 \quad (4.36)$$

$$D = \frac{h(2-3h)(1-h)}{2(-6h^3 + 11h^2 - 6h + 1)} \quad (4.37)$$

It is an easy matter to verify that the above expression reduces to $D = 1/8 + \frac{5}{88} \sqrt{33}$ when $h = \frac{\sqrt{33}-1}{8}$ (ie, $m_0 = m_1$), obtained previously in [96].

Case 5.

One can note from Fig(4.2e) that $h + \frac{h}{m_1} + \frac{h}{m_0} = 1$. On solving this relation with eq. (4.11), we have

$$m_0 = \frac{1}{3-4h} \quad m_1 = \frac{h}{3h-2} \quad (4.38)$$

In this generalisation we allow h to vary in the range $\frac{1}{\sqrt{2}} \leq h < 0.75$. When h is increasing from $\frac{1}{\sqrt{2}}$ to .75, m_0 increases from $3 + 2\sqrt{2}$ to infinity whereas m_1 decreases from $3 + 2\sqrt{2}$ to 3. This means in the above range of h $m_0, m_1 > 1$ ($m_0 \geq m_1$) ie, the map is an expanding one. Invariant probabilities obtained from $\overline{H}_{\mu\nu}$ are

$$p_1 = p_7 = \frac{(1-h)(3-4h)}{(6h^2 - 8h + 3)} \quad p_2 = p_6 = \frac{(3h-2)(1-h)}{(6h^2 - 8h + 3)}$$

$$p_3 = p_5 = \frac{(2h-1)(3h-2)}{(6h^2 - 8h + 3)} \quad p_4 = \frac{(2h-1)(3-4h)}{6h^2 - 8h + 3} \quad (4.39a)$$

We get the invariant densities as

$$\rho_1 = \rho_2 = \rho_6 = \rho_7 = \frac{(1-h)}{(6h^2 - 8h + 3)} \quad \rho_3 = \rho_4 = \rho_5 = \frac{(2h-1)}{(6h^2 - 8h + 3)} \quad (4.39b)$$

p_ν and ρ_ν are positive ensuring that λ is positive. So, the map is fully chaotic. On solving the eigenvalue equation of (\overline{H}_q) we note that four eigenvalues are zeros. The remaining 3 are the solutions of the general cubic eq. (4.22) with

$$\begin{aligned} A &= -[3(3-4h) + 4\frac{(3h-2)}{h} \cosh q] \\ B &= 3\frac{(3h-2)^2}{h^2} + 4(3-4h)\frac{(3h-2)}{h} \cosh q \\ C &= -(3-4h)\frac{(3h-2)^2}{h^2} \end{aligned} \quad (4.40)$$

when $q = 0$ the solution set reduces to $\{1, \frac{3h-2}{h}, (3-4h)\frac{(3h-2)}{h}\}$. That is, $\phi_0^{(0)} = 1$. Hence λ_0 and D can be evaluated using eqs. (4.24) and (4.25). We get

$$\lambda_0 = 0 \quad (4.41)$$

$$D = \frac{h(3h-2)(2h-1)}{14h^2 - 6h^3 - 11h + 3} \quad (4.42)$$

When $m_0 = m_1$, $h = \frac{1}{\sqrt{2}}$. Eq. (4.42) gives $D = \frac{1}{4}\sqrt{2}$, the result reported in [96].

Case 6.

Finally we consider fig(4.2f). We have the relation $h + \frac{1}{m_0} = 1$ in addition to eq. (4.11). On solving

$$m_0 = \frac{1}{1-h} \quad m_1 = \frac{4h}{3h-2} \quad (4.43)$$

where we substituted $c_1 = \frac{3}{2}(1 - h)$; $c_2 = \frac{3h-2}{2h}$. From λ_q we can obtain λ_0 and D as

$$\lambda_0 = 0 \tag{4.48}$$

$$D = \frac{h(3h - 2)}{2(3h^2 - 4h + 2)} \tag{4.49}$$

This expression reduces to $D = \frac{1}{4} + \frac{1}{132}\sqrt{33}$ for $h = \frac{1+\sqrt{33}}{8}$ (ie $m_0 = m_1$), the result obtained previously in [96].

4.4 Variation of diffusion coefficient and fluctuation spectrum.

The figure (4.3) show the variation of D with parameter h . In all cases we note that the diffusion coefficient D increases when the peak-shape becomes flat. In figure 4.2(b, c, and d) this effect is found to be very remarkable. In these cases D -tends to infinity as the peak shape becomes maximum flat.

When the characteristic function λ_q is known, the fluctuation spectrum pertaining to the probability density function can be obtained in a parametric form effecting the Legendre transforms mentioned in subsection 1.2.4. We take case 6 as an example, though the conclusions are valid in all cases. Using eqs. (1.55) and (4.47) we have

$$\alpha = \frac{c_2 \sinh q [\sqrt{c_1^2 + c_2^2 \cosh^2 q + \frac{2c_1c_2}{3} \cosh q} + c_2 \cosh q + \frac{c_1}{3}]}{\sqrt{c_1^2 + c_2^2 \cosh^2 q + \frac{2c_1c_2}{3} \cosh q} \times [c_1 + c_2 \cosh q + \sqrt{c_1^2 + c_2^2 \cosh^2 q + \frac{2c_1c_2}{3} \cosh q}]} \tag{4.50}$$

$$\sigma(\alpha) = -\ln [c_1 + c_2 \cosh q + \sqrt{c_1^2 + c_2^2 \cosh^2 q + \frac{2c_1c_2}{3} \cosh q}] + q\alpha \tag{4.51}$$

When q is replaced by $-q$, α becomes $-\alpha$, $\sigma(\alpha)$ does not change, ie, $\sigma(\alpha)$ is a symmetric function of α . $\lim_{q \rightarrow \pm\infty} \alpha(\theta = \pm)$ give the extreme values of α . For

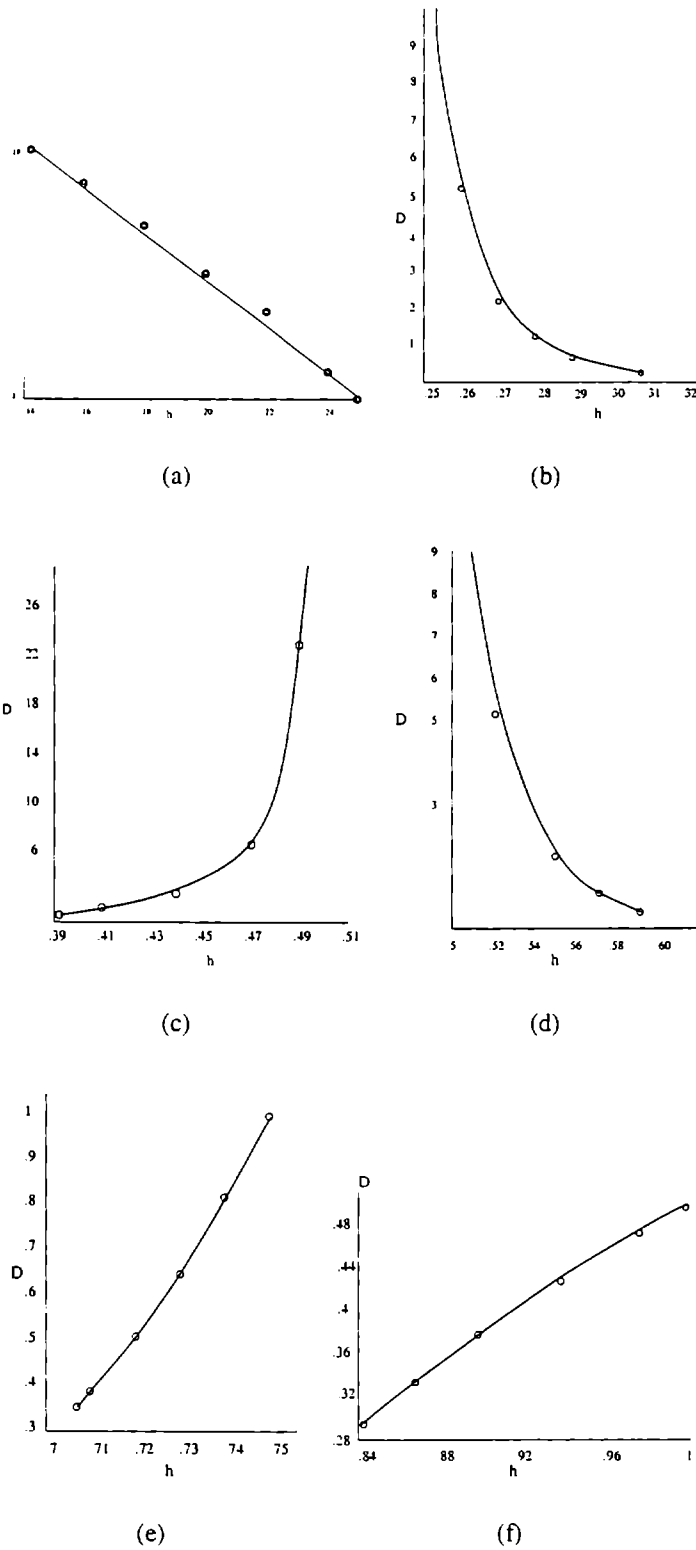


Figure 4.3: Variation of diffusion coefficient D with peak height h for the 6 cases of GPLM maps (a to f) in Fig. 4.2. On both axes units are arbitrary.

$|q| \ll b$, using eqs. (1.36) and (1.55), one can get $\sigma(\alpha)$ as a function of α . We get

$$\alpha = \lambda_0 + 2Dq \quad (4.52)$$

$$\sigma(\alpha) = \frac{(\alpha - \lambda_0)^2}{4D} \quad (4.53)$$

For the present case λ_0 and D are given by equations eq. (4.48) and eq. (4.49).

For $\theta q \gg b$, eqs. (1.55) and (1.59) give

$$\alpha \approx \lambda_{\theta\infty} - \theta c_{\theta} \eta_{\theta} \exp(-\eta_{\theta}|q|) \quad (4.54)$$

$$\sigma(\alpha) \approx \frac{1}{\tau_{\theta}} - \frac{1}{\eta_{\theta}} |\alpha - \lambda_{\theta\infty}| \ln \left[\frac{a_{\theta}}{|\alpha - \lambda_{\theta\infty}|} \right] \quad (4.55)$$

where $\eta_{\theta} \sim O(\frac{1}{b})$ and $a_{\theta} \equiv e c_{\theta} \eta_{\theta}$. For case 6 we get the following values.

$$\lambda_{+\infty} = 1; \quad \tau_{+} = \tau_{-} = \frac{1}{\ln(\frac{2h}{3h-2})}; \quad c_{+} = c_{-} = \frac{4h(1-h)}{(3h-2)}; \quad \eta_{+} = \eta_{-} = 1 \quad (4.56)$$

$$\lambda_{-\infty} = -1$$

The probability distribution function for N_t , the distance from the origin, can be obtained using the fluctuation spectrum $\sigma(\alpha)$. From eq. (1.53) we have

$$P_t(N) \sim \frac{1}{\sqrt{t}} \exp[-\sigma(\frac{N}{t})t] \quad (4.57)$$

$P_t(N)$ being the PDF that N_t takes values between N and $N + dN$. This PDF is approximately Gaussian by central limit theorem. In fact eq. (4.53) gives the part of $\sigma(\alpha)$ corresponding to the Gaussian part of the PDF, which is valid for $|q| \ll b$, ie, low absolute values of α . In fig(4.4) we plot $\sigma(\alpha)$ against α . For comparison the Gaussian form eq. (4.53) also is shown. When α approaches extreme points deviation from Gaussian character is noticed. At these points figure 4.4

and eq. (4.55) show that the derivative $\frac{d\sigma(\alpha)}{d\alpha}$ diverges logarithmically. For Gaussian approximation to hold good in this part of the curve one has to maximise the slope. Since slope is inversely proportional to D (eq. (4.53)) we note that Gaussian character will become more pronounced when D is a minimum. That is, for a particular kind of Markov map, maps with sharp peaks exhibit more Gaussian character than those with flat peaks.

4.5 Results and conclusions.

From the observations made above, we note that the shape of the map has considerable influence in determining the diffusion coefficient and the PDF. For all GPLM maps, the Gaussian character of the PDF will become stronger when the diffusion coefficient D is a minimum which happens when the peak-shape becomes sharp. Conversely, when the maps become more and more flat, non-Gaussian character of the PDF predominates as a result of intermittency. This fact becomes important in time series analysis of experimental data of chaotic systems exhibiting deterministic diffusion [113]. For describing chaotic motion similar to Brownian motion, maps showing Gaussian PDF is necessary. GPLM maps with constant slope are more suited for this. On the contrary, for systems showing intermittency maps with flat peaks will have to be preferred.

We note that in maps shown in figures 4.2 (b, c and d) diffusion coefficient tends to infinity as the peak-shape becomes maximum flat. This remarkable dependence is to be attributed to the effect of pruning. For example, in fig 4.2b we note that the probability for the phase point to move from one short line segment with $\Delta(x) = +1$ to another short line segment $\Delta(x) = -1$ is reduced when the peak-shape becomes flat. This means, the probability for jumping numbers cancelling each other becomes less resulting in large value of N_i . Standard deviation of N_i increases and this leads to large value of diffusion coefficient.

Considering the variation of D with the height of the map (when the line seg-

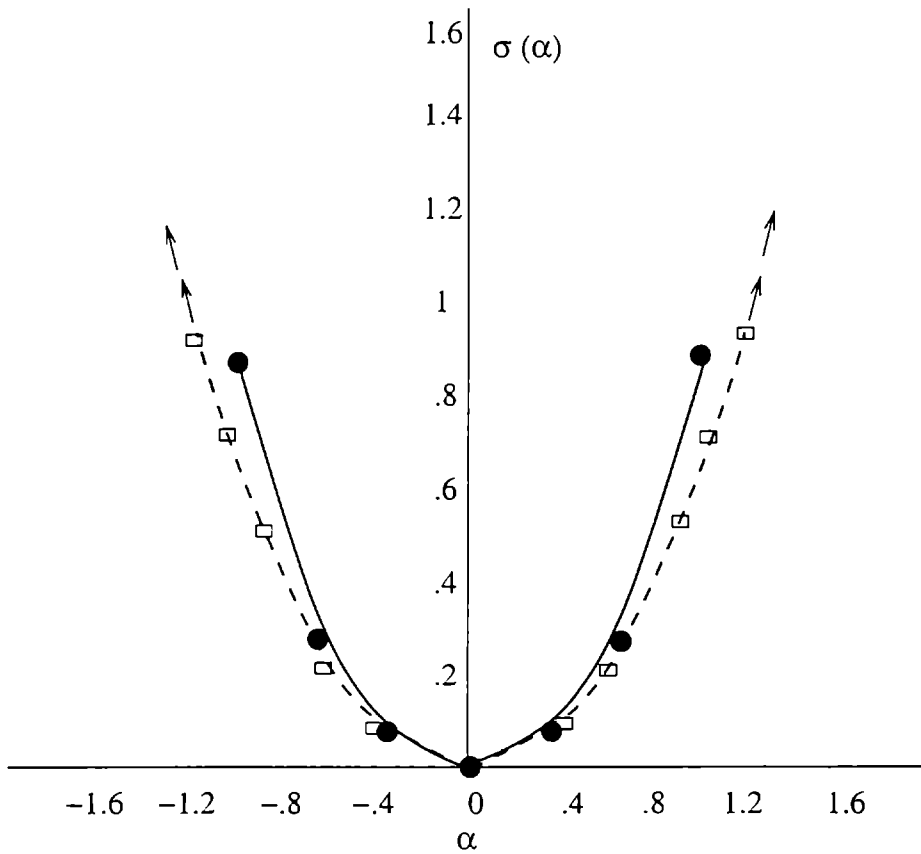


Figure 4.4: Fluctuation spectrum $\sigma(\alpha)$ vs α for the map shown in Fig. 4.2(f) [$h = 0.9$]. Solid line with black dots represents actual $\sigma(\alpha)$ while the dotted line with small squares gives the corresponding Gaussian form. On both axes units are arbitrary.

ments have the same slope), we note that there is a difference between the present case and the generalized piecewise linear (GPL) map discussed in chapter 3. In the GPL map it was found that as the peak-height (taking integer values) is increased, D increases appreciably. When $m_0 = m_1$, in the case of GPLM maps, D increases first with height, and then it decreases. D for case 3 has a maximum value of 0.48507. For case 1 and 6 it is 0.1 and 0.29351 respectively. This is understandable because in the case of GPLM map, no change in jump numbers occur as height is increased. The remarkable increase in diffusion coefficient is solely due to the change in invariant density.

In this paper, we have shown that for a wide range of fractional peak height ' h ' in the interval $[0, 1]$ an exactly solvable GPLM model exists. The ranges of h for which maps are not available are $[0-0.142]$, $[0.3125-0.39]$, $[0.594-0.7]$, $[.75-.84]$. The range $[0-0.142]$ has been excluded in case 1, since in this range of h , the GPLM map will not be expanding everywhere since m_1 is less than 1. For all other cases in the interval $[0, 1]$ a GPLM map exists when the parameter h is varied continuously. Our generalized maps are very good approximations for sine maps which can be treated only numerically. Looking through literature we note that so far there has been no such analytical results for exactly solvable maps when peak-height is varied continuously. We expect that these models will be very useful in time series analysis of [113] chaotic systems showing diffusion.

Finally we want to make a comment regarding the conclusion in ref [98], where a piecewise linear mapping with Markov partition has been shown to exhibit a fractal diffusion coefficient as the peak-height h is varied. The conjecture of the authors that fractal nature might be a characteristic of all piecewise linear maps is not justifiable since D is analytical and exact in all of our GPLM maps. We note that fractal nature of D stems from the fact that piecewise linear mappings of [98] have line segments with equal slopes. When line segments have equal slopes, Markov partitioning will be different for different values of h , resulting in a change in the order of the transition matrix. In our GPLM maps, we

have considered line segments with unequal slopes so that Markov partitioning and order of the transition matrix will not change. When h is varied, there will be no topological instability and hence GPLM maps do not give rise to fractal diffusion coefficient.

4.6 Appendix A.

It is easy to prove that the operator H can be represented by a 7×7 matrix as far as it operates on a step function on the Markov partition. For example note that invariant density $\rho(x)$ is a step function. We define

$$K_\mu(x) = \begin{cases} 1 & \text{if } x \in I_\mu, \\ 0 & \text{otherwise} \end{cases} \quad (\text{A1})$$

Then any step function $G(x)$ can be written as $G(x) = \sum_{\mu=1}^7 G_\mu K_\mu(x)$. Further let us define

$$\Gamma_{\mu\nu} = \begin{cases} 1 & \text{if } f(I_\nu) \supseteq I_\mu, \\ 0 & \text{otherwise} \end{cases} \quad (\text{A2})$$

Then

$$HK_\mu(x) = \sum_\nu K_\mu(x) \Gamma_{\mu\nu} |f'_\nu|^{-1} \quad (\text{A3})$$

$$HG(x) = \sum_\mu \sum_\nu G_\mu K_\mu(x) \Gamma_{\mu\nu} |f'_\nu|^{-1} = \sum_\mu \tilde{G}_\mu K_\mu(x) \quad (\text{A4})$$

where f'_ν denotes the value of the slope $f'(x)$ in the partition I_ν and

$$\tilde{G}_\mu = \sum_\nu G_\nu \Gamma_{\mu\nu} |f'_\nu|^{-1} \quad (\text{A5})$$

We find that the operator H transforms a step function $G(x)$ to a step function $\tilde{G}(x) = \sum_{\mu} \tilde{G}_{\mu} K_{\mu}(x)$. This means that H can be represented by $\bar{\tau} \times \bar{\tau}$ matrix

$$H_{\mu\nu} = \Gamma_{\mu\nu} |f'_{\nu}|^{-1} \quad (\text{A6})$$

4.7 Appendix B.

We give below the generalized transition matrix $(\bar{H}_q)_{\mu\nu}$ for the different cases from 2 to 6.

Case 2.

$$(\bar{H}_q)_{\mu\nu} = \begin{bmatrix} (4h-1) & \frac{(4h-1)e^q}{h} & \frac{(4h-1)e^q}{h} & (4h-1) & 0 & 0 & (4h-1) \\ (1-3h) & \frac{(1-3h)e^q}{h} & \frac{(1-3h)e^q}{h} & (1-3h) & 0 & 0 & (1-3h) \\ (1-3h) & 0 & 0 & (1-3h) & 0 & 0 & (1-3h) \\ (4h-1) & 0 & 0 & (4h-1) & 0 & 0 & (4h-1) \\ (1-3h) & 0 & 0 & (1-3h) & 0 & 0 & (1-3h) \\ (1-3h) & 0 & 0 & (1-3h) & \frac{(1-3h)e^{-q}}{h} & \frac{(1-3h)e^{-q}}{h} & (1-3h) \\ (4h-1) & 0 & 0 & (4h-1) & \frac{(4h-1)e^{-q}}{h} & \frac{(4h-1)e^{-q}}{h} & (4h-1) \end{bmatrix}$$

Case 3.

$$(\bar{H}_q)_{\mu\nu} = \begin{bmatrix} (1-2h) & \frac{(1-2h)e^q}{h} & \frac{(1-2h)e^q}{h} & (1-2h) & 0 & 0 & (1-2h) \\ \frac{(3h-1)}{2} & \frac{(3h-1)e^q}{2h} & \frac{(3h-1)e^q}{2h} & \frac{(3h-1)}{2} & 0 & 0 & \frac{(3h-1)}{2} \\ \frac{(3h-1)}{2} & \frac{(3h-1)e^q}{2h} & \frac{(3h-1)e^q}{2h} & \frac{(3h-1)}{2} & 0 & 0 & \frac{(3h-1)}{2} \\ (1-2h) & 0 & 0 & (1-2h) & 0 & 0 & (1-2h) \\ \frac{(3h-1)}{2} & 0 & 0 & \frac{(3h-1)}{2} & \frac{(3h-1)e^{-q}}{2h} & \frac{(3h-1)e^{-q}}{2h} & \frac{(3h-1)}{2} \\ \frac{(3h-1)}{2} & 0 & 0 & \frac{(3h-1)}{2} & \frac{(3h-1)e^{-q}}{2h} & \frac{(3h-1)e^{-q}}{2h} & \frac{(3h-1)}{2} \\ (1-2h) & 0 & 0 & (1-2h) & \frac{(1-2h)e^{-q}}{h} & \frac{(1-2h)e^{-q}}{h} & (1-2h) \end{bmatrix}$$

Case 4.

$$(\overline{H}_q)_{\mu\nu} = \begin{bmatrix} (2h-1) & \frac{(2h-1)e^q}{h} & \frac{(2h-1)e^q}{h} & (2h-1) & 0 & 0 & (2h-1) \\ \frac{(2-3h)}{2} & \frac{(2-3h)e^q}{2h} & \frac{(2-3h)e^q}{2h} & \frac{(2-3h)}{2} & 0 & 0 & \frac{(2-3h)}{2} \\ \frac{(2-3h)}{2} & \frac{(2-3h)e^q}{2h} & \frac{(2-3h)e^q}{2h} & \frac{(2-3h)}{2} & 0 & 0 & \frac{(2-3h)}{2} \\ (2h-1) & \frac{(2h-1)e^q}{h} & \frac{(2h-1)e^q}{h} & (2h-1) & \frac{(2h-1)e^{-q}}{h} & \frac{(2h-1)e^{-q}}{h} & (2h-1) \\ \frac{(2-3h)}{2} & 0 & 0 & \frac{(2-3h)}{2} & \frac{(2-3h)e^{-q}}{2h} & \frac{(2-3h)e^{-q}}{2h} & \frac{(2-3h)}{2} \\ \frac{(2-3h)}{2} & 0 & 0 & \frac{(2-3h)}{2} & \frac{(2-3h)e^{-q}}{2h} & \frac{(2-3h)e^{-q}}{2h} & \frac{(2-3h)}{2} \\ (2h-1) & 0 & 0 & (2h-1) & \frac{(2h-1)e^{-q}}{h} & \frac{(2h-1)e^{-q}}{h} & (2h-1) \end{bmatrix}$$

Case 5.

$$(\overline{H}_q)_{\mu\nu} = \begin{bmatrix} (3-4h) & \frac{(3-4h)e^q}{h} & \frac{(3-4h)e^q}{h} & (3-4h) & 0 & 0 & (3-4h) \\ (3h-2) & \frac{(3h-2)e^q}{h} & \frac{(3h-2)e^q}{h} & (3h-2) & 0 & 0 & (3h-2) \\ (3h-2) & \frac{(3h-2)e^q}{h} & \frac{(3h-2)e^q}{h} & (3h-2) & \frac{(3h-2)e^{-q}}{h} & \frac{(3h-2)e^{-q}}{h} & (3h-2) \\ (3-4h) & \frac{(3-4h)e^q}{h} & \frac{(3-4h)e^q}{h} & (3-4h) & \frac{(3-4h)e^{-q}}{h} & \frac{(3-4h)e^{-q}}{h} & (3-4h) \\ (3h-2) & \frac{(3h-2)e^q}{h} & \frac{(3h-2)e^q}{h} & (3h-2) & \frac{(3h-2)e^{-q}}{h} & \frac{(3h-2)e^{-q}}{h} & (3h-2) \\ (3h-2) & 0 & 0 & (3h-2) & \frac{(3h-2)e^{-q}}{h} & \frac{(3h-2)e^{-q}}{h} & (3h-2) \\ (3-4h) & 0 & 0 & (3-4h) & \frac{(3-4h)e^{-q}}{h} & \frac{(3-4h)e^{-q}}{h} & (3-4h) \end{bmatrix}$$

Case 6.

$$(\overline{H}_q)_{\mu\nu} = \begin{bmatrix} (1-h) & \frac{(1-h)e^q}{h} & \frac{(1-h)e^q}{h} & (1-h) & 0 & 0 & (1-h) \\ \frac{(3h-2)}{4} & \frac{(3h-2)e^q}{4h} & \frac{(3h-2)e^q}{4h} & \frac{(3h-2)}{4} & \frac{(3h-2)e^{-q}}{4h} & \frac{(3h-2)e^{-q}}{4h} & \frac{(3h-2)}{4} \\ \frac{(3h-2)}{4} & \frac{(3h-2)e^q}{4h} & \frac{(3h-2)e^q}{4h} & \frac{(3h-2)}{4} & \frac{(3h-2)e^{-q}}{4h} & \frac{(3h-2)e^{-q}}{4h} & \frac{(3h-2)}{4} \\ (1-h) & \frac{(1-h)e^q}{h} & \frac{(1-h)e^q}{h} & (1-h) & \frac{(1-h)e^{-q}}{h} & \frac{(1-h)e^{-q}}{h} & (1-h) \\ \frac{(3h-2)}{4} & \frac{(3h-2)e^q}{4h} & \frac{(3h-2)e^q}{4h} & \frac{(3h-2)}{4} & \frac{(3h-2)e^{-q}}{4h} & \frac{(3h-2)e^{-q}}{4h} & \frac{(3h-2)}{4} \\ \frac{(3h-2)}{4} & \frac{(3h-2)e^q}{4h} & \frac{(3h-2)e^q}{4h} & \frac{(3h-2)}{4} & \frac{(3h-2)e^{-q}}{4h} & \frac{(3h-2)e^{-q}}{4h} & \frac{(3h-2)}{4} \\ (1-h) & 0 & 0 & (1-h) & \frac{(1-h)e^{-q}}{h} & \frac{(1-h)e^{-q}}{h} & (1-h) \end{bmatrix}$$

Chapter 5.

Periodic orbits and the complementary dynamics of diffusion and intermittency in chaotic maps.

5.1 Introduction.

In chapter 3 and 4, we introduced two classes of spatially extended maps climbing along the bisector — GPL maps and GPLM maps — exhibiting deterministic diffusion. We introduced these maps by generalising the maps studied by R. Artuso and Tseng et al. GPL maps have variable peak-shape and can take integer peak-heights. GPLM maps also have variable peak-shape but peak-height in this case can take fractional values less than unity. For analysing the chaotic motion and its shape dependence in these maps, we applied the characteristic function method introduced by Fujisaka and his co-workers. We found that this method is a better tool than the cycle expansion technique applied by Artuso and Tseng et.al. Cycle expansion, it appears, aims only at the evaluation of exact diffusion coefficient.

But, as we have seen, the chaotic motion in such spatially extended maps has two complementary aspects — diffusion and intermittency. Characteristic function method is a powerful tool for analysing both these aspects of stochasticity in such maps. It can be noted that this method can be applied to study other types of chaos-induced diffusion like the one produced by fluctuations of local expansion rates (LER).

One can note that there is a close connection between the characteristic function method and the cycle expansion technique. Though this connection between cycle expansion technique and characteristic function method has been hinted in literature [77, 79], we note that it can be exploited further so as to enhance the applicability of cycle expansion technique. In this paper we show how periodic orbits can be used for analysing the probability density function (PDF) of chaotic maps. PDF based on fluctuation spectrum can be used for studying not only diffusion but intermittency aspects of chaotic motion also. Analysis of exactly solvable piecewise linear mappings has been added as illustrative examples for both types of dynamics referred to above - chaotic diffusion in spatially extended maps and the one associated with LER (statistics of trajectory separation). Periodic orbit expansion is a perturbation theory and can be applied to even situations where analytical treatment is not possible. Hence an attempt for enhancing the applicability of cycle expansion technique assumes significance. Moreover, an approach based on periodic orbits will play a major role in understanding quantum counterpart of classical chaotic transport.

In section 5.2, we discuss the connection between Fujisaka's theory and cycle expansion technique. Then we show how cycle expansion can be used for obtaining the fluctuation spectrum relating to the PDF. In section 5.3, illustrative examples are presented. Section 5.4 is devoted to results and conclusions.

5.2 Probability density function via periodic orbits.

The salient features of the characteristic function based theory of diffusion and intermittency developed by Fujisaka et al have been presented in chapter 1. Some of the most important relations appearing in the theory are rewritten below for the sake of completeness.

Using characteristic function, one can study the dynamics of A_t governed by

$$A_{t+1} = B(x_t)A_t \quad t = 0, 1, 2, \quad (5.1)$$

with $A_0 = 1$. $B(x_t)$ is a steady positive-definite function of x_t evolving according to the chaotic map

$$x_{t+1} = f(x_t) \quad (0 \leq x_t < 1) \quad (5.2)$$

Equivalently, one can study the dynamics of the local time average α_t of a time series $\{u_j\} = u_0 \cdot u_1 \cdot u_2 \cdot u_3$

$$\alpha_t = \frac{1}{t} \sum_{j=0}^{t-1} u_j \quad (5.3)$$

where $u_j = u(x_j) = \ln B(x_j)$. The long time dynamics of A_t (or α_t) can be analysed using λ_q , the characteristic function

$$\lambda_q = \frac{1}{q} \lim_{t \rightarrow \infty} \frac{1}{t} \ln \langle A_t^q \rangle = \frac{1}{q} \lim_{t \rightarrow \infty} \frac{1}{t} \ln \langle \exp (qt\alpha_t) \rangle \quad (5.4)$$

$\langle A_t^q \rangle$ is the average over a steady ensemble and is the q -order moment of A_t . Cumulant expansion of λ_q converges for $|q| \ll b$, where b is the convergence radius. In this range of q we can make the approximation

$$\lambda_q = \lambda_0 + Dq \quad (5.5)$$

λ_0 is the long time average $\alpha_\infty = \lim_{t \rightarrow \infty} 1/t \sum_{j=0}^{t-1} u_j$ which is no longer a fluc-

tuating quantity. It is called the drift velocity. D is the diffusion coefficient satisfying, $\langle(\alpha_t - \alpha_\infty)^2\rangle \approx \frac{2D}{t}$ for large t . On the other hand for $\theta q \gg b(\theta = \pm) \lambda_q$ can be set as

$$\lambda_q \simeq \lambda_{\theta\infty} - \frac{1}{q} \left[\frac{1}{\tau_\theta} - c_\theta \exp(-\eta_\theta |q|) \right] \tag{5.6}$$

where τ_θ, c_θ and η_θ are positive constants.

For evaluating λ_q one has to solve the eigenvalue equation for the linear operator H_q defined by (eq. (1.63))

$$H_q G(x) = \int_0^1 \delta(f(y) - x) e^{qu(y)} G(y) dy = H[e^{qu(x)} G(x)] \tag{5.7}$$

$H_0 = H$ gives the operator defined by eq. (1.12). Let the eigenvalues $\phi_q^{(n)}$, $n = 0, 1, 2 \dots$ be ordered as $\phi_q^{(0)} \geq |\phi_q^{(1)}| \geq |\phi_q^{(2)}|$. Then,

$$\lambda_q = \frac{1}{q} \ln \phi_q^{(0)} \tag{5.8}$$

where $\phi_q^{(0)} = \max_n \{ \text{Re } \phi_q^{(n)} \}$.

In order to determine the spectrum of H_q one can study the Fredholm determinant $d(z) = [1 - zH_q]$ for complex z . It's zeros give the reciprocal eigenvalues of H_q . To evaluate d , one can use the standard relations [77].

$$d = \det[1 - zH_q] = \exp \left[- \sum_{n=1}^{\infty} \frac{z^n}{n} \text{tr}(H_q)^n \right] \tag{5.9}$$

The technical utility of introducing Fredholm determinant stems from the possibility of expressing trace in eq.(5.9) in terms of fixed point of f^n . We can write [77, 113].

$$\text{tr}[(H_q)^n] = \sum_{x^* \in \text{fix}(f^n)} \frac{\exp(\sum_{j=0}^{n-1} [qu(f^j(x^*))])}{|1 - J|} \tag{5.10}$$

where $J \equiv D_x f^n|_{x=x^*}$ and the sum extends over the fixed points x^* of f^n . In

higher dimensional cases one has to replace $|1 - J|$ with $\det |1 - J|$. The summation over the fixed points of f^n can be converted to a summation over all the prime cycles in a standard way[77]. In general the n^{th} order trace picks up contributions from all repeats of prime cycles (a/b means that a is a divisor of b).

$$\text{tr}((H_q)^n) = \sum_{p, n_p/n} n_p t_p^{n/n_p} \quad (5.11)$$

p denoting a prime cycle with period n_p , t_p being the contribution from this prime cycle. Then [77]

$$\begin{aligned} \det[1 - zH_q] &= \exp\left(-\sum_p \sum_{r=1}^{\infty} \frac{(z^{n_p} t_p)^r}{r}\right) = \exp\left(\sum_p \ln(1 - z^{n_p} t_p)\right) \\ &= \prod_p (1 - z^{n_p} t_p) \end{aligned} \quad (5.12)$$

Note that t_p is given by the summand of eq. (5.10) with $n = n_p$ and $x^* = x_p$; x_p being one of the points in the prime cycle denoted by p . For expanding maps $|J| > 1$ so that

$$|1 - J|^{-1} = |J|^{-1} \sum_{m=0}^{\infty} J^{-m} \quad (5.13)$$

Making these substitutions, one can note from eq. (5.10) and eq. (5.12) that the Fredholm determinant d can be written as an infinite product of inverse ζ functions

$$d = \prod_{m=0}^{\infty} \zeta_m^{-1}(z, q) \quad (5.14)$$

where

$$\zeta_m^{-1}(z, q) = \prod_{p, x_p \in pc(f^p)} \left(1 - \frac{z^{n_p} \exp \sum_{j=0}^{n_p-1} (qu(f^j(x_p)))}{|J_p| J_p^m}\right) \quad (5.15)$$

Let z_q^i denote the zeros of d . If

$$z_q^{(0)} < |z_q^{(1)}| \leq |z_q^{(2)}| \leq \quad (5.16)$$

Then, we have

$$\lambda_q = \frac{1}{q} \ln \frac{1}{z_q^{(0)}} = -\frac{1}{q} \ln z_q^{(0)} \quad (5.17)$$

The asymptotic ($t \rightarrow \infty$) PDF of α_t has a Gaussian component resulting from central limit theorem and a non-Gaussian component. For $|q| \ll b$, the q -order moment in eq. (5.4) is determined by the Gaussian component. This range of q is the diffusion branch of q . When $|q| \gg b$, non-Gaussian component will predominate and this range of q is the intermittency branch. For writing the PDF $P_t(\alpha)$ where α_t takes the value between α and $\alpha + d\alpha$, one can use the fluctuation spectrum $\sigma(\alpha)$.

$$P_t(\alpha) \sim \sqrt{t} \exp(-\sigma(\alpha)t) \quad (5.18)$$

As $t \rightarrow \infty$, $P_t(\alpha) \rightarrow \delta(\alpha - \alpha_\infty)$. α and $\sigma(\alpha)$ can be obtained from λ_q in a parametric form.

$$\alpha = \frac{d}{dq}(q\lambda_q), \quad \sigma(\alpha) = q^2 \frac{d}{dq} \lambda_q \quad (5.19)$$

In terms of $z_q^{(0)}$ this becomes

$$\alpha = -\frac{1}{z_q^{(0)}} \frac{d}{dq} z_q^{(0)}, \quad \sigma(\alpha) = \ln z_q^{(0)} - \frac{q}{z_q^{(0)}} \frac{d}{dq} z_q^{(0)} \quad (5.20)$$

For $q \ll b$, λ_q is approximately given by eq. (5.5). In this case one can get

$$\alpha = \lambda_0 + 2Dq \quad (5.21)$$

$$\sigma(\alpha) = \frac{(\alpha - \lambda_0)^2}{4D} \quad (5.22)$$

where λ_0 and D can be evaluated using eq. (5.17).

$$\lambda_0 = \lim_{q \rightarrow 0} \lambda_q = - \lim_{q \rightarrow 0} \frac{1}{q} \ln z_q^{(0)} \quad (5.23)$$

$$D = \lim_{q \rightarrow 0} \frac{d\lambda_q}{dq} = - \lim_{q \rightarrow 0} \frac{d}{dq} \left(\frac{1}{q} \ln z_q^{(0)} \right) \quad (5.24)$$

For $\theta q \gg b$, ($\theta = \pm$) the approximation for λ_q (eq. (5.6)) leads to

$$\ln z_q^{(0)} \approx -q\lambda_{\theta\infty} + \left[\frac{1}{\tau_\theta} - c_\theta \exp(-\eta_\theta|q|) \right] \quad (5.25)$$

τ_θ , c_θ and η_θ being positive constants. Eq.(5.20) gives

$$\alpha \approx \lambda_{\theta\infty} - \theta c_\theta \eta_\theta \exp(-\eta_\theta|q|) \quad (5.26)$$

$$\sigma(\alpha) \approx \frac{1}{\tau_\theta} - \frac{1}{\eta_\theta} |\alpha - \lambda_{\theta\infty}| \ln \left[\frac{a_\theta}{|\alpha - \lambda_{\theta\infty}|} \right] \quad (5.27)$$

where $a_\theta \equiv e c_\theta \eta_\theta$. From $P_t(\alpha)$ one can obtain the distribution of $\ln A_t$ or A_t . PDF of α and $\ln A_t$ will be approximately Gaussian by central limit theorem but that of A_t will be log normal. In fact eq. (5.22) and eq. (5.27) give respectively the Gaussian and non-Gaussian components of the PDF. Thus, $\sigma(\alpha)$ can be used for studying the complementary dynamics of diffusion and intermittency in chaotic maps.

5.3 Illustrative examples.

5.3.1 Spatially extended piecewise linear maps.

As the first example, let us consider case 1 of the spatially extended maps (GPLM models) we analysed in chapter 4. The extended map shown in fig. 4.1 consists of

linear segments with slopes m_0 and m_1 , $m_1 \leq m_0$. For the cells on the bisector, the slope magnitude is m_0 . For cells above and below this bisector, the slope magnitude changes to m_1 . The peak height in these cells is represented as h . We know that climbing maps of this type can be represented as

$$X_{t+1} = X_t + P_r(X_t) = Y_r(X_t); \quad P_r(X + 1) = P_r(X) \quad (5.28)$$

r being the control parameter. With the decomposition $X_t = N_t + x_t$, where N_t is the cell number in which X_t is located and x_t , ($0 \leq x_t < 1$) the distance measured from the relative origin $X = N_t$, the above equation reduces to two dynamical laws

$$N_{t+1} = N_t + \Delta(x_t) \quad x_{t+1} = f(x_t) \quad (5.29)$$

$\Delta(x)$ is the jumping number defined as the largest integer smaller than $x + P_r(x)$ and is free from N_t and $f(x) = x + P_r(x) - \Delta(x)$, $0 \leq f(x) < 1$. $f(x)$ is the reduced map of the extended map. The reduced map corresponding to case 1 of GPLM maps (fig. 4.2a) is redrawn in fig. 5.1 in which solid lines represent $f(x)$ and the dotted lines show the Markov partitions. Extended map can be generated from the reduced map by giving suitable jump numbers $\Delta(x)$ (constant for a line segment). In chapter 4, we have considered this problem using Fujisaka's characteristic function method, by putting

$$A_t = \exp(N_t - N_0), \quad B(x) = e^{\Delta(x)} \quad u(x) = \Delta(x), \quad \alpha_t = \frac{N_t}{t} \text{ with } N_0 = 0 \quad (5.30)$$

Here we treat the problem within the context of cycle expansion. From eq. (5.15) we get

$$\zeta_m^{-1}(z, q) = \prod_p \left(1 - \frac{z^{n_p} \exp(\sigma_p q)}{|J_p| J_p^m} \right) \quad (5.31)$$

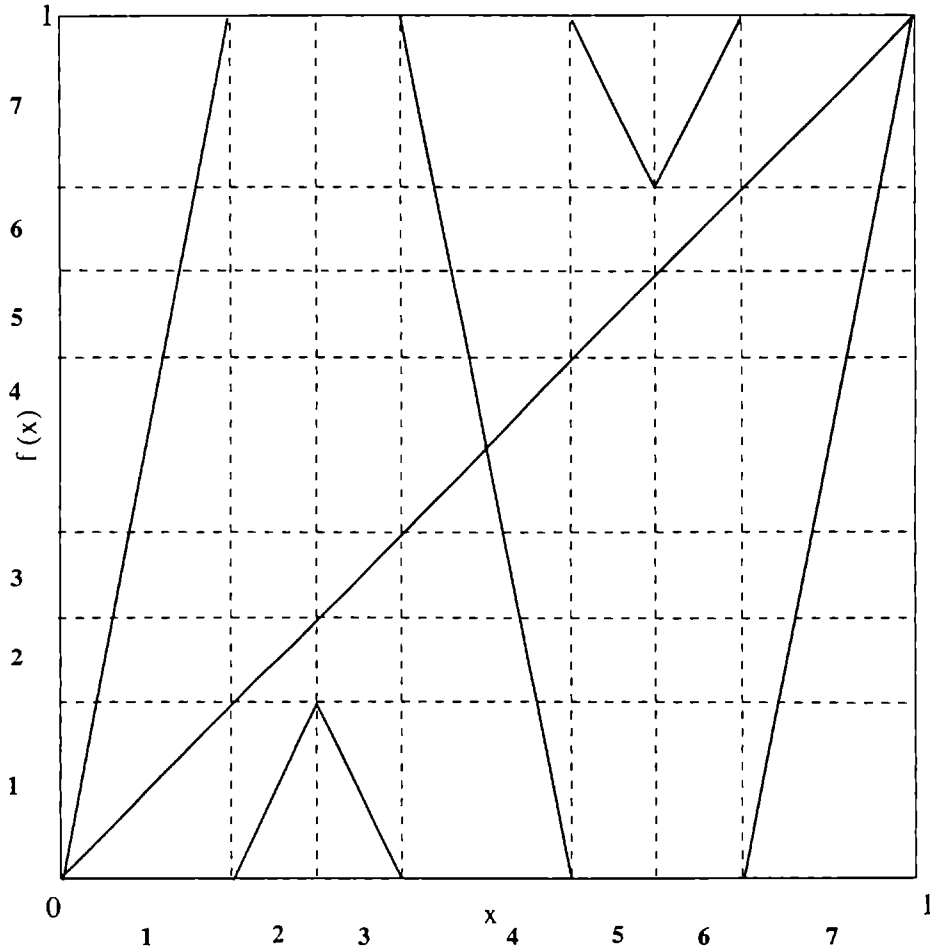


Figure 5.1: Reduced map of the GPLM map (case 1) analysed in chapter 4. The slope magnitude of the 3 longer linear segments is m_0 , whereas the slope magnitude of the 4 shorter segments is m_1 . Dotted lines indicate Markov partitions. Symbols for the 7 branches of $f(x)$ are also shown. On both axes units are arbitrary.

where we substituted

$$\exp \sum_{j=0}^{n_p-1} (qu(f^j(x_p))) = \exp \sum_{j=0}^{n_p-1} (q\Delta(f^j(x_p))) = \exp(\sigma_p q) \quad (5.32)$$

Note that σ_p is the integer part of $Y_r^{n_p}(x_p)$, x_p being a periodic point of a p -cycle. The above expression for $\zeta_m^{-1}(z, q)$ is the same as the one in [95 – 97]. Thus the jumping number $\Delta(x)$ is the required symbolic dynamics. For locating the first zero of d , usually one focus attention on

$$\zeta_0^{-1}(z, q) = \prod_p (1 - T_p) \quad (5.33)$$

where

$$T_p = \frac{z^{n_p} \exp(\sigma_p q)}{|J_p|} \quad (5.34)$$

is the weight factor.

Let us denote the seven branches of $f^{-1}(x)$ by the symbol $\nu = 1, 2, 3, \dots, 7$ (from left). Let l_ν be the slope of the line segment. $l_1 = l_7 = m_0$; $l_2 = l_6 = m_1$; $l_3 = l_5 = -m_1$; $l_4 = -m_0$. From fig. 5.1 we note that the slope magnitudes are connected by relations.

$$\frac{3}{m_0} + \frac{4h}{m_1} = 1 \quad (5.35)$$

$$h = \frac{1}{m_0} \quad (5.36)$$

On solving we get

$$m_0 = \frac{1}{h} \quad (5.37)$$

$$m_1 = \frac{4h}{1 - 3h} \quad (5.38)$$

We consider the situation $\frac{1}{7} < h \leq \frac{1}{4}$. In this range of h . m_0 and m_1 are greater

than 1. ie, the map is an expanding one. Also $m_0 \geq m_1$. Let Δ_ν denote the jumping number for the branch with symbol ν . They are (from left) 0, +1, +1, 0, -1, -1, 0. By observing backward iterations of $f(x)$ in fig. 5.1, one finds that the following sub-sequences are forbidden

$$\begin{aligned}
 & -24-, \quad -27-, \quad -22-, \quad -23-, \quad -25-, \quad -26- \\
 & -34-, \quad -37-, \quad -32-, \quad -33-, \quad -35-, \quad -36- \\
 & -51-, \quad -54-, \quad -52-, \quad -53-, \quad -55-, \quad -56- \\
 & -61-, \quad -64-, \quad -62-, \quad -63-, \quad -65-, \quad -66-
 \end{aligned} \tag{5.39}$$

The pruning rule [77, 78] implies that “2” and “3” must always be followed by “1” and “5”, and “6” by “7” The dynamics is an unrestricted symbolic dynamics with the alphabet $\{1, 4, 7, 21, 31, 57, 67\}$. Let $i, j, k \dots$ represent a symbol sequence indicating line segments which contain the periodic points of a prime cycle. Due to uniformity of slope for a line segment we have

$$T_{i,j,k\dots} = T_i \times T_j \times T_k \times \tag{5.40}$$

This means that the curvatures [77, 78, 95 – 97] will vanish exactly. Thus the zeta function $\zeta_0^{-1}(z, q)$ can be expanded as

$$\zeta_0^{-1}(z, q) = 1 - T_1 - T_4 - T_7 - T_{21} - T_{31} - T_{57} - T_{67} \tag{5.41}$$

We note

$$T_i = \frac{z^1 \exp(\Delta_i q)}{|l_i|} \quad T_{ij} = \frac{z^2 \exp[(\Delta_i + \Delta_j)q]}{|l_i||l_j|} \tag{5.42}$$

Using eqs. (5.37,5.38,5.42), in eq. (5.41) it can be found that $z_q^{(0)}$ is the first zero of the following equation.

$$1 - 3hz - (1 - 3h)z^2 \cos hq = 0 \tag{5.43}$$

from which

$$z_q^{(0)} = \frac{2}{3h + \sqrt{9h^2 + 4(1 - 3h) \cos hq}} \quad (5.44)$$

We get λ_0 and D using eqs. (5.23) and (5.24)

$$\lambda_0 = 0 \quad (5.45)$$

$$D = \frac{(1 - 3h)}{2(2 - 3h)} \quad (5.46)$$

Note that eq. (5.24) is the general relation for obtaining D . The relation given in [95 – 97].

$$D = -\frac{1}{2} \frac{\partial^2 z_q^{(0)}}{\partial q^2} \Big|_{q=0} \quad (5.47)$$

is only a special case of the relation (5.24) and is applicable only when $\lambda_0 = 0$. In a map like the one in fig. 4.1, because of symmetry, the drift velocity λ_0 is always zero. But it is not true generally.

From eq. (5.20), α and $\sigma(\alpha)$ are obtained as

$$\alpha = \frac{(1 - 3h) \sin hq}{3h\sqrt{(9/4)h^2 + (1 - 3h) \cos hq} + \frac{9}{2}h^2 + 2(1 - 3h) \cos hq} \quad (5.48)$$

$$\sigma(\alpha) = -\ln\left[\frac{3h}{2} + \sqrt{\frac{9}{4}h^2 + (1 - 3h) \cos hq}\right] + q\alpha \quad (5.49)$$

The limiting forms eqs. (5.21) and (5.22) applicable for $|q| \ll b$ (small values of α) can be considered with the above values for λ_0 and D . For considering the limiting form eqs. (5.26) and (5.27) for $|q| \gg b$, ie extreme regions of α , we get

the following constants using eq. (5.25).

$$\lambda_{+\infty} = \frac{1}{2} \quad \lambda_{-\infty} = -\frac{1}{2}$$

$$\tau_+ = \tau_- = \frac{1}{\ln\left(\frac{2}{1-3h}\right)^{1/2}} \quad c_+ = c_- = \frac{3h}{\sqrt{2(1-3h)}} \quad \eta_+ = \eta_- = \frac{1}{2} \quad (5.50)$$

Note that the expression for diffusion coefficient D we got (eq. (5.46)) using cycle expansion technique is exactly the same as the one derived in chapter 4 for case 1 (eq (4.19)). In fig. 4.3a we have shown the variation of D with h . It is easy to note that D increases when the map becomes more and more flat (when h decreases from $\frac{1}{4}$ to $\frac{1}{7}$, m_0 increases from 4 to 7 whereas m_1 decreases from 4 to 1). From fluctuation spectrum $\sigma(\alpha)$, one can obtain the PDF of N_t , the distance from the origin. From eq. (5.18), we have

$$P_t(N) \sim \frac{1}{\sqrt{t}} \exp\left[-\sigma\left(\frac{N}{t}\right)t\right] \quad (5.51)$$

$P_t(N)$ being the PDF that N_t takes values between N and $N + dN$. This PDF is approximately Gaussian by central limit theorem. Infact eq. (5.22) corresponds to the Gaussian part of the PDF which is applicable for small values of α and eq. (5.27) corresponds to the non-Gaussian part applicable for extreme values of α . In fig. 5.2 we show the variation of $\sigma(\alpha)$ with α along with Gaussian form. From this graph and also from eq. (5.27) one notes that $\frac{d\sigma(\alpha)}{d\alpha}$ diverges logarithmically at extreme values of α . Since the slope of $\sigma(\alpha)$ in eq. (5.22) is inversely proportional to D , one finds that for minimising deviation from Gaussian character of the PDF, one has to minimise D ie, the peak-shape should become sharp. Conversely when the map becomes flat, the PDF exhibits more non-Gaussian character since the dynamics exhibits intermittency.

As the second example, let us consider the generalized piecewise linear (GPL) map which we analysed in chapter 3. The reduced map shown in fig. 3.2 has 7 line segments and the resulting climbing map has a peak height $h = 1$. Gener-

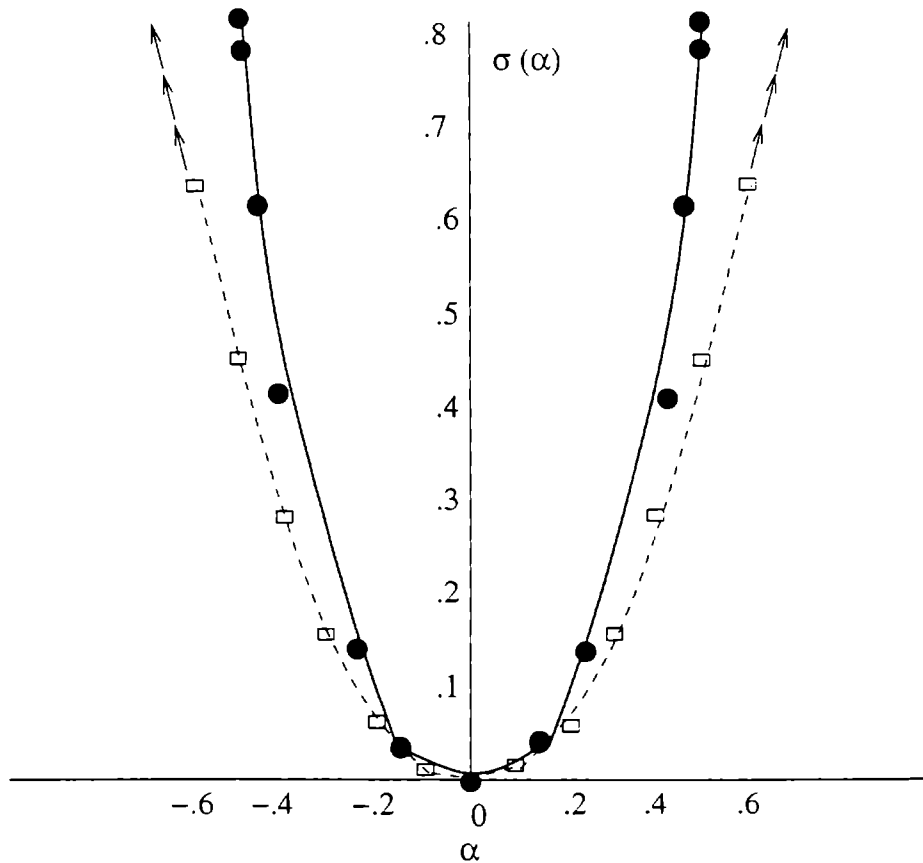


Figure 5.2: Fluctuation spectrum $\sigma(\alpha)$ vs α pertaining to the spatially extended map generated by Fig. 5.1 ($h = 0.2$). Solid line with black dots represents actual $\sigma(\alpha)$ while dotted line with small squares gives the corresponding Gaussian form. On both axes units are arbitrary.

expansion for ζ_0^{-1} gives

$$\zeta_0^{-1}(z, q) = 1 - T_1 - T_4 - T_7 - T_{21} - T_{31} - T_{57} - T_{67} \quad (5.60)$$

$$T_i = \frac{z^1 |l_i|^q}{|l_i|} \quad T_{ij} = \frac{z^2 |l_i|^q |l_j|^q}{|l_i| |l_j|} \quad (5.61)$$

It follows from (5.37), (5.38), (5.61).

$$1 - 3z\left(\frac{1}{h}\right)^{q-1} - 4z^2\left(\frac{4}{1-3h}\right)^{q-1} = 0 \quad (5.62)$$

from which

$$z_q^{(0)} = \frac{2}{3\left(\frac{1}{h}\right)^{q-1} + \sqrt{9\left(\frac{1}{h}\right)^{2(q-1)} + 16\left(\frac{4}{1-3h}\right)^{q-1}}} \quad (5.63)$$

One can obtain (eqs. (5.23) and (5.24))

$$\lambda_0 = \frac{-3h \ln h + (1-3h) \ln\left(\frac{4}{1-3h}\right)}{(2-3h)} \quad (5.64)$$

$$D = \frac{3h(1-3h)}{2(2-3h)^3} \left[\ln\left(\frac{4h^2}{1-3h}\right) \right]^2 \quad (5.65)$$

From eq. (5.20) we get

$$\alpha = \frac{\{-\ln h \times (\sqrt{1 + \frac{16}{9}\left(\frac{4h^2}{1-3h}\right)^{q-1}} + 1) + \frac{8}{9} \ln\left(\frac{4}{1-3h}\right) \times \left(\frac{4h^2}{1-3h}\right)^{q-1}\}}{[1 + \sqrt{1 + \frac{16}{9}\left(\frac{4h^2}{1-3h}\right)^{q-1}}] \sqrt{1 + \frac{16}{9}\left(\frac{4h^2}{1-3h}\right)^{q-1}}} \quad (5.66)$$

$$\sigma(\alpha) = -\ln\left[\frac{3}{2}\left(\frac{1}{h}\right)^{q-1} \pm \sqrt{\frac{9}{4}\left(\frac{1}{h}\right)^{2(q-1)} + 4\left(\frac{4}{1-3h}\right)^{q-1}}\right] + q\alpha \quad (5.67)$$

One can consider the limiting forms of $\sigma(\alpha)$, given by eqs. (5.22) and (5.27) (Gaussian and non-Gaussian parts respectively). For the Gaussian part λ_0 and D are given above. We can evaluate the following constants using eq. (5.25)

$$\begin{aligned} \lambda_{+\infty} &= -\ln h & \tau_+ &= -\frac{1}{\ln 3h} & c_+ &= \frac{1-3h}{9h^2} & \eta_+ &= \ln\left(\frac{1-3h}{4h^2}\right) \\ \lambda_{-\infty} &= \ln\left(\frac{4}{1-3h}\right)^{1/2} & \tau_- &= -\frac{1}{\ln(1-3h)^{1/2}} & c_- &= \frac{3}{2}\left(\frac{h^2}{1-3h}\right)^{1/2} \\ & & & & \eta_- &= \frac{\ln\left(\frac{1-3h}{4h^2}\right)}{2} \end{aligned} \quad (5.68)$$

As the second example, we consider $f(x)$ given by the reduced map of the GPL model discussed in chapter 3. The dynamics is an unrestricted symbolic dynamics with the alphabet $\{1, 2, \dots, (4h+3)\}$. Curvatures cancel exactly and the cycle expansion is given by

$$\zeta_0^{-1}(z, q) = 1 - T_1 - \dots - T_{(4h+3)} \quad (5.69)$$

which implies

$$1 - z[3m_0^{q-1} + \sum_{i=1}^h 4m_i^{q-1}] = 0 \quad (5.70)$$

from which

$$z_i^{(0)} = \frac{1}{3m_0^{q-1} + \sum_{i=1}^h 4m_i^{q-1}}. \quad (5.71)$$

We get

$$\lambda_0 = \frac{3}{m_0} \ln m_0 + \sum_{i=1}^h \frac{4}{m_i} \ln m_i \quad (5.72)$$

$$D = \frac{\frac{3}{m_0} (\ln m_0)^2 + \sum_{i=1}^h \frac{4}{m_i} (\ln m_i)^2 - [\frac{3}{m_0} \ln m_0 + \sum_{i=1}^h \frac{4}{m_i} \ln m_i]^2}{2} \quad (5.73)$$

As shown in chapter 3, we can consider a special case with

$$\frac{m_i}{m_{i-1}} = r \quad 0 < r < 1 \quad (5.74)$$

The problem becomes an exactly solvable one for all values of r . Solving with eq. (5.52) we have

$$m_0 = 3 + \frac{4(1 - r^h)}{r^h(1 - r)} \quad (5.75)$$

$$m_i = m_0 r^i \quad (5.76)$$

Summations appearing in eqs. (5.72) and (5.73) can be performed and we get

$$\lambda_0 = \frac{3}{m_0} \ln m_0 + \frac{4}{m_0} \frac{(r^h - 1)}{r^h(r - 1)} \left\{ \ln m_0 + (\ln r) \times \frac{r}{r - 1} \right\} - \frac{4 \ln r}{m_0} \times \frac{h}{(r - 1)r^h} \quad (5.77)$$

$$D = \frac{2(\ln r)^2 \{4r - h^2 r^h - (h + 5)(h + 1)r^{h+1} + h(5h + 12)r^{h+2} - 3(h + 1)^2 r^{h+3} + r^{2h+1} + 3r^{2h+2}\}}{(1 - r)^2 [4 - r^h - 3r^{h+1}]^2} \quad (5.78)$$

α and $\sigma(\alpha)$ can be got from eq. (5.71) using eq. (5.20) as

$$\alpha = \ln m_0 + 4 \ln r \times \left\{ \frac{r^{h+q+1} - (h + 1)r^{hq+q+1} + hr^{(h+2)q}}{(3r^{h+1} + r^{h+q} - 4r^{(h+1)q})(r - r^q)} \right\} \quad (5.79)$$

$$\sigma(\alpha) = - \ln \left\{ m_0^{(q-1)} \left[\frac{3r^{h+1} + r^{h+q} - 4r^{(h+1)q}}{r^h(r - r^q)} \right] \right\} + q\alpha \quad (5.80)$$

Using the values of λ_0 and D Gaussian component applicable for small values of α ($q \ll b$) can be obtained from eq. (5.22). Non-Gaussian component corresponding to extreme values of α are given by eq. (5.27). The constants appearing in

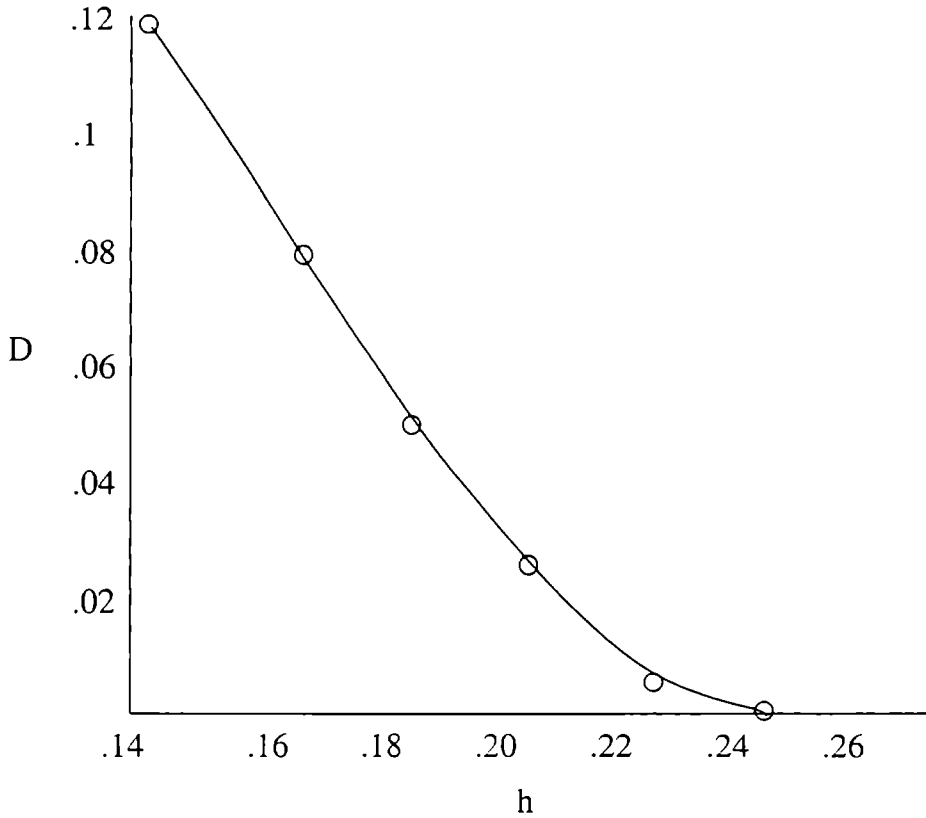


Figure 5.3: Variation of diffusion coefficient D pertaining to the dynamics of local expansion rates with h for the map shown in Fig. 5.1. On both axes units are arbitrary.

equation (5.27) are given by

$$\begin{aligned}
 \lambda_{+\infty} &= \ln m_0 & \tau_+ &= \frac{1}{\ln(m_0/3)} & c_+ &= \frac{4}{3r} & \eta_+ &= \ln\left(\frac{1}{r}\right) \\
 \lambda_{-\infty} &= \ln m_h & \tau_- &= \frac{1}{\ln\left(\frac{m_h}{4}\right)} & c_- &= r & \eta_- &= \ln\left(\frac{1}{r}\right)
 \end{aligned} \tag{5.81}$$

where $m_h = m_0 r^h$

Fig. 5.3 shows the variation of D with h for the map (GPLM) in fig. 5.1. As h decreases from $\frac{1}{4}$ to $\frac{1}{7}$, the difference between slope magnitudes of the line

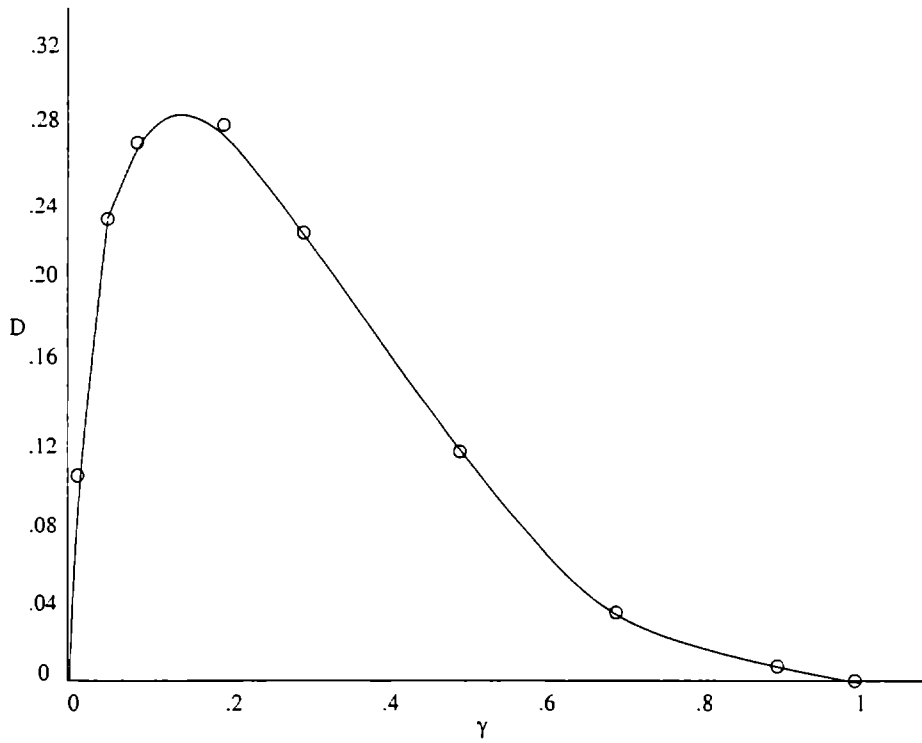


Figure 5.4: Variation of diffusion coefficient D pertaining to the dynamics of local expansion rates with r for the reduced map of GPL model analysed in chapter 3. (with $h = 2$ Eq.(5.78)). On both axes units are arbitrary.

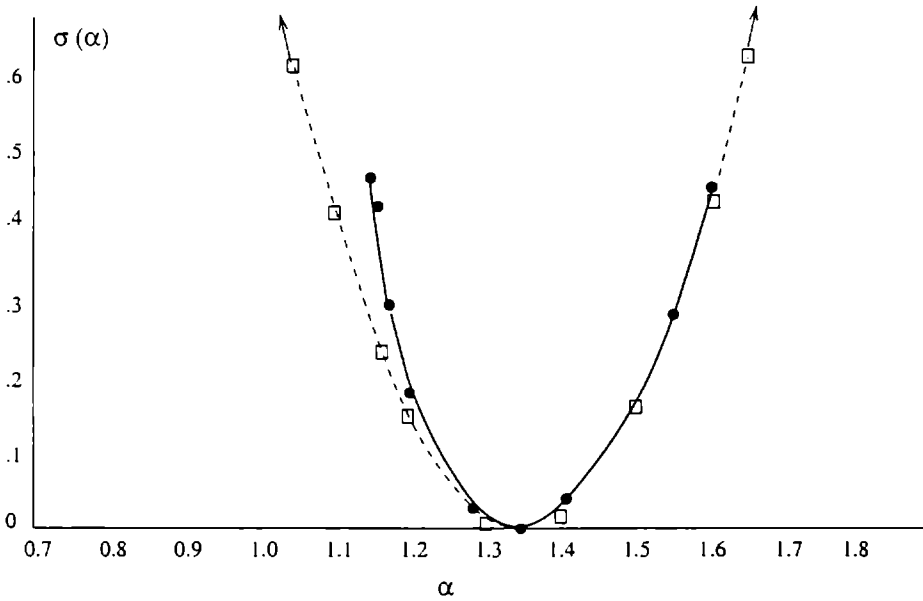


Figure 5.5: Fluctuation spectrum $\sigma(\alpha)$ vs α in relation to the dynamics of local expansion rates for the map in fig. 5.1 ($h = 0.2$). Solid line with black dots represents actual $\sigma(\alpha)$ while dotted line with small squares gives the corresponding Gaussian form. On both axes units are arbitrary.

segments increases and hence diffusion coefficient increases. Fig. 5.4 shows the variation of D with r for the second example i.e. the GPL map with $h = 2$. Here note that as r decreases from 1 to around 0.1, slope magnitudes becomes more and more different and as such D increases. When r is decreased further to zero the probability for the phase point to fall on line segments with slopes m_0 and m_1 (both tending to ∞) tends to zero. The probability will be maximum for the line segments forming the peaks. All these segments have the same slope magnitude $m_2 = 4$. Hence D will decrease. The variation of $\sigma(\alpha)$ with α along with the Gaussian form eq. (5.22) for the map shown in fig. 5.1 is shown in fig. 5.5 with $h = 0.2$. Fig. 5.6 shows the same variation for the second example (GPL map with $h = 2$; $r = 0.5$). As in the case of spatially extended maps, one can reach the conclusion that Gaussian approximation for the PDF will become more and more

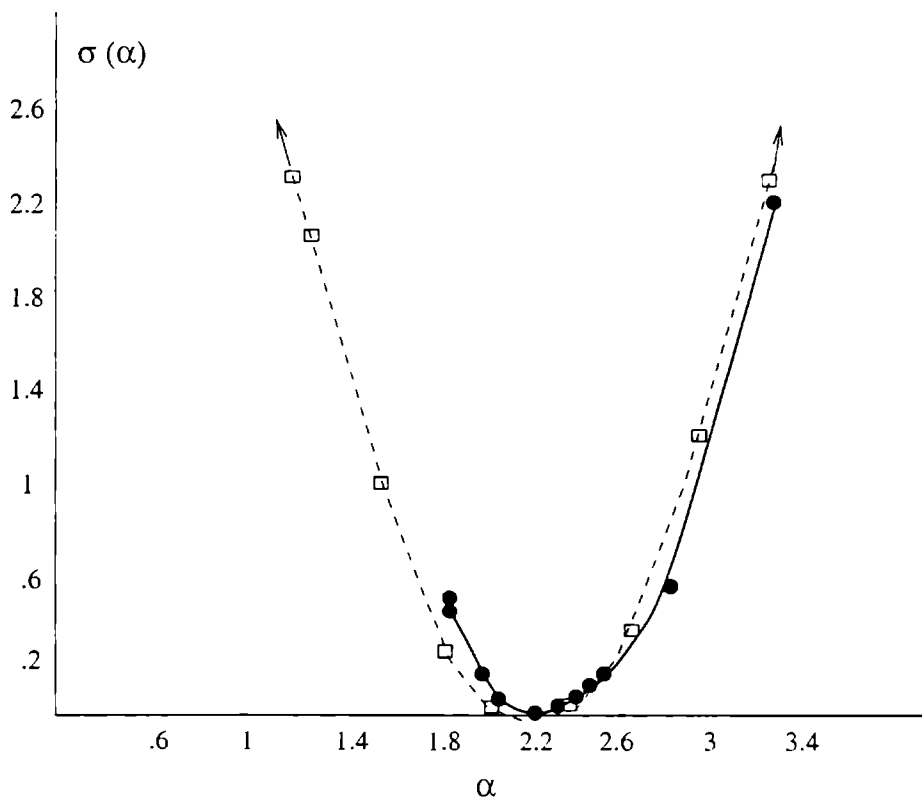


Figure 5.6: Fluctuation spectrum $\sigma(\alpha)$ vs α in relation to the dynamics of local to expansion rates for the reduced map of the GPL model (chapter 3) (with $h = 2$, $r = 0.5$). Solid line with with black dots represents actual $\sigma(\alpha)$ while dotted line with small squares gives the corresponding Gaussian form. On both axes units are arbitrary.

valid when diffusion coefficient $D \rightarrow 0$. This happens when the line segments have almost the same slope.

5.4 Results and conclusions.

In this paper, we show how periodic expansion technique can be used to obtain the probability density in connection with the chaotic maps producing chaos-induced diffusion. We have shown, how cycle expansion can give the fluctuation spectrum which in turn can provide the PDF. PDF has two components - a Gaussian component resulting from central limit theorem and a non-Gaussian component. These lead to a complementary dynamics of diffusion and intermittency in chaos-induced diffusion systems. Our aim is to demonstrate that periodic orbits can be used to analyse the PDF and this complementary dynamics of diffusion and intermittency rather than just obtaining the exact diffusion coefficient.

As examples, we have discussed exactly solvable piecewise linear maps for two types of chaos-induced diffusion (1) deterministic diffusion in spatially extended climbing maps (2) diffusion associated with the dynamics of local expansion rates (trajectory separation statistics). In both cases, we have shown that for enhancing the Gaussian character of the PDF one has to minimise the diffusion coefficient. In this case diffusive characteristics will predominate over intermittency and moments will be determined by D . In the context of spatially extended systems this means that maps with sharp peaks show more Gaussian character than those with flat peaks. This fact is beneficial in the time series analysis of chaotic systems showing diffusion. For describing systems like Brownian motion one should use maps with sharp peaks. For describing systems showing intermittency in time, maps with flat peaks are more suitable. In statistics of trajectory separation resulting from the fluctuations of local expansion rates, logarithmic separation of the trajectory will show more Gaussian character if the studied map has almost the same slope within the interval $[0, 1]$. Otherwise non-Gaussian char-

acteristics and intermittency will predominate.

Periodic orbit expansion is a perturbation method and hence can be applied to get approximate results for systems where analytical treatment is not possible. Moreover, as observed by Dana [114], an approach to chaos-induced diffusion via hierarchical skeleton of periodic orbits should play a major role in the study of the quantum counter part of classical chaotic transport [115]. The reason is that classical periodic orbits are relevant in the study of energy spectrum as well as structure of wave functions at least in the semi-classical regime [116, 117]. In the light of these, we feel that an attempt to enhance the applicability of periodic orbit expansion has both theoretical and practical significance.

Bibliography

- [1] H.Poincare, *Les Methodes Nouvelles de la Mechanique Celeste* (Gauthier-Villars, Paris,1892).
- [2] M.H.Jensen, L.P.Kadanoff, A.Libchaber, I.Procaccia, and J.Stavans, Phys. Rev.Lett. **55**, 2798 (1985).
- [3] D. Bensimon, M.H.Jensen, and L.P.Kadanoff, Phys. Rev.A**33**, 3622 (1986).
- [4] M.Feigenbaum, M.H.Jensen, and I.Procaccia, Phys. Rev.Lett. **57**, 1503 (1986).
- [5] H.G.Schuster, *Deterministic Chaos An Introduction* (Physik-Verlag, Weinheim, 1984).
- [6] Edward Ott, *Chaos in Dynamical Systems* (Cambridge University Press, Cambridge, 1993).
- ✓ [7] Christian Beck and F. Schlögl, *Thermodynamics of Chaotic Systems* (Cambridge University Press, Cambridge, 1993).
- [8] B.B.Mandelbrot, *Fractals: Form, Chance and Dimension* (Freeman, San Francisco, 1977).
- [9] H.G.E. Hentschel and I.Procaccia, Physica **8D**, 435 (1983).
- [10] P.Grassberger, Phys.Lett. **97A**, 227 (1983).

- [11] R.Benzi, G.Paladin, G.Parisi, and A.Vulpiani, *J.Phys.A.Math.Gen.* **17**, 3521 (1984).
- [12] T.C.Halsey, M.H.Jensen., L.P.Kadanoff, I.Procaccia, and B.Shraiman, *Phy.Rev.* **A33**, 1141 (1986).
- [13] G.Paladin and A.Vulpiani, *Phys.Rep.* **156**, 147 (1987).
- [14] T.Bohr and T.Tel, in *Direction in Chaos* edited by Hao-Bai-Lin (World Scientific, Singapore, 1988) Vol.2 and references cited therein.
- [15] J.P.Eckmann and I.Procaccia, *Phys.Rev.* **A34**, 659 (1986).
- [16] R.M.May, *Nature* **261**, 459 (1976).
- [17] M.J.Feigenbaum, *J.Stat. Phys.* **19**, 25 (1978).
- [18] M.J.Feigenbaum, *Phys.Lett.* **74A**, 375 (1979)
- [19] M.Henon, *Commun. Math. Phys.* **50**, 69 (1976).
- [20] J.L.Kaplan and J.A.Yorke, in *Functional Differential Equations and Approximation of Fixed Points*, *Lecture Notes in Mathematics*, **730**, 204, eds. H.O.Peitgen and H.O.Walther (Springer, Berlin. 1979).
- [21] J.L.Kaplan, J.Mallet-Paret, J.A.Yorke, *Ergod. Th. Dynam.Syst.* **4**, 261 (1984).
- [22] D.H.Mayer, G.Roepstorff, *J. Stat. Phys.* **31**, 309 (1983).
- [23] C.Beck. *Commun. Math.Phys.* **130**, 51 (1990).
- [24] A.J.Lichtenberg, M.A.Liebermann, *Regular and Stochastic Motion* (Springer. Berlin, 1983).

- [25] G.L.Baker and J.P.Gollub, *Chaotic Dynamics An Introduction* (Cambridge University Press, Cambridge, 1996).
- [26] R.C.Hilborn, *Chaos and Non-linear Dynamics An Introduction for Scientists and Engineers* (Oxford University Press, Oxford, 1994).
- [27] E.N.Lorenz, *The Essence of Chaos* (University of Washington Press, Seattle, 1993).
- [28] S.H.Strogatz, *Non-linear Dynamics and Chaos* (Addison Wesley, Reading, M A., 1994).
- [29] V.I.Arnold and A.Avez, *Ergodic Problems of Classical Mechanics* (W.A.Benjamin Inc, New York, 1968).
- [30] D.Ruelle, Prog.Theor.Phys.Suppl. No **64**, 339 (1978)
- ✓ [31] H.Mori, B.C.So,and T.Ose, Prog.Theor.Phys **66**, 1266 (1981).
- [32] S.Grossmann and S.Thomae, Z.Naturforsch **32A**, 1353 (1977).
- [33] P.Manneville and Y.Pomeau, Phys.Lett **75 A**, 1 (1979).
- [34] P.Manneville and Y.Pomeau, Physica **D1**,219 (1980).
- [35] P.Manneville and Y.Pomeau, Commun. Math. Phys. **74**, 189(1980).
- [36] I. Procaccia and H.Schuster, Phys. Rev. A **28**, 1210 (1983).
- [37] K. Sobu, T. Ose,and H.Mori, Prog. Theor. Phys. **71**, 458 (1984).
- [38] B.C.So and H. Mori, Physica D **21**, 126 (1986).
- [39] Y. Aizawa, Prog. Theor. Phys.. **72**, 659 (1984).
- [40] D.Ruelle and F.Takens, Commun. Math. Phys. **20**, 167 (1971).

- [41] S.Newhouse, D.Ruelle,and F.Takens Commun. Math. Phys. **64**, 35 (1978).
- [42] L.D.Landau, C.R.Dokl, Acad.Sci.USSR **44**, 311 (1944).
- [43] H.Fujisaka, Prog.Theor.Phys. **71**, 513 (1984).
- [44] H.Fujisaka and M. Inoue, Prog.Theor.Phys. **74**, 20 (1985).
- [45] M. Inoue and H.Fujisaka, Prog.Theor.Phys. **77**, 1077 (1987).
- [46] H.Fujisaka, M. Inoue,and H.Uchimura, Prog.Theor.Phys. **72**, 23 (1984).
- [47] H.Fujisaka and M.Inoue, Prog. Theor. Phys. **77** , 1334 (1987).
- [48] H.Fujisaka and M.Inoue, Prog. Theor. Phys. **79**, 758(1988).
- [49] H.Fujisaka, A. Yamaguchi,and M.Inoue, Prog.Theor.Phys. **81**, 1146 (1989).
- [50] H.Shibata, S.Ando,and H.Fujisaka, Phys.Rev. A**45**,7049 (1992).
- [51] H.Fujisaka and M.Inoue, Prog.Theor.Phys. **78**, 268 (1987).
- [52] H.Fujisaka and M.Inoue, Phys.Rev. A**41**, 5302 (1990).
- [53] H.Fujisaka , R.Hagihara,and M.Inoue, Phys. Rev. A **38**, 3680(1988).
- [54] H.Fujisaka, M.Inoue, Phys.Rev. A **39**,1376 (1989).
- [55] H.Fujisaka, Prog.Theor. Phys. **70**, 1264 (1983)
- [56] C.F.F.Karney, A.B.Rechester,and R.B.White, Physica **4D**, 425 (1982).
- [57] H.Koga. H.Fujisaka,and M.Inoue, Phys.Rev. A **28**, 2370 (1983).
- [58] H.Fujisaka and S. Grossmann, Z Phys. B **48**, 261 (1982).
- [59] H.Fujisaka and T. Yamada, Z. Naturforsch **33a**, 1455 (1978).

- [60] A.S. Monin and A.M. Yaglom, *Statistical Fluid Mechanics* (MIT Press, Cambridge, Massachusetts, 1975).
- [61] U. Frisch, P.L. Sulem, and M. Nelkin, *J. Fluid Mech.* **87**, 719 (1978).
- [62] D. Ruelle, *Thermodynamic Formalism* (Addison-Wesley, Reading, M A 1978).
- [63] Ya. G. Sinai, *Russ. Math. Surveys* **166**, 21 (1972).
- [64] R. Bowen, in *Equilibrium States and Ergodic Theory of Anosov Diffeomorphisms*, Lecture Notes in Mathematics Vol **470** (Springer, New York, 1975).
- [65] P. Collet, J. Lebowitz, and A. Porzio, *J. Stat. Phys.* **47**, 609 (1987).
- [66] A. Arneodo and M. Holschneider, *J. Stat. Phys.* **50**, 995 (1988).
- [67] D. Bessis et al., *J. Stat. Phys.* **51**, 109 (1988).
- [68] V. Baladi, J.P. Eckmann, and D. Ruelle, *Non-linearity* **2**, 119 (1989).
- [69] A.O. Lopes, *SIAM J. Math. Anal.* **20**, 1243 (1989).
- [70] C. Beck, *Physica* **50D**, 1 (1991).
- [71] U. Frisch and G. Parisi, in *Turbulence and Predictability in Geophysical Fluid Dynamics and Climate Dynamics*, International School of Physics, "Enrico Fermi" Course L XXX VIII. ed. M. Ghil, R. Benzi, and G. Parisi. (North Holland, New York, 1985) P.84.
- [72] T.C. Halsey, P. Meakin, and I. Procaccia, *Phys. Rev. Lett.* **56**, 854 (1986).
- [73] C. Amitrano, A. Coniglio, and F. di Liberto, *Phys. Rev. Lett.* **57**, 1016 (1986).
- [74] P. Szepefalussy, *Phys. Scr. T* **25**, 226 (1989).

- [75] T.Tel, Phys.Rev. A **36**, 2507 (1987).
- [76] Wolfram Just, T.Kobayashi, and H.Fujisaka, Phys.Lett. A **180**, 87 (1993).
- [77] R.Artuso, E.Aurell, and P.Cvitanovic, Nonlinearity **3**, 325 (1990).
- [78] R.Artuso, E.Aurell, and P.Cvitanovic, Nonlinearity **3**, 361 (1990).
- [79] F.Christiansen, G. Paladin, and H.H.Rugh, Phys.Rev.Lett **65**, 2087 (1990).
- [80] S.Smale, Bull.Am.Math.Soc. **73**, 747 (1967).
- [81] D. Ruelle, *Elements of Differentiable Dynamics and Bifurcation Theory* (Academic: New York, 1989).
- [82] R.S. Mac Kay and J.D. Miess. *Hamiltonian Dynamical Systems* (Hilger, Bristol, 1987).
- [83] D.S. Ornstein, in *Statistical Mechanics*, ed. S.A. Rice, K.F.Freed, and J.C.Light (University Chicago Press, 1972) p.13.
- [84] B.A. Huberman and J.Rudnick, Phys. Rev. Lett. **45**, 154(1980).
- [85] J.P.Crutchfield and B.A. Huberman, Phys. Lett. **77 A**, 407 (1980).
- [86] T.Kobayashi, H.Fujisaka, and Wolfram Just, Phys. Rev. E **47**, 3196 (1993).
- [87] N.Mori, T. Kobayashi, H. Hata, T. Morita, T. Horita, and H. Mori, Prog. Theor. Phys. **81**, 60 (1989).
- [88] W.Jezewski, Phys.Lett. A **183**, 63 (1993)
- [89] T.Geisel and J.Nierwetberg, Phys.Rev. Lett. **48**, 7 (1982).
- [90] M.Schell, S.Fraser, and R.Kapral, Phys.Rev.A **26**, 504 (1982).
- [91] S. Grossmann and H. Fujisaka, Phys. Rev. A **26**, 1779 (1982).

- [92] M.Inoue and H.Koga, Prog. Theor. Phys. **68**, 2184 (1982).
- [93] T.Geisel, in *Non Equilibrium Co-operative Phenomena in Physics and Related Fields*, ed. M.G. Velarde. (Plenum, New York,1984).
- [94] S. Grossmann and S. Thomae, Phys. Lett. **97A**, 263 (1983).
- [95] R. Artuso,Phys. Lett. A **160**,528 (1991).
- [96] H.C.Tseng, H.J.Chen, P.C.Li, W.Y. Lai, C.H.Chou, and H.W. Chen, Phys. Lett. A **195**, 74 (1994)
- [97] Chia- Chu Chen, Phys.Rev E **51**, 2815 (1995).
- [98] R.Klages and J.R.Dorfman, Phys.Rev.Lett. **74**,387 (1995).
- [99] R.Klages and J.R.Dorfman, Phys.Rev. E **59**, 5361 (1999).
- [100] R.Klages and J.R.Dorfman,Phys. Rev. E **55**, R 1247 (1997).
- [101] P. Gaspard and R. Klages, Chaos **8**, 409 (1998).
- [102] P.Gaspard, J.Stat.Phys. **68**, 673 (1992).
- [103] P.Gaspard, Phys. Lett. A **168**, 13(1992).
- [104] P.Gaspard, Chaos **3**, 427(1993).
- [105] R. Klages. *Deterministic Diffusion in One Dimensional Chaotic Dynamical Systems* (Wissenschaft and Technik-Verlag, Berlin, 1996).
- [106] S.Wiggins, *Chaotic Transport in Dvnamical Systems* (Springer-Verlag, New York, 1992).
- [107] B.A.Huberman, J.P.Crutchfield, and N.H.Packard, Appl. Phys.Lett. **37**, 750 (1980).

- [108] M.Cirillo and N.F. Pedersen, Phys.Lett. A **90**,150 (1982).
- [109] E.Ben-Jacob, J.Goldhirsch, Y.Imry,and S.Fishman, Phys.Rev. Lett. **49**,1599 (1982).
- [110] R.W.Leven and B.P.Koch, Phys. Lett. A **86**,71 (1981).
- [111] Yuji Ono and Kazuhiro Fukushima, Phys. Lett. A **163**, 173 (1992).
- [112] B.V. Chirikov, Phys.Rep. **52**, 263 (1979).
- [113] Wolfram Just, J.Phys.A.Math.and Gen. **27**, 3029 (1994).
- [114] I. Dana., Physica **D 39**, 205 (1989).
- [115] G. Casati, B.V. Chirikov, F.M. Izrailev, and J. Ford, in Lecture notes in Physics. Vol. **93**, *Stochastic Behaviour in Classical and Quantum Hamiltonian Systems.*, eds. G. Casati and J. Ford (Springer, Berlin, 1979).
- [116] M.C. Gutzwiller, J.Math.Phys. **12**, 343 (1971).
- [117] E. J. Heller, Phys. Rev. Lett. **53**. 1515 (1984).